DEVELOPMENT OF A TRAUMATIC BRAIN INJURY ASSESSMENT SCORE USING NOVEL BIOMARKERS DISCOVERED THROUGH AUTOIMMUNE PROFILING

by

MAJ John E. Buonora, CRNA

Dissertation submitted to the Faculty of the
Neuroscience Graduate Program
Uniformed Services University of the Health Sciences
in partial fulfillment of the requirements for the degree of
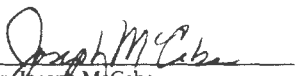Doctor of Philosophy 2013

DISSERTATION APPROVAL FOR THE DOCTORAL DISSERTATION IN THE NEUROSCIENCE
GRADUATE PROGRAM

Title of Dissertation: "Development of a Traumatic Brain Injury Assessment Score Using Novel
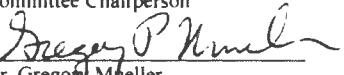Biomarkers Discovered Through Autoimmune Profiling"

Name of Candidate: John Buonara
Doctor of Philosophy Degree
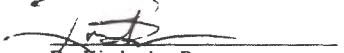July 3, 2013

DISSERTATION AND ABSTRACT APPROVED:

DATE:

07/31/13

Dr. Joseph McCabe
DEPARTMENT OF ANATOMY, PHYSIOLOGY, AND GENETICS
Committee Chairperson

07/3/2013

Dr. Gregory Mueller
DEPARTMENT OF ANATOMY, PHYSIOLOGY, AND GENETICS
Dissertation Advisor
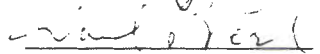
7/3/13

Dr. Kimberley Byrnes
DEPARTMENT OF ANATOMY, PHYSIOLOGY, AND GENETICS
Committee Member
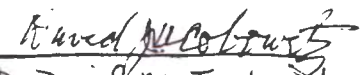
7/3/13

Dr. Brian Schaefer
DEPARTMENT OF MICROBIOLOGY AND IMMUNOLOGY
Committee Member

July 3, 2013

Dr. Daniel Perl
DEPARTMENT OF PATHOLOGY
Committee Member

7/3/13

De David M Jacobowitz
Dept Anatomy, Physiology + Genetics
Committee Member

ACKNOWLEDGMENTS

In 2012 I wrote these words describing Dr. Gregory P. Mueller, in support of him receiving the 2012 Cinda Helke Award:

> Those of us who have had the privilege of working side by side with Dr. Mueller at the bench have witnessed his patient instruction and attention to detail in the use of scientific equipment and techniques in the lab. For a student, there is no substitute for this level of one-on-one mentoring. He is an optimistic mentor who sees success in every failure. In both the laboratory and the classroom, he creates an atmosphere of scientific learning and discovery, all while pursuing hypotheses with clinical relevance. When teaching, Dr. Mueller ensures that a thorough understanding of the neuroscience coursework has taken place. Dr. Mueller has taken students to the white board after an exam and reviewed the subject matter repeatedly to confirm that the foundation and knowledge base they will need for their future research is well established. The common thread of our graduate student experiences is easy to summarize: Dr. Mueller's professional demeanor, intellectual enthusiasm at the bench and unwavering support have been instrumental in his students reaching their academic and professional goals.

Dr. Mueller created an atmosphere of educational opportunities and future success. I would not have completed my vision quest without his mentorship, support, guidance, patience and optimism. I owe my graduate school success to him. I trust that he recognizes that my future scientific endeavors will forever be guided by his mentorship. It has been a great privilege and an honor to work beside Dr. Gregory P. Mueller.

The Gregory P. Mueller Lab:

As a graduate student, bench work is rarely a solo performance. James Freedy, Michael Mousseau and Rachel Lazarus have all been integral parts of this project. Jim and Mike's work laid the foundation for the entire project and their contribution to the advancement of our research was immeasurable. Despite all of her other responsibilities,

Rachel always made time to proofread documents and create professional quality graphics.

Dr. David Jacobowitz:

I was blessed with the extraordinary opportunity to work with a scientist of outstanding experience and commitment to educating graduate students. Dr. Jacobowitz trained and guided me until he was satisfied that the fundamental principles were understood and that I could complete the task to his satisfaction and standards. For a neuroscientist in training to apprentice under a neuroanatomist and scientist of Dr. Jacobowitz's caliber is an unparalleled gift.

We have lots of Data…But No Information:

Dr. Cara Olsen was instrumental in guiding me through the statistical design and methodology for the interpretation of the results.

Despite being on the same four-year Army PhD timeline, CPT Angela Yarnell was always available to discuss, interrogate and interpret the tremendous amount of raw data this project generated. Her commitment to my success was a testament to the Army Values. CPT Yarnell is by all definitions a true officer and scientist.

The Committee:

I would like to acknowledge and thank my dissertation advisory committee: chair Dr. Joseph McCabe; advisor Dr. Gregory Mueller; members Dr. Kimberly Byrnes, Dr. David Jacobowitz, Dr. Brian Schaefer and Dr. Daniel Perl. Each of you agreed to take on

one more responsibility in your already filled academic lives to advise and guide me through this project. You believed in the project and most importantly, you believed in me. I thank each of you for your time and dedication to this cause.

Collaborators:

I have been extremely fortunate that Dr. Mueller assembled a rich and diverse group of collaborators. Without the support and assistance of all of these individuals, I could not have completed this project. It was only because of the generous tissue sharing, equipment sharing, and sharing of personnel that I was able to accomplish so much in such a short period of time.

> USUHS – Dr. H. Pollard, Dr. M. Braga and Ms. C. Almeida-Suhett, Dr. W. Watson, Dr. J. Cole and Ms. M. D'Acchille, Dr. M. Selak, Dr. B. Cox and Mr. S. Gouty
>
> Center for Neuroscience and Regenerative Medicine – Clinical Collaborators: Dr. R. Diaz-Arrastia and Ms. C. Moore, Dr. L. Latour
>
> The Department of National Defence and the Canadian Forces - clinical collaborators: Dr. S. Rhind, Dr. S. Rizoli, Dr. A. Baker

The Army Nurse Corps:

In 2009 the US Army Nurse Corps initiated a pilot program to recruit experienced nurse anesthetists capable of educating the next generation of CRNAs. COL Bruce Schoneboom believed I was the right man for the job. His support has been constant and true from the beginning; I would not be here were it not for him. I owe this entire phase

vi

A few words to:

My family, Robert P., Anne, Robert G., Catherine, Paul, Loretta, Ellen and Elizabeth: You have been a lifetime of faith, love and support.

My son, SPC Andrew P. Buonora: Had it not been for you I would have withdrawn from this program three years ago. The words *acta non verba* are ours to live by.

My wife, Mary Louise Marasco: I have spent half of my life and all of my existence with you; anything written here would not do justice to what we have in our hearts.

DEDICATION

I began my military service to this country to support and care for its service members and their families. Therefore, I dedicate this dissertation to the men and women of the armed forces.

Quiet friend who has come so far,
feel how your breathing makes more space around you.
Let this darkness be a bell tower
and you the bell. As you ring,

what batters you becomes your strength.
Move back and forth into the change.
What is it like, such intensity of pain?
If the drink is bitter, turn yourself to wine.

In this uncontainable night
be the mystery at the crossroads of your senses,
the meaning discovered there.
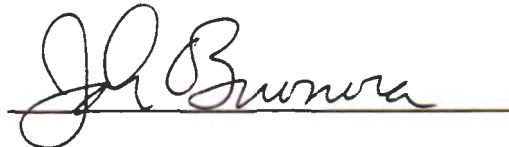
And if the world has ceased to hear you,
say to the silent earth: I flow.
To the rushing water, speak: I am.

Sonnets to Orpheus II, 29
Rainer Maria Rilke

COPYRIGHT STATEMENT

ABSTRACT

Development of a Traumatic Brain Injury Assessment Score Using Novel Biomarkers Discovered Through Autoimmune Profiling:

John E. Buonora, Doctor of Philosophy, 2013

Dissertation directed by: Gregory P. Mueller Ph.D., Professor, Department of Anatomy, Physiology and Genetics

The high rate of head trauma in deployed military personnel and in civilians involved in automobile accidents and in contact sports is well recognized. The extent to which these head traumas result in mild brain injury, however, cannot be determined due to the lack of suitable diagnostic tools, including biomarkers. At present, there is no effective way to assess mild traumatic brain injury (TBI) and the risks it brings for underlying neuropathology and second injury syndrome. For more than a decade, traditional approaches in biomarker research have failed to identify a means for diagnosing mild TBI. Much of this work has focused on single proteins thought to be relevant to TBI but subsequently shown to be ineffective for the diagnosis of mild TBI. It is now clear that new approaches to the discovery of biomarkers and their applications in diagnosis are needed. The goals of this research were to identify novel brain proteins targeted by TBI-induced autoantibodies and to determine if these proteins contribute to a circulating biomarker signature for TBI. We reasoned that the humoral immune response

to brain injury may serve as a pathway for the discovery of novel biomarker proteins for TBI.

Autoimmune profiling for TBI-induced autoantibodies was carried out by immunoblotting in rodents and protein microarray in humans. Serum from control and brain-injured rats was used to interrogate immunoblots of the entire rat brain proteome fractionated on large 2-dimensional gels. Proteins revealed by autoreactive immunoglobulins were then mapped to corresponding protein gels and identified proteomically by peptide mass fingerprinting. A related analysis of the human autoimmune response to TBI was performed using a protein microarray platform containing over 9,000 human proteins. Within-subject comparisons were made between samples that were collected immediately following TBI and 30 days post-injury, times that would reveal the full expression of a TBI-induced autoimmune response. A total of 43 proteins showed enhanced antigenicity following TBI; the proportion of central nervous system proteins in this group was an order of magnitude higher than the representation of brain-centric proteins on the entire array. These findings suggest there is an autoimmune response to TBI that is directed towards the central nervous system.

Findings from the two autoimmune profiling approaches were used to create a list of 12 proteins considered to be the best candidates for having roles as novel TBI biomarkers. This selection was based upon their reported localization and functions in the brain. These proteins, which include peroxiredoxin 6, cyclin-dependent kinase 5, collapsin response mediator protein 2, neuronal pentraxin 1, and presynaptic cytomatrix protein, have been formally recorded in an invention disclosure document. Immunosorbent assays developed for peroxiredoxin 6 and cyclin-dependent kinase 5

demonstrated that these two proteins were informative biomarkers for TBI. It was shown

that the plasma profiles of these novel biomarkers, when considered in conjunction with

the profiles of other established biomarkers, could be interpreted to create an assessment

score that identifies mild TBI. Specifically, it was demonstrated how fold changes in

plasma levels of a panel of biomarker proteins can be formulated to produce a TBI

Assessment Score that identifies mild TBI in humans. This score offers a long-sought

solution to the need for a sensitive and objective tool for diagnosing mild TBI in adult

patients. Because the TBI Assessment Score is based upon definitive measures of

circulating biomarkers, it is an objective assessment that is easily standardized across

clinical settings.

In summary, this research has two major outcomes. First, it demonstrates that

autoimmune profiling can be used to identify novel biomarkers for TBI. Second, this

investigation demonstrates for the first time that a profile of biomarker responses can be

used to formulate a diagnostic assessment score that is sensitive for the detection of mild

TBI.

TABLE OF CONTENTS

LIST OF TABLES

LIST OF FIGURES

LIST OF ABBREVIATIONS

1-D: one-dimensional

2-D: two-dimensional

ACTH(1-17): cleaved fragment of adrenocorticotropic hormone

BBB: blood brain barrier

BCA: bicinchoninic acid assay

BDNF: brain derived neurotrophic factor

BSA: bovine serum albumin

$^\circ$C: degree Celsius

$CaCl_2$: calcium chloride

CCD: charge-coupled device

CCI: controlled cortical impact

CDK5: cyclin-dependent kinase 5

CHAPS: 3-[(3-Cholamidopropyl)dimethylammonio]propanesulfonic acid

CI-P: Chebyshev's inequality value

CKBB: creatine kinase brain type

cm: centimeter

CNS: central nervous system

CO_2: carbon dioxide

CPB: cardiopulmonary bypass

CRMP2: collapsin response mediator protein 2

CSF: cerebral spinal fluid

CT or CAT: computed axial tomography

DTT: dithiothreitol

ECMO: extracorporeal membrane oxygenation

EDTA: ethylenediaminetetraacetic acid

ELISA: enzyme-linked immunosorbent assay

FBS: fetal bovine serum

FDA: Food and Drug Administration

fmol: femtomole

g: force of gravity

gm: gram

GFAP: glial fibrillary acidic protein

GSC: Glasgow Coma Scale

GST: glutathione S-transferase

HRP: horseradish peroxidase

ICAM-5: intercellular adhesion molecule 5

IEA: immunosorbent electrochemiluminescent assay

IgG: immunoglobulin G

IgM: immunoglobulin M

IHC: immunohistochemistry

KCL: potassium chloride

kDa: kilodalton

kg: kilogram

LAM: laboratory animal medicine

LIPS: luciferase immunoprecipitation system

LOD: level of detection

LOQ: level of quantification

M: molar

mA: milliamp

MALDI-TOF: matrix-assisted laser desorption/ionization-time of flight

MANOVA: multivariate analysis of variance

MBP: myelin basic protein

MCP-1/CCL2: monocyte chemotactic protein 1 / chemokine (C-C motif) ligand 2

mg: milligram

$MgCl_2$: magnesium chloride

min: minute

mL: milliliter

mmHg: millimeter of mercury

mM: millimolar

mm: millimeter

MOPS: 3-(N-morpholino) propanesulfonic acid

MOWSE: molecular weight search

MRI: magnetic resonance imaging

ms: millisecond

MS: multiple sclerosis

MS-Fit: proteomic tool for mining peptide sequence databases in conjunction with mass spectrometry

MSD: Meso Scale Discovery

MW: molecular weight

NaAc: sodium acetate

NaCl: sodium chloride

NaEDTA: sodium ethylenediaminetetraacetic acid

Na^2HPO_4: disodium phosphate

ng: nanogram

$NaHCO_3$: sodium bicarbonate

NH_4HCO_3: ammonium bicarbonate

NSE: neuron specific enolase

OEF: Operation Enduring Freedom

OIF: Operation Iraqi Freedom

OND: Operation New Dawn

PBS: phosphate buffered saline

PCLO: presynaptic cytomatrix protein

pg: picogram

pH: negative log of hydrogen ion concentration

PI: isoelectric point

ppm: parts per million

PRDX6: peroxiredoxin 6

PTSD: post-traumatic stress disorder

PVDF: polyvinylidene fluoride

RFU: relative florescent units

RPM: revolutions per minute

Ru(bpy)3: ruthenium(II) tris-bipyridine

S100B: S100 calcium binding protein B

SDS: sodium dodecyl sulfate

SDS-PAGE: sodium dodecyl sulfate-polyacrylamide gel electrophoresis

TBI: traumatic brain injury

TBST: tris-buffered saline and Tween 20

TFA: trifluoroacetic acid

Tris: tris(hydroxymethyl)aminomethane

Tris-HCL: tris(hydroxymethyl)aminomethane-hydrochloric acid

µg: microgram

µL: microliter

UCH-L1: ubiquitin carboxy-terminal hydrolase-L1

USUHS: Uniformed Services University of the Health Sciences

V: volt

v/v: volume to volume

w/v: weight per volume

X: times

y/o: year old

yrs: years

CHAPTER 1: INTRODUCTION

Mild traumatic brain injury (TBI) is often described as an invisible wound. This is primarily due to the fact that a cascade of intracerebral events including inflammation, overt tissue injury and cell loss can all occur following mild TBI without any outwardly apparent signs. At present, TBI assessment is conducted by acute injury surveillance, neuropsychological testing, brain imaging and recording of signs and symptoms. A critical challenge for the care of mild TBI is defining when a head trauma has actually resulted in brain injury and when it has not. Missed diagnosis of TBI undermines necessary clinical treatments and masks the need for behavioral measures designed to prevent the occurrence of a second, compounding head injury (124). Additionally, missed diagnoses are key factors hindering preclinical and clinical TBI investigations (32; 79). Conversely, incorrect diagnoses of TBI burden our health care system unnecessarily and can adversely affect one's eligibility for health care coverage and career opportunities. Because there currently are no effective means for accurately diagnosing mild TBI, this research sought a new approach for the discovery and application of TBI biomarkers. The findings presented here demonstrate the effectiveness of autoimmune profiling for the discovery of novel TBI biomarkers and show how both novel and recognized biomarkers can be used together for the formulation of a TBI Assessment Score that is sensitive for the detection of mild TBI.

The prevalence of mild TBI is impossible to determine simply because so many cases go unreported or undiagnosed. TBI has been referred to as the "Signature Injury" of Operations Iraqi Freedom (OIF), Enduring Freedom (OEF), and New Dawn (OND), where blast injuries were the leading cause of injury (1; 86; 132). In the civilian

population of the United States, there are 1.7 million emergency room visits annually that are directly related to head injury and TBI (33; 109). The clinical importance of TBI is further reflected by the Centers for Disease Control and Prevention's estimation that TBI-related healthcare costs exceed $60 billion annually (22; 39). Considering the overall scope of head injuries, it is reasonable to conclude that undiagnosed mild TBI is a very significant clinical entity. This is particularly true for high school and collegiate athletes as well as soldiers where the culture-of-care does not support medical follow-up on suspected mild TBI. Moreover, in the absence of a diagnosis, the long-term clinical consequences of mild TBI remain unknown because they cannot be linked to the injury. Accordingly, effective biomarkers for the diagnosis of mild TBI will both improve clinical care and facilitate research designed to increase our understanding of brain injury.

The National Research Council recognizes "biomarkers of effect" as those that reflect a condition or disease state through measurable variations in bodily fluids (83). To be effective, these markers must meet the criteria of high specificity and sensitivity and ease of detection. Also important are ease of sample collection and sufficient sample volume to allow for repeated testing. The fundamental limitation of all current TBI biomarkers is clear: when studied individually, none of the established biomarkers for TBI have sufficient specificity or sensitivity for accurate diagnosis of mild TBI. The research proposed here presents a straightforward approach that effectively utilizes the strengths of currently available biomarkers in combination with newly discovered biomarkers to develop a diagnostic tool that is sensitive to mild TBI.

Novel TBI biomarkers were discovered here by using the humoral immune response to brain injury as a pathway for discovery. We hypothesize that TBI triggers the expression of brain-specific autoantibodies against proteins that can serve as blood-borne indicators of brain injury and early biomarkers for the varying degrees of TBI. The approach of autoimmune profiling offers an innovative strategy for discovery and has resulted in the identification of candidate biomarkers that had escaped detection by the conventional experimental approach. Unlike the conventional approach which is based upon the biased *a priori* selection of each specific protein to be studied, autoimmune profiling investigates the immune response to identify proteins that are directly involved in TBI. In this manner, autoimmune profiling is unbiased and evaluates the entire proteome in the search for candidates that are functionally involved in the injury as judged by the expression of TBI-induced autoantibodies.

Use of this innovative approach has led to the discovery of a panel of completely novel candidate biomarkers for brain injury. An additional outcome of potential clinical relevance is the possibility that the autoantibodies involved may themselves constitute a diagnostic signature for TBI. This latter outcome points to the potential involvement of the humoral immune system in the long-term pathology of TBI.

In summary, this dissertation introduces a new approach for the discovery of TBI biomarker proteins. This approach has resulted in the identification of a panel of novel biomarker candidates. The findings presented here demonstrate how patterns in biomarker responses for both novel and established biomarker proteins can be formulated to create a single, objective, multivariate TBI Assessment Score that is sensitive to mild TBI.

CHAPTER 2: BACKGROUND

BIOMARKERS IN MEDICINE

The use of circulating biomarkers has been invaluable in identifying and assessing a wide array of disease states. Conditions of the heart, kidney, pancreas, colon, ovaries, uterus and prostate are all examples of organs for which biomarkers have been developed and successfully used for both diagnosis and disease assessment (63). Sampling for blood-borne biomarkers is minimally invasive, a better predictor of illness than self-reporting, and offers an objective and quantitative measure of disease processes (40; 96). Health care professionals rarely rely exclusively on biomarkers for a diagnosis, but their addition to the armamentarium of decision-making tools has been extremely beneficial for a variety of medical conditions.

Biomarkers can be viewed as having three roles: they function as diagnostics, prognostics, and predictors (98). The diagnostic role pertains to their ability to aid in diagnosing a condition before it is detectable by overt signs or symptoms. A biomarker's prognostic ability refers to its ability to forecast the aggressiveness of a disease process, or how a specific medical condition will be affected by direct intervention (98). Finally, the predictive aspect of a biomarker relates to its quantitative nature, which can be interpreted in the assessment of disease status and the response to care and treatment.

Biomarkers can also be broken down into three types: (1) molecular or biochemical, which are often genes or proteins; (2) physiological, which pertains to functional processes such as blood flow after a stroke; and (3) anatomical, which are related to structures and relationships between parts, such as that seen in the movement

disorder resulting from specific neurological deficits in Huntington's disease (98). The research undertaken here focused on biochemical biomarkers relevant to TBI.

The use of diagnostic biomarkers requires assays that are evaluated on the basis of their specificity, sensitivity, validity, and reliability. Specificity refers to the accuracy of a biomarker test in identifying a positive result that is an accurate reflection of the patient's true condition. A high degree of specificity results in a low rate of false positives. Sensitivity describes the likelihood that the patient has a positive result when the protein is present: thereby a high sensitivity biomarker assures sensitive detection. Validity of a biomarker is often described in two terms. Clinical validity pertains to a biomarker's ability to accurately predict clinical outcome. Assay validity is the confirmation that the assay measures what it reports to measure. One example of a test to confirm validity would be the demonstration of an expected finding using an independent measure. For example, an antibody's specificity for a protein of interest in an immunosorbent electrochemiluminescent assay (IEA) could be confirmed by immunoblotting. Reliability of a biomarker requires that its assay is consistently repeatable and accurate. Having addressed the characteristics and clinical use of biomarkers, our attention will turn to a brief consideration of the evolution of TBI biomarkers, specifically pertaining to development and shortcomings.

BIOMARKERS IN TBI: GAPS TO BE FILLED

It is well recognized that blood-borne biomarkers have the potential to be useful and important tools in clinical medicine relating to brain injury. An objective assessment of the TBI biomarker field over the last decade reveals that an extraordinarily large volume of work has been conducted at considerable cost to the taxpayer and private

5

investor. Much of this work has involved the selection of likely candidates, chosen based on deductive reasoning. If the protein was known to be brain-specific and was shown to produce a distinct peptide signature when digested with proteases known to be activated in TBI, then that protein and its fragments were pursued as candidate TBI biomarkers. Table 1 presents a list of proteins widely recognized as potential biomarkers for TBI. Unfortunately, none of these biomarkers when used independently has proven useful in the diagnosis of mild TBI.

Table 1. Summary of the TBI biomarker literature for commonly cited markers

Known TBI Markers	Reported findings and references
GFAP	Increased levels are seen after TBI (84; 91; 128; 136). Elevated levels are predictive of poorer outcome and correlate with Glasgow Coma Scale and mortality. Good sensitivity (85%) but poor specificity (52%) for predicting poor outcome at 6 months (128).
S100b	Serum and CSF levels increase following TBI, and were shown to predict outcome, differentiates mild and severe injury and correlates with CT scans (12; 49; 73; 90; 91; 97; 104; 128; 140; 145). S100b is a sensitive marker for TBI (95%) but with low specificity (31%) and not always specific to brain injury (2; 12; 50; 101; 103; 128).
NSE	Shown to be a marker of brain injury severity, and levels have been correlated with poor outcome in TBI patients (49; 102; 111). Good sensitivity (80%) but poor specificity (55%) (89).
CKBB	One of the first TBI biomarkers studied. 2009 study in military personnel with suspected mild TBI serving in Iraq demonstrated poor sensitivity (11%) and good specificity (97%) (6; 19; 43; 48; 51; 59; 61; 92; 111; 121; 137).
UCH-L1	Serum levels increase with TBI and levels are associated with severity of injury and CT scan results (75; 87). Also shown as a predictor of in-hospital mortality and strongly predicted death within 6 months. Not significantly elevated in mild TBI (9).
MBP	Levels show some correlation with outcome but lack specificity (8; 119).
α II-spectrin proteolysis products	Shown to correlate with severity of injury (130; 133; 134). Another study correlated levels with severity and outcome 6 months post-injury in severe TBI (93). Higher levels are found in patients with poor outcome (18).
BDNF	A body of evidence is forming that points to dysregulation of BDNF following TBI and post-traumatic stress disorders (7; 11; 58; 100; 110).

The leader in TBI biomarker research, Banyan Biomarkers, Inc., has received more than $75 million in grants and contracts over the last ten years to support its discovery efforts (118). The company has made significant progress in developing and clinically validating many enzyme-linked immunosorbent assays (ELISAs) for TBI. While Banyan's scientists have created an extensive portfolio of intellectual property and a large pipeline of potential biomarkers, the fact remains that neither Banyan nor any other research enterprise has been successful in developing biomarkers for assessing anything other than the more severe forms of TBI: that is, conditions where the obviousness of the injury diminishes the need for biomarker assessment. The two lead candidates under development for Food and Drug Administration approval, ubiquitin carboxy-terminal hydrolase - L1 (UCH-L1) and a proteolytic fragment of glial fibrillary acidic protein (GFAP), have proven ineffective at identifying milder forms of TBI. There is no compelling evidence that any other Banyan candidates have any better potential (24; 74; 76; 87). Accordingly, a new approach to biomarker discovery is needed.

HOW THIS RESEARCH FILLS GAPS IN TBI SCIENCE

This research introduces a new strategy for the discovery of novel TBI biomarkers and demonstrates how a panel of biomarkers can be used to formulate an assessment score sensitive for mild TBI. The research is based upon the proposal that the humoral immune response to brain injury can serve as a pathway for the discovery of TBI biomarkers. The underlying hypothesis for this investigation is that brain-specific autoantibodies can be used to identify proteins that will serve as circulating biomarkers for the assessment of mild TBI. The objectives for this project, therefore, were to identify and investigate brain proteins that are targeted by autoimmune recognition in response to

7

TBI. The ultimate goal for this work was to utilize this approach of autoimmune profiling to discover novel biomarkers useful in the diagnosis and assessment of TBI.

AUTOIMMUNE RESPONSE TO TBI: ANTIBODIES, AUTOANTIBODIES AND TOLERANCE

Humoral immunity is mediated by immunoglobulin antibodies produced by B lymphocytes. The immune system expands and contracts its inventory of B cells as needs determine. In the process, B cells progress through distinct phases of development beginning with their formation in bone marrow and culminating in highly specific cell proliferation and antibody production in the periphery (88). The intervening developmental stages involve the expression and rearrangement of heavy- and light-chain immunoglobulin genes to produce novel receptor molecules capable of recognizing antigens. These early events in B cell development occur in the bone marrow where B cells recognizing self-antigens are generally eliminated through a process referred to as negative selection. Nearly 75% of immature B cells have some affinity for self-antigens and thus are eliminated by either apoptosis or a form of cellular senescence known as anergy (88).

Many, but not all self-antigens, are presented to developing B cells. Accordingly, some B cells exit the marrow compartment with the capability of self-recognition and, thus, the potential to marshal an autoimmune attack. Normally, these self-recognizing B cells are held in a quiescent state through immune mechanisms that constitute positive selection and result in peripheral tolerance. Under certain pathological conditions, however, the immune environment permits B cells to become fully active and produce self-directed autoantibodies. This reversal of peripheral tolerance is proposed as one mechanism by which TBI induces the expression of brain-specific autoantibodies.

8

B cells that survive negative selection travel from the bone marrow to secondary lymphoid organs where they complete maturation. Mature B cells function as reactive sentinels of the immune system, responding to foreign proteins with cellular activation, clonal expansion and antibody production. The specific steps involved are exceedingly complex and involve precise interactions among antigen presenting cells, activated T lymphocytes and a spectrum of immune signaling and co-stimulatory molecules. During the course of an immune response, some B cells develop into memory B cells, which are long lived and retain high-affinity antigen receptors tailored to their respective foreign antigens. These memory cells provide for a rapid and enhanced response to reinfection.

AUTOIMMUNE RESPONSE TO TBI: MECHANISMS FOR THE EXPRESSION OF AUTOANTIBODIES

The autoimmune response to TBI is triggered by immune surveillance of brain proteins previously sequestered by the blood brain barrier, and also by the generation of injury-induced chemical modifications that increase the antigenicity of brain proteins (41; 105; 113; 115). While the mechanisms involved are not fully understood, critical features underlying the immune response include a weakening of the blood brain barrier, invasion of immune cells into the injured tissue, and the subsequent reaction of these cells with specific proteins and their posttranslational modifications (resulting in the expression of autoantibodies) (3; 127; 129; 135). The appearance of circulating autoantibodies can occur within one week post-injury (113; 115). A growing body of experimental evidence is now beginning to confirm that some of the specific proteins targeted by autoantibodies are shed into the general circulation (56; 64; 77; 80; 106; 131), where they may be evaluated as biomarkers. It is likely, therefore, that the presence of these autoantigens in

9

blood precedes the appearance of their respective autoantibodies due to the time required to marshal a humoral immune response. Accordingly, we propose that the humoral immune response to brain injury will reveal novel, brain-specific proteins as early biomarkers for TBI.
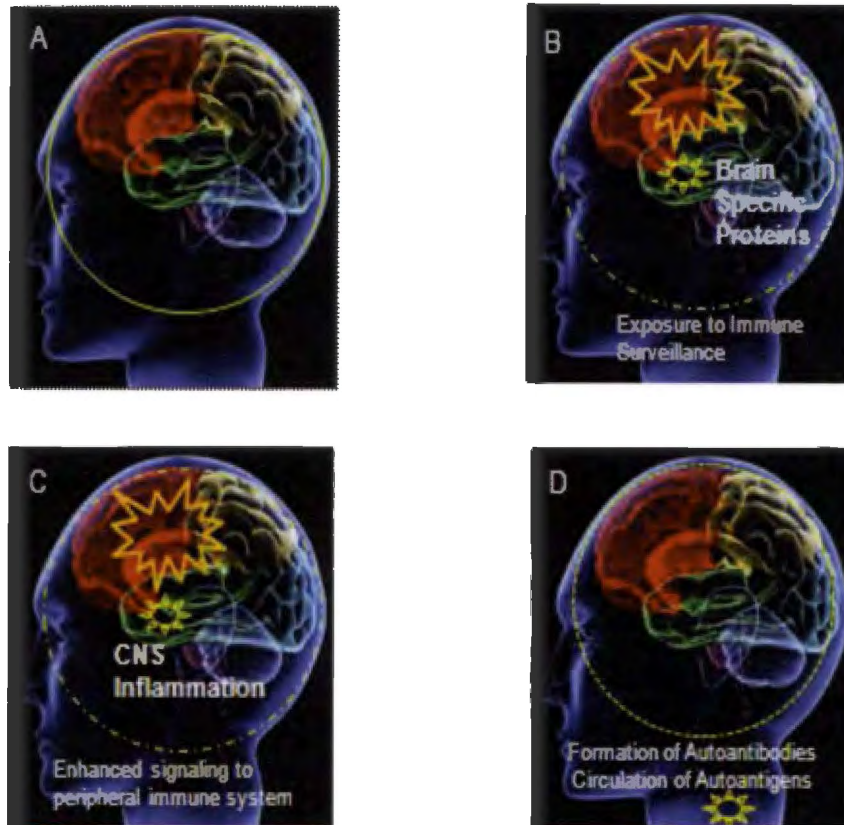
Figure 1. Mechanisms for the autoimmune response to brain injury. Panels A-D present proposed mechanisms that underlie the expression of brain-specific autoantibodies in response to TBI. These mechanisms involve direct immune surveillance of novel brain proteins that become accessible when the blood brain barrier is disrupted (panels A and B) and reversal of peripheral immune tolerance in response to enhanced immune signaling due to the inflammatory state of the brain following injury (panel C). Both processes can result in the expression of brain-specific autoantibodies in response to TBI (panel D) (Figure adapted from ryanspringer.com).

The concept that brain-specific autoantibodies contribute to the negative long-term consequences of TBI gained recognition in 1974, with the proposal by Berry and Riches that the immune system plays an important role in the failure of axonal regeneration in the mammalian central nervous system (CNS) (10). This proposal was based upon a body of evidence that the brain harbors "sequestered antigens" or "encephalitogenic factors" that, once exposed by injury, are targeted for deleterious actions by the autoimmune system (10). Regarding the proposal that autoantibodies impair neuronal repair mechanisms, most recent attention has focused on spinal cord injury where B cell-mediated responses were shown to interfere with neuronal recovery (4; 27; 107). These findings have led to the hypothesis that immune-based therapies may have a place in treating injuries of the CNS, particularly in conjunction with stem cell repair (38; 46; 66; 123). It should be emphasized, however, that the overall immune response to CNS injury is highly complex and involves well-documented, beneficial T-cell responses (15; 44; 99; 108; 143). Accordingly, therapeutic modulation of the immune responses for TBI will require a sophisticated understanding of the processes involved.

There is a recent precedent for head trauma eliciting an autoimmune response. Marchi and coworkers reported that in collegiate football players, repeated subconcussive hits to the head resulted in the formation of autoantibodies against S100b (69). Additionally, serum titers of anti-S100b antibodies were proportional to the number and severity of the hits experienced. The authors speculate that the autoimmune response was due to repetitive disruption of the blood-brain barrier and subsequent immune activation. This is the first report in humans of a CNS autoimmune response resulting from head

trauma. Importantly, the response occurred in the absence of any positive findings with current clinical assessment tools.

RELATION OF DISSERTATION RESEARCH TO TBI FIELD

An important challenge facing discovery efforts for novel TBI biomarker proteins is the need for a discovery approach that does not rely upon an *a priori* search paradigm. This dissertation project was designed to meet this challenge. The research presented here has added to the field of TBI biomarkers with two major outcomes. First, it was demonstrated that novel biomarkers for TBI can be discovered by autoimmune profiling. Importantly, the candidate biomarkers discovered by this approach are generally unique and have not been detected by conventional strategies for TBI biomarker discovery. The second major outcome from this dissertation project is the demonstration that a profile of biomarker responses can be used to formulate a diagnostic score that is sensitive for the detection of mild TBI.

Finally, an additional important outcome of this research is the identification of specific TBI-induced autoantibodies. The presence of these molecules introduces new mechanisms through which the immune system may contribute to the long-term negative consequences of TBI. The concept of centrally directed autoantibodies mediating long-term neuropathology is not without precedent, especially in the case of multiple sclerosis (MS) where autoimmune mechanisms are a well-recognized underpinning for the neuropathology of the disease (60). It is proposed here that, similar to MS, autoantibodies generated in response to TBI may contribute to the long-term comorbidities associated with brain injury including seizures, epilepsy, chronic traumatic encephalopathy and post-traumatic stress disorder.

12

CHAPTER 3: METHODOLOGIES

REAGENTS

All reagents were obtained from Sigma-Aldrich (St. Louis, MO) unless otherwise specified.

ANIMAL MODEL

All housing, surgical, pre and postoperative care procedures were performed in accordance with the Uniformed Services University of the Health Sciences (USUHS) Institutional Animal Care and Use Committee. Adult male and female Sprague Dawley rats, Charles River (Raleigh, NC), 8-9 weeks of age, were used in all experiments. Animals arrived at the USUHS Laboratory Animal Medicine (LAM) facility weighing between 226-250 grams (approximately 53-56 days of age) for the males and 176-200 grams (approximately 51-56 days of age) for the females; they were double housed in standard clear plastic shoebox containers (46 cm x 25 cm x 20 cm) containing Harlan Teklad Laboratory Aspen Bedding #7093 (Madison, WI). All animals were housed as a cohort in a single room, with room temperature and humidity maintained at 22°C ± 4° and 30-70%, respectively. Standard rat chow Teklad Global, 18% Protein Rodent Diet, Harlan Laboratories #2018 (Madison, WI) and fresh tap water were provided *ad libitum.* Full spectrum light was cycled for 12 hours on beginning at 0600. Animals were allowed to acclimate to the LAM environment for 3-4 days prior to experimentation. Rats were individually housed postoperatively in clean cages containing a plastic/polyvinyl chloride tunnel as an environmental enrichment (95).

RODENT BLOOD COLLECTION AND SERUM PREPARATION

Whole blood was collected from the animals by two methods: retro-orbital plexus bleeding performed under general anesthesia or trunk blood collection at the time of euthanasia.

Retro-Orbital Plexus Bleeding

Animals received approximately 1 - 2 minutes of a mixture of 100% medical grade oxygen and 4% 2-chloro-2-(difluoromethoxy)-1,1,1-trifluoro-ethane (isoflurane) (Abbott, North Chicago, IL) administered in a rodent anesthesia induction chamber. Following unconsciousness, a heparinized capillary tube was inserted into the medial canthus of the eye under the nictitating membrane at approximately a 30° angle to the nose. The tube was directed in a ventrolateral direction while rotating, rolling it between the thumb and forefinger of the dominant hand. The rat was positioned in such a way that the end of the capillary tube in the medial canthus was higher than the end that dripped into the glass collection tube. The average amount of serum collected utilizing this technique was 600 µL regardless of gender.

Trunk Blood Collection

The rats were rendered unconscious by low flow compressed gas CO_2 narcosis administered in a clear clamshell delivery device. The gas flow rate was sufficient to fill 20% of the chamber volume per minute. Following loss of consciousness and lack of response to a tail pinch, the rats were decapitated using a rodent guillotine and trunk blood was collected.

Whole blood was processed in the same manner regardless of the collection technique. Following collection, blood samples were allowed to clot at room temperature for 30 to 45 minutes and then the samples were transferred to a 4°C refrigerator for 2 hours. Prior to centrifugation the clot was ringed from the side of the container. A Sorvall RT6000B Refrigerated Centrifuge, Dupont (Wilmington, DE) was cooled to 4°C and the blood samples were centrifuged for 10 minutes at 3600 rpm (2500 x g). The resulting sera were transferred to new storage vials. The clots were removed from the collection tubes and the remaining fluids were centrifuged a second time using the same parameters. The resulting sera were combined with those from the first spin and the samples were stored at -80°C until analyzed. The average amount of serum collected from male and female rats utilizing this technique was 4 mLs and 5.6 mLs, respectively.

TRAUMATIC BRAIN INJURY BY MEANS OF CONTROLLED CORTICAL IMPACT

Following acclimation to the USUHS rodent housing quarters, rats were weighed and anesthetized with 4% 2-chloro-2-(difluoromethoxy)-1,1,1-trifluoro-ethane (isoflurane) (Baxter Healthcare Corporation, Deerfield, IL) vaporized in medical grade oxygen (100%, Roberts Oxygen Company Inc, Rockville, MD). The crown of the head was shaved and surgically prepped (povidone-iodine scrub, Purdue Products, Stanford CT and 70% alcohol, Sigma Aldrich, St. Louis, MO). Animals were then placed in a digital cranial stereotactic device (Leica Microsystem, Buffalo Grove, IL) utilizing non-penetrating ear bars. Anesthesia was maintained by nose cone administration of 2-3% isoflurane. Ophthalmic ointment (CVS Pharmacy, Rockville, MD) was placed on the corneas to prevent drying. Body temperature was maintained by a thermocouple probe (inserted 5 cm rectally) connected to a feedback warming blanket, which maintained the

15

rat's core temperature at 37°C ± 3°C. Prior to incision, 5 mLs of lactated ringers (Baxter, Deerfield, IL) was injected subcutaneously in the region of the withers followed by 0.03 to 0.05 mg/kg of buprenorphine (Roxane Laboratories, Columbus, OH) subcutaneously approximately 3 cm from previous injection. A midline scalp incision was made over the cranium and the fascia was reflected. A free hand craniotomy was performed at -3.8 mm from bregma in males and -3.0 mm from bregma in females. A 3x5 mm bone flap was removed and discarded. Care was taken to not damage the sagittal sinus or disrupt the dura mater. A 3 mm flat tip impactor was then slowly lowered to the surface of the dura. A low-voltage detector along with visual inspection was used to confirm when the tip contacted the dura mater. Once the tip was correctly positioned, a TBI was administered by means of a controlled cortical impact device (CCI) (Impact One™ Stereotaxic Impactor; Leica, Buffalo Grove, IL) controlling the impactor. The TBI consisted of the delivery of a 3 mm impactor at a 20 degree angle to a depth of 2 mm at 5 m/sec with a dwell time of 500 ms. Following injury a piece of Gelfoam® (purified pork Skin Gelatin USP Pfizer, New York, NY) was placed over the injury site to treat any uncontrolled bleeding. The Gelfoam was removed and the craniotomy covered with a thin layer of bone wax (Medline, Mundelein, IL). The scalp incision was closed with the 9 mm AutoClip® wound closure system (Alzet, Cupertino, CA). The rats were then transferred to pre-warmed clean cages where they emerged from anesthesia. Control rats received similar handling, but no anesthesia, incision or craniotomy. All animals were provided water and food *ad libitum* immediately post-operatively. Anesthesia, surgical and emergence times were all recorded as well as any unique intra or postoperative events.

1-Dimensional (1-D) Gel Electrophoresis and Immunoblotting

Rat brain cytosol and membrane homogenates were prepared as described in section; 2-D gel electrophoresis. Both homogenates were prepared as master mixes containing final protein concentrations of 25 µg/10 µL or 10 µg/4 µL using a 3X reducing loading buffer (1.25 M dithiothreitol (DTT), 6% (w/v) MOPS [3-(N-morpholino)propanesulfonic acid] SDS [sodium dodecyl sulfate] (Life Technologies, Grand Island, NY), 30% glycerol, 0.03% (w/v) bromophenol blue and 187.5 mM Tris-HCl [tris(hydroxymethyl)aminomethane-HCl] with a pH 6.8 at 25°C). The 25 µg master mix consisted of 400 µL of brain extract with 200 µL of 3X loading buffer, while the 10 µg master mix consisted of 200 µL of brain extract with 250 µL of loading buffer and 300 µL of distilled water. Samples were heated to 70°C for 10 min and then loaded into the wells of 10% Bis Tris gels (1.5 mm, 15 well, NuPAGE®, Life Technologies, Grand Island, NY). Samples were loaded at 25 µg and 10 µg for both brain cytosol and membrane samples. Novex® Sharp Pre-stained Protein Standard (10 µL/lane, Life Technologies, Grand Island, NY) was used for estimating molecular weights. Gels were placed in a NovexTM 1-D apparatus (Novel Experimental Technology, San Diego, CA) containing a stir bar and freshly prepared 1X NuPAGE MOPS SDS running buffer (50 mM MOPS, 50 mM Tris base, 0.1% SDS, 1 mM ethylenediaminetetraacetic acid (EDTA), pH 7.7) (Life Technologies, Grand Island, NY). The entire apparatus was then placed in a bucket filled with crushed iced water and positioned on top of a platform stirrer set at a medium stir rate. Proteins were fractionated with a limiting potential of 200 volts. Upon completion of the run, gels were removed from their cassettes, briefly immersed in distilled water and then transferred to polyvinylidene fluoride (PVDF) or

nitrocellulose membranes (iBlot® Gel Transfer Apparatus and Transfer Stacks; Invitrogen, Grand Island, NY). Following transfer, membranes were blocked with 5% fetal bovine serum (FBS) in Tris-buffered saline and Tween 20 (50 mM Tris, 150 mM NaCl, 0.05% Tween 20, pH adjusted to 7.6 with HCL) (TBST) for 60 min at room temperature and then probed overnight at 4°C using a 1:250 final dilution of control or CCI serum in 5% FBS/ TBST. The next day blots were washed 3X with TBST and probed with an anti-rat IgG-horseradish peroxidase (HRP) antibody conjugate (1:5000 in TBST; R&D, Minneapolis, MN) for 2 hours at room temperature. Next, the blots were washed extensively at room temperature for at least 3 hours with multiple changes of TBST. Finally, the blots were visualized using the Enhanced Chemiluminescent Substrate reagent Kit (Novex® ECL – HRP) (Invitrogen, Invitrogen, Camarillo, CA) and imaged using a FUJI LAS 3000 charge-coupled device camera and Mutli Gauge v3.0 software (Stanford, CT). Immunoreactive signals that were unique to TBI blots were mapped to the corresponding protein features on Coomassie stained gels. The mapping procedures involved the combined use of simple transparency overlays and sophisticated image analyses using both Multi Gauge and Progenesis (Shimadzu Biotech, Columbia, MD) image analysis software suites. Proteins of interest were carefully excised and processed for identification by peptide mass fingerprint analysis.

PROTEIN IDENTIFICATION BY PEPTIDE MASS FINGERPRINTING

Silver stained gel fragments were excised and destained with 100 μL of a 1:1 mixture of 30 mM potassium ferricyanide and 100 mM sodium thiosulfate then rinsed with distilled water until the gel appeared clear. Gel fragments were then equilibrated with 0.2 ml of 100 mM NH_4HCO_3/50% acetonitrile for 45 minutes at 37°C followed by

dehydration in 100 μL 100% acetonitrile using a Freeze Mobile G® speed vacuum (Virtis Company, Gardner, NY). The dried gel pieces were re-hydrated to saturation with 40 mM NH_4HCO_3/10% acetonitrile containing 20 ng/μL trypsin (Trypsin Gold, Mass Spec Grade, Promega, Madison, WI) and incubated overnight at 37°C.

Peptide fragments were recovered by first adding 75 μL 1.0% trifluoroacetic acid (TFA) and incubating for 1 hour at room temperature. The first wash/recovery solution was removed and saved. A second and third wash consisting of 50 μL of 50% acetonitrile/5% TFA were carried out similarly and pooled with the first. The combined recovery solution was dried under vacuum, dissolved in 10 μL of 1% TFA and peptides were then purified and concentrated using a C18 Zip Tip® (protocol per Millipore Corporation, Billerica, MA). Purified tryptic digests were mixed with alpha-cyanohydroxycinnamic acid matrix (10 mg/mL in 50% acetonitrile/0.1% TFA) and analyzed by matrix-assisted laser desorption ionization time-of-flight (MALDI-TOF) mass spectrometry using a Voyager MALDI-TOF DE STR instrument (PE Biosystems, Framingham, MA). The mass spectrometer was operated in reflectron mode with an accelerating voltage of 20,000 V, a grid voltage of 76.13% and a guidewire voltage of 0.003%. The instrument was calibrated using the protonated monoisotopic masses of bradykinin (1060.5692 daltons) and adrenocorticotropic hormone fragment 18-39 (2465.1989 daltons) (AnaSpec, San Jose, Ca) which were incorporated in the matrix as internal standards in amounts corresponding to 50 fmol and 150 fmol, respectively. The peptide mass spectra data was used to query the National Center for Biotechnology Information protein sequence database accessed through the ProteinProspector MS-Fit search engine (http://prospector.ucsf.edu/).

MS-FIT (MASS SPECTROMETRY BEST FITS)

Peptide masses obtained from the MALDI-TOF were uploaded to the database search program Protein Prospector v 5.9.4 operated out of the University of California, San Francisco. This software is specifically designed for searching sequence databases in conjunction with mass spectrometry experiments. For the search engine to determine a MOWSE (molecular weight search) score the following parameters were used: Database – SwissProt current version, taxonomy – Rattus Norvegicus, protein MW 1000-125,000, protein PI (set according to gel – i.e., if gel 4-7, set point was 3-9), maximum reported hits = 10, minimum # peptides required to match = 4, masses are = monoisotopic, Total ppm = 35, contaminant masses, included standards added = 1060 and 2465, Digest = trypsin, maximum missed cleavages = 1, constant mods and possible modifications were not set. The MOWSE score is a similarity score, using a statistical algorithm to determine the probability that the submitted peptide peaks obtained by MALDI-TOF analysis have come from a specific protein based upon the *in silico* tryptic map for that protein (5).

PREPARATION OF BRAIN PROTEINS FOR IMMUNOPROFILING

Adult male Sprague Dawley rats were anesthetized by intraperitoneal injection of 10% chloral hydrate solution (0.4 mL/100 gm). Following complete loss of responsiveness to a noxious stimulus, the rats were decapitated and the brains rapidly removed. The brains were quick frozen with finely powdered dry ice and stored at -80°C until used. Brain cytosol and membrane protein fractions were prepared as follows. Whole brain tissue was weighed, minced, and homogenized in 8 volumes/weight extraction buffer (0.25 M sucrose, 20 mM *N*-tris[hydroxymethyl]-methyl-2-

aminoethanesulfonic acid (TES), 1 mM ethylenediaminetetraacetic (EDTA), 0.6 M

potassium chloride (KCL), pH 7.0 and 1X Complete® protease inhibitor mix (Roche,

Indianapolis, IN) using a Polytron tissue homogenizer (setting 6-7; 15-20 seconds). The

resulting tissue homogenates were then subjected to Potter-Elvehjem glass/teflon

homogenization for five down/up strokes followed by slow speed centrifugation (4,900 x

g; 4°C; 15 min) to remove cellular debris. The supernatant was then centrifuged at high

speed (100,000 x g, 4°C, and 1 hour) to prepare cytosol and membrane fractions. The

resulting supernatant (cytosol) was removed, assayed for total protein using a

bicinchoninic acid protein assay (BCA) (112), aliquoted and stored at -80°C until used.

The pellet (membrane fraction) was re-suspended by sonication in 20 mM

Tris(hydroxymethyl)aminomethane, pH 8.0 extraction buffer (1 mL per gram of starting

weight), assayed for total protein, aliquoted and stored at -80°C until used.

Samples of brain cytosol or membrane were delipidated by Folch extraction prior

to first dimension electrophoresis. Folch extraction was carried out by mixing 1 part

protein sample with 5 parts chloroform/methanol (2:1) followed by centrifugation (3000

x g, 5 min, room temp) (35). Delipidated proteins were physically recovered as a pad

positioned at the aqueous/organic interface; protein recovery was typically 95-99%

through the extraction procedure (N=6). Extracted proteins were dissolved in isoelectric

focusing rehydration buffer consisting of 1% dithiothreitol, 2% pH 3-10 pharmalytes (GE

Healthcare Life Sciences, Pittsburgh, PA), a trace of Bromophenol blue, 2M thiourea, 6M

urea, and 1% 3-[(3-cholamidopropyl) dimethylammonio]-1-propanesulfonate (CHAPS)

at a concentration of 1 mg/450 μL.

2-Dimensional (2-D) Gel Electrophoresis

2-dimensional gel electrophoresis was performed according to the methods originally developed by O'Farrell (1975) with minor modifications as described by Jacobowitz and coworkers (53; 85). Samples of brain cytosol or membrane-bound proteins were pipetted into ceramic strip holders (450 uL, 1 mg total protein) and equilibrated with an isoelectric focusing Dry Strip® (24 centimeter, pH 3-10, GE Healthcare Bio-Sciences, Uppsala, Sweden). Mineral oil was applied as a cover fluid to prevent drying of the strip during the first dimension isoelectric point separation. The ceramic trays were placed in the first dimension electrophoresis apparatus (Amersham Ettan IPGphor, GE Healthcare Bio-Sciences, Uppsala Sweden) and subjected to a standard 22 hour isoelectric focusing protocol at 16°C (30 volts for 12 hours, 500 volts for 1 hour, 1000 volts for 1 hour and 8000 volts for 8 hours).

Upon completion of the first dimension, strips were removed from the ceramic trays, blotted on paper, and sequentially treated to reduce and alkylate the fractionated proteins. For reduction, the strips were equilibrated in 1% dithiothreitol (DTT), 6 M urea, 75 mM Tris-HCL, 29.3% (v/v) glycerol, 2% (v/v) sodium dodecyl sulfate (SDS) and 1% Bromophenol Blue (15 min). This was followed by the alkylation step where the strips were incubated in a solution consisting of 2.5% iodoacetemide, 6 M urea, 75 mM Tris-HCL, 29.3% (v/v) glycerol, 2% (v/v) SDS, and 1% Bromophenol Blue (15 min). The DTT served to reduce cysteine disulphide bonds and iodoacetemide, a sulfhydryl-reactive alkylating reagent, capped the reduced cysteine residues. Following reduction and alkylation, the gel strips were positioned on a second dimension gel and the union sealed with agarose. Second dimension fractionations were performed on 255 x 196 x 1

mm Dalt Gels 12.5 (GE Healthcare Bio-Sciences, Uppsala Sweden) over 3 hours. The composition of the second dimension anode and cathode buffers were as follows: anode buffer (5 M diethanolamine, 5 M glacial acetic acid); cathode buffer (1% SDS, 1.92 M glycine, 0.25 M Tris). The second dimension fractionation was carried out with the following settings for one gel: step 1: 30 minutes at 2.5 watts followed by step 2: 5 hours at 30 watts.

Upon completion of the second dimension, fractionated proteins were transferred to Amersham Hybond-P PVDF Membranes (GE Healthcare, Buckinghamshire, UK). The PVDF membranes were wetted in 100% methanol and then equilibrated in transfer buffer 10% methanol/3-(N-morpholino) propanesulfonic acid, (MOPS) buffer system (40 mM MOPS, 10 mM sodium acetate (NaAc), 1 mM EDTA pH 7.7) (Nupage® Invitrogen). Transfer stacks were assembled from the bottom up with several sheets of hydrated filter paper, PVDF membrane, 2-D gel, and additional sheets of hydrated filter paper. Immuno transfer was accomplished using a Pharmacia Multiphor II electrophoresis unit operated at 600 volts/cm^2, 400 mA (limiting) for 90 minutes.

SILVER STAINING OF 2-D GELS FOLLOWING ELECTROPHORESIS

One or two gels per run were visualized by silver staining. These gels served as the replicate protein gels to which autoimmune features were mapped for subsequent proteomic identification. The standard, per gel, protocol for this procedure was to: (1) fix in 200 mL ethanol, 50 mL glacial acetic acid, 250 mL water over night; (2) sensitize in 75 mL ethanol, 10 mL 5% sodium thiosulfate, 17 g sodium acetate, 165 mL water (30 min); (3) wash five times with water (8 min per wash); (4) stain with a solution of 0.625 g silver nitrate in 250 ml water (20 min); (5) wash four times with water (1 min per

23

wash); (6) develop with 6.25 g sodium carbonate, 0.1 mL 37% formaldehyde, 250 mL water to a desired degree of spot resolution; and (7) stop the silver reaction with 3.65 g EDTA in 250 mL water. After 30 minutes, the stop solution was removed and the gel was placed in water.

IMMUNOPROFILING

Following transfer, PVDF immunoblots were blocked with 5% FBS (Gibco, Grand Island, NY) in TBST for 60 minutes at room temperature. The immunoblots were then probed overnight at 4°C using a 1:250 final dilution of control or CCI rat serum in 5% FBS/TBST. The following day, immunoblots were washed 3 times for 20 minutes each with TBST. Horseradish peroxidase labeled anti-rat IgG secondary antibody (HAF005, Lot# XGO0210021, R&D, Minneapolis, MN), diluted 1:5,000 in TBST, was applied for 2 hours at room temperature. The immunoblots were then extensively washed over several hours with multiple changes of TBST and visualized by Novex ECL – HRP using a FUJI LAS 3000 imager and Multi Gauge V3.0 software. Immunoreactive signals that were unique to CCI immunoblots, as compared to control, were mapped to the corresponding protein features on silver-stained gels. Criteria for the selection of an immunoreactive signal of interest were as follows; a dramatic appearance or increase in signal as a consequence of TBI and the repeated identification of the feature with different pools of CCI serum (N= 2 to 6). Proteins of interest were excised and processed for proteomic identification.

IMMUNOSORBENT ELECTROCHEMILUMINESCENT ASSAYS (IEA)

Singleplex IEA

Immunosorbent electrochemiluminescence assays (IEA) were built to validate proteins of interest discovered through immunoprofiling. These IEAs were used to measure levels of protein candidates in serum or plasma using electrochemiluminescence detection technology developed by Meso Scale Discovery (MSD®, Gaithersburg, MD). MSD incorporates a proprietary SULFO-TAG® in their electrochemiluminescence detection platform. The SULFO-TAG emits light when the assay complex is electrochemically activated and this technique allows for greatly enhanced sensitivity with low background and wide dynamic range as compared to conventional ELISA detection systems.

Singleplex sandwich IEAs were constructed on MSD MULTI-ARRAY™ 96-well plates as follows. A carrier-free monoclonal antibody specific to the biomarker candidate of interest was applied to the bottom surface of the MULTI-ARRAY 96-well plate. This "capture" antibody was diluted in 0.22 µm filtered PBS to a concentration of 2 µg/mL and plated in a volume of 25 µL/well. Following brief mixing (5 min; 800 RPM), the capture antibody was incubated anywhere from 1 hour at room temperature to overnight at 4°C, with longer times resulting in slightly greater degrees of coating (capture). When an overnight incubation was used, plates were allowed to equilibrate to room temperature prior to the proceeding steps. Many of the capture antibodies tested were commercially prepared in a solution containing bovine serum albumin (BSA) or gelatin carrier and/or glycerol. In these cases, the antibody was purified by protein G affinity chromatography (Protein G HP SpinTrap, GE Healthcare, Uppsala, Sweden, utilizing the vendor's

protocol) prior to plating. After the incubation period, the capture antibody solution was discarded and plates were blocked with 3% BSA or 5% FBS (Gibco, Grand Island, NY) diluted in 0.22 μm filtered PBS. The time for blocking ranged from 1 to 2 hours after which the wells were washed 3 times with TBST, 150 μL/well.

The next step involved the addition of varying amounts of standard protein to the wells to create standard curves, and serum or plasma samples to the wells for biomarker quantitation. Control serum or plasma samples were obtained from untreated rats or normal human subjects (20-30 y/o, males and females, purchased from Innovative Research, Novi, MI). Standard curves were constructed using commercially available purified recombinant proteins. The specificities of these assays were confirmed by immune blot analyses showing that the capture and primary antibodies were specific for recognizing single bands of appropriate molecular weight in the brain homogenates. Plasma samples were diluted to 25% in 1% BSA/PBS and assayed at 100 uL/well. Standard proteins were plated in 2- or 3-fold serial dilutions in concentrations ranging from 100 ng/mL to 0 ng/mL. Incubation times were typically 1 – 2 hours after which plates were washed 3 times with TBST, 150 μL/well.

Primary antibodies were usually polyclonal antibodies developed in rabbits against the proteins of interest. In a few instances anti-protein mouse or rabbit monoclonal antibodies were used effectively. When creating a monoclonal – monoclonal IEA using antibodies from the same species it was imperative that the primary antibody was directly SULFO-TAGged, thereby avoiding the need for an anti-species detection antibody that would cross react with the capture antibody. Primary antibodies were diluted in either 1% BSA or 1% FBS, depending on the block used, to a concentration of

2 µg/mL and plated at 25 µL/well. The incubation time was typically 1 hour after which plates were washed 3 times with TBST, 150 µL/well.

As noted above, IEA detection is by way of ruthenium (II) tris-bipyridine-(4-methylsulfone) [Ru(bpy)3] -based (SULFO-TAG) light emission that occurs when a voltage potential is applied to the base of the IEA plate. Electrochemiluminescence is only activated by SULFO-TAG reagent located within close proximity of the plate surface. Accordingly, only antibody bound SULFO-TAG reagent is detected. This geometry results in a greatly reduced background as compared to conventional ELISA assays. The inherent sensitivity of light detection technology accounts for the enhanced sensitivity IEAs which are characteristically at least 10-fold more sensitive than the colorimetric detection method of standard ELISAs. The SULFO-TAG detection reagent can be incorporated as a conjugate to the primary antibody, or as a conjugated anti-species IgG directed against the primary antibody. Both approaches were used here.

SULFO-TAG primary antibody was prepared using proprietary reagent and a standard protocol provided by the vendor (MSD). This involved simply mixing the SULFO-TAG reagent with purified IgG (1000x [protein concentration (mg/mL) divided by protein MW] x 13X volume of protein solution (µL)) and allowing the two to react for 2 hours (in darkness) after which unconjugated SULFO-TAG reagent was removed by size filtration chromatography using a Zeba™ Spin desalting column (Thermo Scientific, Rockford IL). Alternatively, SULFO-TAG labeled anti-species IgGs (purchased from MSD) were diluted 1:500 in either 1% BSA or 1% FBS, depending on the block used and plated at 25 µL/well. Following a 1 hour incubation, plates were washed 3 times with TBST, 150 µL/well. Plates were then treated with MSD Read Buffer with Surfactant

(MSD, Gaithersburg, MD) (150 µL/well) and immediately read using a SECTOR Imager

6000 instrument (MSD). The Imager 6000 uses an ultra-low noise, charge-coupled device

(CCD) camera with custom-designed telecentric lenses for rapid multiplex detection

(MULTI-ARRAY or MULTI-SPOT® plates; MSD).
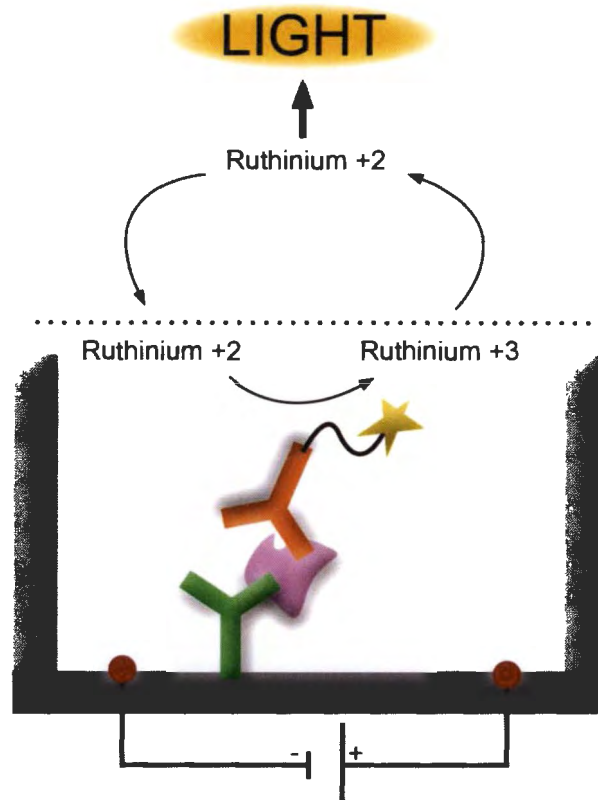
Figure 2. Functional design of a singleplex immunosorbent electrochemiluminescence
assay (IEA). The assay platform consists of a conventional sandwich
immunosorbent assay fabricated onto a proprietary microtiter plate especially
designed for the application of a voltage potential across the bottom of each
well (Meso Scale Diagnostics). The primary, or detection antibody, is labeled
with a ruthenium compound that generates light in response to the voltage
potential. The light generated is directly proportional to the amount of primary
antibody bound, which in turn is a direct measure of the amount of analyte
protein immobilized by the capture antibody. This technology offers the
specificity of independent recognition by two different antibodies that recognize
unique epitopes on the same protein analyte, and the sensitivity, wide dynamic
range and low background achieved with electrochemiluminescence detection.

28

Multiplex IEA

In some cases, singleplex IEAs were assembled in a multiplex format by printing capture antibodies at addressable locations on the base surface of each well. This was accomplished using the proprietary printing service and special multiplex plates (MULTI-SPOT plates) provided by MSD. All subsequent steps were carried out using cocktails of standards and SULFO-TAG labeled primary antibodies at concentrations optimized through the development of singleplex assays. Similarly, washing, blocking and reading steps followed procedures optimized in singleplex.
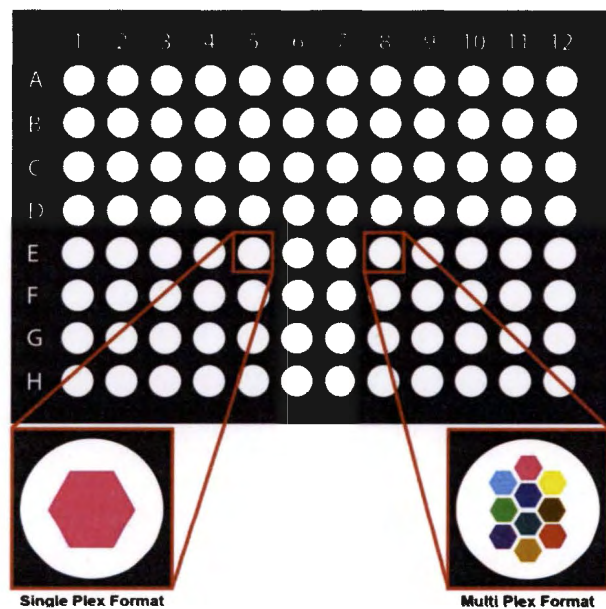
Figure 3. Schematic diagram for the multiplex platform used to simultaneously analyze multiple biomarkers in a single plasma sample.

An important part of the IEA development was the discovery of the best conditions that minimized the effects of sample matrix on the performance of the assay. Matrix effects are the sum of all of the interferences from all the components in a sample

29

that influence the measurement of the target analyte. The source of a matrix effect can arise from the sample's composition, diluents, buffers, antibodies and detection labels. Each IEA developed here was optimized to ascertain the best possible operating conditions. For example, as discussed above, either BSA or FBS was incorporated into the assay buffer to limit the nonspecific effects of serum or plasma matrix. Other approaches employed included: varying times of incubation, use of 4°C vs. room temperature and the inclusion of off-species plasma or serum in the standard curves (e.g., chicken, donkey, and horse). This approach was based upon the determination that the off-species sample exhibited the same matrix effects as the target sample but, due to species specificity, did not contain an immunoreactive form of the protein of interest. These properties were established by evaluating the effects of the matrix material over a wide range of doses in the IEA.

REAGENTS SPECIFIC TO THE IEA(S) DEVELOPED AS PART OF THIS PROJECT
Peroxiredoxin 6:

Combinations of 7 monoclonal and 5 polyclonal anti-PRDX6 antibodies were screened for compatible pairs. A mouse anti-PRDX6 monoclonal antibody (Clone 1A11, GenWay Biotech, catalog #20-007-280008, San Diego, California) and a rabbit monoclonal anti-PRDX6 antibody (Clone EPR3755, Epitomics, catalog # 2769-1, Burlingame, California) were selected for optimization as capture and primary antibodies, respectively. Standard curves were constructed using serial dilutions of PRDX6 recombinant human protein (GenWay Biotech, catalog #GWB-F65D50, San Diego, California). The monoclonal capture antibody was first purified by protein G affinity chromatography (Protein G HP SpinTrap, GE Healthcare, Uppsala, Sweden, vendors

protocol), to remove glycerol. Standard curves were prepared in PBS-1%BSA containing either 25% horse serum or 25% chicken plasma (both from Innovative Research) to control for the non-specific effects of serum or plasma matrix. Detection was carried out using goat anti-rabbit MSD SULFO-TAG antibody (MSD, R32AB-1). The assay is quantitative to 1 ng/mL (lower limit of quantitation, LOQ) and can detect 0.7 ng/mL (lower limit of detection; LOD) as defined by three and ten times the standard deviation of readings obtained for 0 pg/mL standard, respectively (n=10). Intra- and inter-assay variability were 4% and 13%, respectively (n=10).

Creatine Kinase BB:

Combinations of 5 monoclonal and 5 polyclonal anti-PRDX6 antibodies were screened for compatible pairs. A mouse anti-creatine kinase MB antibody (Clone CK1, Abcam, catalog #ab404, Cambridge, Massachusetts) and a rabbit polyclonal anti-creatine kinase B type antibody (Abcam, catalog #ab36082, Cambridge, Massachusetts) were selected for optimization as capture and primary antibodies, respectively. Standard curves were constructed using serial dilutions of CKBBI recombinant human protein (GenWay Biotech, catalog #GWB-BS271B, San Diego, California). Standard curves were prepared in PBS-1%FBS containing 25% horse serum (Innovative Research) to control for the non-specific effects of serum matrix. Detection was carried out using goat anti-rabbit MSD SULFO-TAG antibody (MSD, R32AB-1). The assay is quantitative to 4 ng/mL (lower limit of quantitation, LOQ) and can detect 3 ng/mL (lower limit of detection; LOD) as defined by three and ten times the standard deviation of readings obtained for 0 pg/mL standard, respectively).

Cyclin Dependent Kinase 5:

Combinations of 4 monoclonal and 4 polyclonal anti-CDK5 antibodies were screened for compatible pairs, and a mouse anti-CDK5 monoclonal antibody (Clone 2G2, Abcam, catalog #ab28441, Cambridge, Massachusetts) and a rabbit monoclonal anti-CDK5 antibody (Abcam, catalog #ab21249, Cambridge, Massachusetts) were selected for optimization as capture and primary antibodies, respectively. Standard curves were constructed using serial dilutions of CDK5 recombinant human protein (Abcam, catalog #ab56282, Cambridge, Massachusetts). The monoclonal capture antibody was first purified by protein G affinity chromatography (Protein G HP SpinTrap, GE Healthcare, Uppsala, Sweden, vendors protocol), to remove glycerol. Standard curves were prepared in PBS-1%BSA containing 25% horse plasma (Innovative Research) to control for the non-specific effects of plasma matrix. Detection was carried out using goat anti-rabbit MSD SULFO-TAG antibody (MSD, R32AB-1). The assay is quantitative to 7 ng/mL (lower limit of quantitation, LOQ) and can detect 2 ng/mL (lower limit of detection; LOD) as defined by three and ten times the standard deviation of readings obtained for 0 pg/mL standard, respectively.

TBI 6-Plex Multiplex Assay

This project involved the use of a multiplex assay platform developed in the lab for the analysis of 6 TBI biomarker proteins in human plasma. Because this platform has not been published, details for its development and performance are included here in Appendix I. It should be recognized that the development of this platform was not a part

of this project per se; however, its application was integral to the findings and conclusions presented here.

The candidates evaluated with this platform were brain derived neurotrophic factor (BDNF), S100 calcium binding protein B (S100b), neuron specific enolase (NSE), GFAP, monocyte chemotactic protein 1/chemokine (C-C motif) ligand 2 (MCP-1/CCL2) and intercellular adhesion molecule 5 (ICAM-5). These analytes were selected based upon their established role(s) as candidate TBI biomarkers (BDNF, S100b, NSE, GFAP), as an inflammatory signaling molecule (MCP-1/CCL2) and as a potential marker for the integrity of the intercellular adhesion apparatus of the brain (ICAM-5).

PROTEIN MICROARRAY FOR AUTOIMMUNE PROFILING IN HUMANS

Invitrogen (Branford, CT) protein microarrays have 3 major applications; the investigation of immune response biomarker profiling, protein-protein interactions and kinase substrate identification developed for the ProtoArray® protein microarray platform. The ProtoArray platform was used here for immune response biomarker profiling of human serum to identify the expression of autoantibodies directed against human proteins in response to TBI. Version 5 of the ProtoArray platform consists of more than 9000 full-length human proteins that represent all major signaling pathways, biologic regulatory mechanisms, and structural relations among proteins. Importantly, the array contains a majority of protein post-translational modifications, thus representing many of the conformations that occur naturally *in vivo*. The full-length human proteins are part of two proprietary collections: Invitrogen Ultimate™ ORF collection and the Gateway® kinase collection. Nucleotide sequences for clones were verified by full sequencing prior to being expressed as recombinant proteins in insect cells using a

33

baclovirus expression system manufactured by Invitrogen. N-terminal glutathione-s-transferase tagging of proteins enabled affinity purification of the expressed proteins. Expressed proteins were verified by confirmation of predicted molecular weight using sodium dodecyl sulfate polyacrylamide gel electrophoresis. Each protein concentration was determined prior to printing on the array. In order to calculate the amount of protein in each control spot, a dilution series of purified GST protein was run for each slide. The signal obtained was used to generate a standard curve that was used to calculate the amount of protein in each spot. The printed protein concentrations for the control proteins ranged from 0.5 - 250 ng/μL. Protein spots were printed in duplicate on 1 inch x 3 inch nitrocellulose-coated glass slides with a spot-to-spot spacing of 200 μm. The sensitivity of the level of detection of autoantibodies against autoantigens on the array has been reported at < 1 ng/μL of serum (2011; L. T. Corporation, Branford, CT, Invitrogen).

Ten sets of patient plasma samples were profiled to identify autoantibodies and thus, candidate protein biomarkers for TBI. Within-patient comparisons were made using samples collected within 24 hour of injury (baseline), before an immune response could be marshaled, and at 30 day post-injury, a time when full expression of an autoimmune response would be expected.

SUBJECTS AND SAMPLE PREPARATIONS

Serum samples were obtained from Dr. R. Diaz-Arrastia, a principal investigator directing the "The Citicoline Brain Injury Treatment (COBRIT)" trial. The COBRIT trial was a "two-arm, double-blind, placebo-controlled, phase III, multi-center clinical trial designed to determine the effects of citicoline on functional and cognitive outcome in patients with complicated mild, moderate, and severe TBI (144)." The samples were from

ten males between the ages of 27 and 58 with a mean age of 34.6. All patients submitted

for analysis by the ProtoArray® were in the placebo arm of the study and were admitted

to emergency rooms of their respective hospitals with a Glasgow Coma Scale of 3-15

with a mean score of 9. The mechanisms of injury ranged from (4) falls, (2) motorcycle

collisions, (3) motor vehicle accidents and (1) assault. Admission injury severity was

rated as severe in 5 patients and complicated mild in the remainder of the group. For the

purposes of the COBRIT trial, complicated mild was defined as a patient who was alert

and oriented on admission yet exhibited the following findings on an admission

computed tomography scan: a subarachnoid hemorrhage on at least 2 slices, a contusion

of at least 10 mm and a subdural or epidural hematoma of 5 mm. The thirty-day extended

Glasgow outcome scale ranged from 2 to 7 with an average of 5 for the group. Baseline

serum samples (time point 1) were obtained within 24 hours of injury and follow up

serum collection occurred thirty days post-injury (time point 2). The samples were stored

frozen until analyzed.

The Protoarray Microarray

The ProtoArray Microarray is a single use analytical tool that was processed as

follows. Samples were centrifuged at 12,000 x g for 30 seconds to remove any aggregates

and then diluted 1:500 with Invitrogen washing buffer (final concentration: 1X PBS,

0.1% Tween 20, and 1X Synthetic Block [proprietary] in deionized water). Once

removed from frozen storage, each microarray was immediately placed at 4°C to

equilibrate for 15 minutes prior to blocking. Invitrogen blocking buffer (Branford, CT)

consists of: 50 mM HEPES, pH 7.5, 200 mM NaCl, 0.08% Triton® X-100, 25% glycerol,

reduced glutathione, 1 X synthetic block in deionized water, and 1 mM DTT as final

concentrations. Before application to the array, the pH was adjusted to 7.5 with NaOH and DTT was added once the reagent was chilled to 4°C. The chilled microarrays were placed in a four chamber sealable tray and incubated with blocking buffer for 1 hour (5 mL at 4°C). Following one hour incubation the blocking buffer was removed and 5 mL of washing buffer was added to the arrays. The washing buffer was aspirated and the diluted samples (1:500) were applied to the each of the arrays (≤ 20 µL per sample equally ~ 5 mL per array). After 90 minute incubation the samples were aspirated off and the arrays were washed 5 times (5 minutes each) with 5 mL of washing buffer. The arrays were then reacted with a solution of Alexa Fluor® 647 goat anti-human IgG antibody (1 µg/mL, 5 mL) prepared in washing buffer. After 90 minutes of incubation (at 4°C) the detection antibody was aspirated from the incubation tray and the array was washed with repeated applications of 5 mL of washing buffer, 5 times for 5 minute each. All incubations were performed with gentle rotary mixing.

The arrays were then removed from the incubation tray, rinsed once in a large volume of deionized water and immediately centrifuged for 1 minute at 200 x g, to completely dry the reaction surface. Scanning of the array was carried out using a GenePix® Pro microarray scanning system and GenePix data acquisition software (Sunnyvale, CA). The scanner settings were as follows: Wavelength: 650 nm; PMT Gain: 600; Laser Power: 100%; Pixel Size: 10 µm; Lines to Average: 1.0; Focus Position: 0 µm. Data acquisition was obtained using Invitrogen's ProtoArray Human Protein Microarray v5.0 for Immune Response BioMarker Profiling (IRBP) software (2011; L. T. Corporation, Branford, CT, Invitrogen).

Data Analysis

A pairwise comparison was carried out between time point 1 (baseline) and time point 2 (30 days post-TBI). One negative and one positive control sample was also run in parallel to evaluate array performance. Additionally, each array contained several reagent controls printed at specific locations to guide the data acquisition software and confirm the performance of the detection system. The negative and positive control arrays were set up in an identical manner to the experimental arrays with the exception that the negative array was incubated with buffer containing no human serum prior to the application of the Alexa Fluor 647 goat anti-human IgG detection reagent. Proteins that exhibited significant non-specific background signal (Relative Florescent Units [RFU] > 10,000) were eliminated from the analysis. The positive control array was treated with human serum from a patient with a well-established autoimmune profile resulting from systemic lupus erythematous. This array positively identified the expected lupus autoantigens. Assay performance was also assessed by dynamic range. All of the arrays demonstrated uniformly low backgrounds and a maximum relative fluorescence (RFU $\geq$ 65,000) that surpassed minimum specifications with an overall working detection range of >2 logs.

Identification of Autoantibodies

Data generated by the protein microarrays were used to evaluate autoimmune signals in response to TBI. Proteins identified as candidate autoantigens met four criteria: a p-value less than 0.05, a RFU reading of greater than 500 for time point 1, an average signal used value of greater than 1000 RFUs for time point 2, a signal used value for the

negative control of less than 10,000 RFU, and a ratio of greater than 3 for the average

signal used value (average of time point 2 divided by the average signal used value for

time point 1). In other words, time point 2 samples had to demonstrate an increased

autoantibody signal at least three-fold to be considered significant. The analyses included

background subtraction and determinations of: Z-score, Z-factor, Chebyshev's Inequality

(CI-P value), replicate spot coefficient of variation, group characterization of individual

proteins across all samples and finally M-statistics.

The Z-score was calculated by subtracting signal used value from the mean signal

used value for all protein features on the array, divided by the standard deviation of the

all the protein features. Because the population mean and population standard deviation

are known for the entire array, not just a sample set, it was possible to use the Z-score for

statistical comparisons as opposed to a Student's t-statistic. The Z-factor is a measure of

statistical effect size. It was used in this analysis as a confidence factor; the signal used

was significantly different from the negative control and provided a means by which to

judge whether the response was large enough. CI-P value was used to minimize

assumptions about the negative control distribution. The mean and the standard deviation

from the observed signals in the negative control distribution were used to calculate the

probability that a signal used value came from the negative control distribution. Replicate

spot coefficient of variation was used to establish a cutoff for a signal difference whereby

poorly printed spots were eliminated from analysis. Seven specific group characterization

evaluations were performed on the data: the cutoff signal for determining a positive "hit",

the number of arrays in each group that had signals larger than the cutoff, estimated

prevalence of a marker in each group, the P-value for the most significant difference due

to M-statistics, and whether normalized signal values were used. Finally, the M-statistic

utilizes an algorithm that counts the number of assays in one group where a signal value

for a specific protein was larger than the largest observed signal value for this protein in

another group. This calculation is then carried out sequentially, second largest, third

largest, etc. The p-value was then calculated as a probability of having an M value greater

or equal to the M value of the other group. The analysis workflow and

processing/quantification of spot files were carried out using ProtoArray Prospector

software. The software performed all aspects of the measurements and statistical analysis.
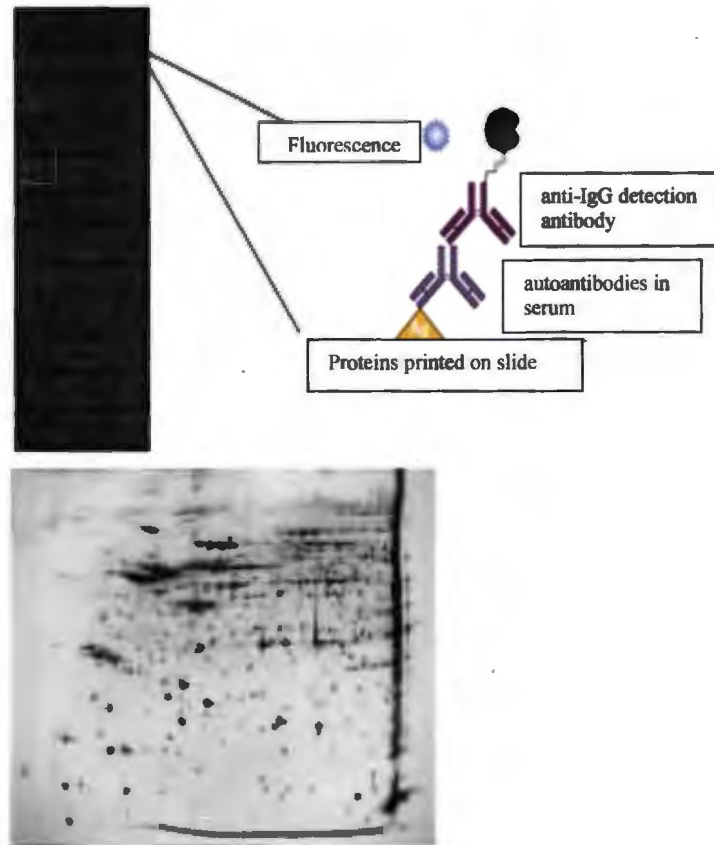
Figure 4. Protein microarray and global autoimmune profiling: complementary strategies for the discovery of novel biomarkers for TBI. The protein microarray (panel A) contains ~9470 human proteins expressed and printed under native conditions. The array was reacted with patient serum and bound autoantibodies were visualized fluorescently using an anti-human IgG labeled with Cy dye (blue star in schematic of panel A). Global autoimmune profiling identifies autoantibodies that recognize brain proteins fractionated by large-scale, 2-D gel electrophoresis and transferred to PVDF. Panel B presents an example of fractionated rat brain proteome visualized by silver staining. (Modified from original Invitrogen.com and piercenet.com)

HUMAN BRAIN AND BLOOD SAMPLE PREPARATION

Matched pairs of human serum and plasma (ethylenediaminetetraacetic acid (NaEDTA) anticoagulant) were prepared from single blood draws collected from healthy, adult Caucasian (76%) male and female volunteers (ages 19-50) (Innovative Research,

Novi, MI). Platelets were prepared from separate sets of control Caucasian (76%) male and female normal volunteers (ages 19-50) as follows. Platelet rich plasma (Innovative Research) was combined with equal volume of Tyrode's buffer (137 mM NaCl, 2.7 mM KCl, 1 mM MgCl$_2$, 1.8 mM CaCl$_2$, 0.2 mM Na^{2}HPO$_4$, 12 mM NaHCO$_3$ and 5.5 mM D-glucose) containing prostacyclin (100 ng/mL) and centrifuged at 1800 x g for 15 minutes at 15°C. The pelleted platelets were gently washed, resuspended in 30 mL of the Tyrode's buffer containing 1X protease inhibitor cocktail (cOmplete, EDTA-free protease inhibitor mix, Roche Applied Science, Indianapolis, IN) and assessed microscopically for purity (> 99% routinely) and appearance (spherical with little or no sign of activation). Platelet proteins were prepared by repeated freeze/thawing and sonication 3X. The extracts were then centrifuged at 14,000 x g for 10 minutes at 4°C, supernatants collected and assayed for protein content (BCA, Thermo Fisher Scientific Inc., Rockford, IL). Platelet extracts were diluted in phosphate buffer saline (PBS) containing 1% BSA, for evaluation.

Human cerebral cortex (52 y/o; African American male; cause of death was atherosclerotic cardiovascular disease; postmortem interval was 2 hours; neuropathologic evaluation revealed brain to be normal) was obtained from the Brain and Tissue Bank for Developmental Disorders of the National Institute of Child Health and Human Development, University of Maryland (Baltimore, MD). A homogenate of soluble brain protein was prepared by (glass/Teflon) homogenization (five down/up) and centrifugation at 4,900 x g (4°C, 15 min) to remove cellular debris (36). The resulting supernatant was centrifuged at 150,000 x g (4°C, 60 min). The supernatant was collected, assayed for total protein (BCA) and aliquoted for storage at -80°C until use.

Brain Perfusion and Fixation via Transcardial Approach

Perfusion and fixation were performed according to the methods of Jacobowitz and coworkers, with minor modifications (52; 54). Rats received an intraperitoneal injection of 0.4 mL/100 gm body weight of a 10% chloral hydrate solution. A surgical-plane of anesthesia was confirmed by the absence of a response to noxious stimuli (toe or tail pinch) (34; 36). Once a surgical plane of anesthesia was reached, each limb was secured to a dissecting board. Using a heavy toothed forceps, the distal end of the sternum was grasped, elevated and an incision was made at the distal end of the xiphoid process. The incision was extended down and through the diaphragm, taking care not to injure any internal organs. Thoracotomy continued with far-lateral cuts up each side of the rib cage, reflecting the sternum up and over the head, widely exposing the entire chest cavity. A blood sample was collected by direct cardiac puncture using an 18 gauge needle and a 3 mL syringe. Following the blood draw a blunt instrument was used to reflect the left lung toward the mid-line, exposing the descending aorta which was cross-clamped. Next a weighted retaining clamp was attached to the apex of the heart's right ventricle providing gentle caudal traction.

Using Baby Mayo dissecting scissors, an incision was made in the left ventricle and a blunt 13 gauge needle (primed with PBS) was advanced through the heart and into the ascending aorta. A bulldog clamp was used to secure the needle in place and a piece of the right atrium was excised to provide perfusion outflow. Gravity flow of PBS (approximately 50 mmHg) was started and continued for 5 minutes or until 100 mL was perfused. Once clear exsanguinate was confirmed, a gravity flow of 10% buffered formalin (Fischer Scientific, Pittsburgh, PA) was started and continued for 30 minutes or

42

100 mL. Following perfusion, the head was decapitated and the brain was removed. Placing the brain in a Jacobowitz® brain block, dorsal surface down, a block cut was performed just posterior to the peduncular notch to remove the cerebellum. Both pieces of the brain were then placed in a sealable jar containing 10% formalin and stored for 24 hours at 4°C. Following formalin post-fixation the brain was transfer into 20% sucrose in PBS and stored for 48 hours at 4°C after which the brain was rinsed with distilled water, blotted dry, frozen with powdered dry ice and stored at -80°C until used.

IMMUNOHISTOCHEMISTRY – RAT BRAIN TISSUE

Immunohistochemistry (IHC) was performed according to the methods of Jacobowitz and coworkers, with minor modifications (54). Twenty micron cryostat sections were prepared from formalin fixed naïve and CCI brains with a Leica CM1900 cryostat (Leica Microsystems, Bannockburn, IL) cooled to -20°C. All brains were sectioned according to the same protocol. For CCI brains, a center point of the injury was determined with outer limits marked at 2.5 mm rostral and 2.5 mm caudal from the center point. Therefore, the surveyed area consisted of a 5 mm block centering on the injury site. Naïve brain blocks were sectioned similarly based upon coordinates that replicated those of the CCI brains. All useable sections were saved with every other section being distributed to create two separate slide sets. This created an active set and a matching backup set for replicating findings. After every twenty sections, a single section was collected for histological characterization of the physical injury. These sections were floated and stained with a 9 second 0.1% thionin stain (Fisher Scientific, Pittsburgh, PA). All other slides were stored at -80°C until IHC was performed.

Immunohistochemical analysis of each candidate TBI protein was performed on a series of slides representing the entire rostral-caudal span of the injury. Immunoblot was used to document antibody specificity. Antibody dilutions ranging from 1:100 to 1:10,000 were tested, with 1:1000 and 1:10,000 yielding the best signal-to-noise ratio. The negative immune control for antibodies was use of secondary antibody only prior to imaging. A typical analysis involved approximately 12 sections collected from across the lesion, or a comparable tissue span from control brain. Slides were removed from the freezer, condensation wiped away and a circumferential barrier was drawn around all the sections with an ImmunoPen™ (CalBioChem, Billerica, MA). Sections were then probed with the desired primary antibody diluted 1:1000 to 1:10,000 in PBS containing 0.3% Triton-X 100 in a solution of PBS/distilled water (1:10) and 1% donkey serum (gift from Dr. Jacobowitz, USUHS). Slides were incubated overnight at 4°C in a humidified covered container. The following day all slides were examined to confirm full hydration had been achieved. The slides were then washed 3X for 10 min each in PBS containing 0.2% Triton-X. The ImmunoPen lines were freshened and a secondary antibody was added. Depending upon the species of the primary antibody, either Alexa Fluor® 488 donkey anti-rabbit (green) or Alexa Fluor® 488 donkey anti-mouse (red) (Invitrogen, Grand Island, NY) detection antibody was used at a concentration of 1:100 in PBS containing 0.3% Triton-X. The secondary antibody was incubated at room temperature in a covered humidified box for 30 minutes. Next, the slides were washed 3X for 10 min with PBS containing 0.2% Triton-X 100, followed by a 5 minute wash with PBS. The final step involved the application of a few drops of P-phenylenediamine mounting medium (1mg /mL p-phenylenediamine, 10% PBS/glycerol; buffered to a pH

of 8.0 with 0.5 M carbonate-bicarbonate) and a cover slip. Slides were stored at 4°C until imaged.

Co-localization

An analysis of cellular co-localization was carried out using antibodies directed against GFAP (Lot # 1940527; catalogue # MAB360; Millipore, Billerica, Massachusetts, 1:1000) for astrocytes; IBA-1 ([1022-5]; catalogue # ab15690, Abcam, Cambridge, Massachusetts, 1:1000) and ED-1 (clone ED1, catalogue # MCA341R, AbD Serotec, Raleigh, North Carolina, 1:150) for quiescent and activated microglia, respectively; and Neu N (Lot # NG1876252; catalogue # MAB377; Millipore, Billerica, Massachusetts, 1:1000) for neurons.

CHAPTER 4: RESULTS

AUTOIMMUNE PROFILING OF TBI-INDUCED AUTOANTIBODIES BY PROTEIN MICROARRAY

The Invitrogen ProtoArray platform was used to investigate the expression of autoantibodies in response to TBI. This array simultaneously evaluates autoimmune reactivity against 9,740 human proteins expressed and printed under native conditions. Table 2 lists 43 proteins targeted by autoantibodies that were elicited in response to TBI. Proteins are ordered according to their fold-increase over baseline values. Baseline values were established using samples collected within 24 hours of injury, at a time before any autoimmune response could be marshaled. In contrast, the 30-day post-injury sampling time allowed for the full expression of an autoimmune response. Each of the 43 proteins identified exhibited a significant increase ($p < 0.05$) in autoimmune reactivity by 30 days post-TBI; none of the 9,740 proteins evaluated had a reduced responsiveness following TBI. The "Ultimate ORF ID" shown in Table 2 is a commercial identifier that references the expression clones used by Invitrogen to produce the proteins. The term "Database ID" refers to the database in which the proteins were identified. For example, "NM_002363.1" refers to NCBI Reference Sequence.

Based upon their identification as antigenic, as well as their established roles in important neuronal functions and pathology, cyclin-dependent kinase 5 (CDK5) and presynaptic cytomatrix protein (piccolo, PCLO) were selected for the development of IEAs and further analysis as blood-borne biomarkers for TBI. A working IEA was developed for CDK5 and showed a characteristic response of plasma CDK5 levels in

response to brain injury in human patients. Our efforts to develop an IEA for PCLO were

not successful due to the lack of suitable antibodies available commercially.

Table 2. Proteins identified as TBI-induced autoantigens by protein microarray autoimmune profiling.

Database ID	Ultimate ORF ID	Baseline	30 days Post-Injury	Fold Increase	P-Value	Description
CCP_10BSA		596	5072	8.5	4.33E-02	Citrullinated protein (CCP_10BSA)
NM_002363	1OH10928	2196	15778	7.2	3.57E-04	melanoma antigen family B, 1 (MAGEB1), transcript variant 1
PV4676		628	3995	6.4	4.33E-02	cyclin-dependent kinase 5 (CDK5) and p25: CDK5 and p25 sequences are separated by -- (in protein list file).
BC032852.2	1OH27153	3638	16756	4.6	5.42E-03	melanoma antigen family B, 4 (MAGEB4)
NM_002364	1OH11315	1422	6276	4.4	3.49E-02	melanoma antigen family B, 2 (MAGEB2)
BC011804.2	1OH14438	3225	13478	4.2	2.74E-03	chromosome I open reading frame 165 (C1orf165)
BC002493.1	1OH3967	4010	16425	4.1	3.57E-04	transcription factor 19 (SC1) (TCF19)
BC015202.2	1OH39942	1724	7038	4.1	3.57E-04	centromere protein T (CENPT)
BC067735.1	1OH40060	2159	8682	4	3.57E-04	hypothetical protein DKFZp761B107 (DKFZp761B107)
NM_015607	1OH41553	4570	18373	4	5.95E-05	Uncharacterized protein C1orf77
NM_033345	1OH40371	2129	8520	4	9.88E-03	regulator of G-protein signaling 8 (RGS8), transcript variant 1
NM_032848	1OH13466	4073	15829	3.9	5.95E-05	chromosome 12 open reading frame 52 (C12orf52)
NM_153332	1OH27323	1552	6019	3.9	2.86E-02	three prime histone mRNA exonuclease 1 (THEX1)
BC001304.1	1OH45994	3550	13378	3.8	5.95E-05	piccolo (presynaptic cytomatrix protein) (PCLO)
NM_144664	1OH45592	1833	6849	3.7	3.57E-04	Protein FAM76B
BC011924.1	1OH12682	2418	8822	3.6	3.57E-04	unkempt homolog (Drosophila)-like (UNKL)
NM_000122	1OH6320	3291	11995	3.6	5.47E-04	excision repair cross-complementing rodent repair deficiency, complementation group 3 (xeroderma pigmentosum group B complementing) (ERCC3)
NM_006788	1OH10874	10354	37651	3.6	2.74E-03	RalA-binding protein 1
PV3851		4057	14723	3.6	2.74E-03	MAP/microtubule affinity-regulating kinase 4

NM_015891	IOH44384	2159	7570	3.5	5.95E-05	cell division cycle 40 homolog (S. cerevisiae) (CDC40)
NM_004873	IOH26366	2608	9111	3.5	9.88E-03	BCL2-associated athanogene 5 (BAG5), transcript variant 2
BC069677.1	IOH61907	1672	5725	3.4	2.86E-02	Regulator of G-protein signaling 8
NM_153339	IOH22364	2557	8666	3.4	5.95E-05	pseudouridylate synthase-like 1 (PUSL1)
BC096708.1	IOH63336	2922	9905	3.4	1.55E-03	Wilms tumor-associated protein
PHC1475		1452	4907	3.4	5.95E-05	C-C motif chemokine 21
BC000979.2	IOH2932	1108	3734	3.4	4.33E-02	Probable ATP-dependent RNA helicase DDX49
NM_194290	IOH42276	3153	10624	3.4	3.57E-04	cDNA FLJ42001 fis, clone SPLEN2029912 (LOC153684 protein) [Source:UniProtKB/TrEMBL;Acc:Q6ZVW3]
NM_018454	IOH3087	1359	4576	3.4	3.57E-04	nucleolar and spindle associated protein 1 (NUSAP1), transcript variant 2
BC020786.1	IOH14667	1445	4778	3.3	5.41E-06	pleiotropic regulator 1 (PRL1 homolog, Arabidopsis) (PLRG1)
BC029382.1	IOH23139	9392	30092	3.2	3.57E-04	Angiogenic factor with G patch and FHA domains 1
BC001132.1	IOH3853	2557	8191	3.2	3.57E-04	DEAD (Asp-Glu-Ala-Asp) box polypeptide 54 (DDX54)
NM_003221.	IOH25803	2663	8492	3.2	5.42E-03	transcription factor AP-2 beta (activating enhancer binding protein 2 beta) (TFAP2B)
NM_145043	IOH13260	1813	5781	3.2	5.47E-04	nei like 2 (E. coli) (NEIL2)
BC020555.1	IOH10305	6965	22184	3.2	5.95E-05	SERPINE1 mRNA binding protein 1 (SERBP1)
BC014949.1	IOH13331	1557	4952	3.2	2.86E-02	DEXH (Asp-Glu-X-His) box polypeptide 58 (DHX58)
BC015008.1	IOH23029	2394	7534	3.1	2.74E-03	Hydroxyacylglutathione hydrolase-like protein
NM_015640	IOH22934	4758	14788	3.1	3.57E-04	SERPINE1 mRNA binding protein 1 (SERBP1), transcript variant 4
BC002488.1	IOH3970	5682	17629	3.1	3.57E-04	SERPINE1 mRNA binding protein 1 (SERBP1)
BC059405.1	IOH40433	5590	17217	3.1	4.33E-02	Transducin-like enhancer protein 4
NM_001031	IOH58930	1954	6008	3.1	9.88E-03	40S ribosomal protein S28
PHC1244		1552	4752	3.1	1.55E-03	chemokine (C-C motif) ligand 19 (CCL19)
NM_001022	IOH4572	1553	4701	3	5.95E-05	ribosomal protein S19 (RPS19)
BC014298.1	IOH13449	2636	7925	3	1.55E-03	PRKR interacting protein 1 (IL11 inducible) (PRKRIP1)

49

GLOBAL AUTOIMMUNE PROFILING OF TBI-INDUCED AUTOANTIBODIES BY 1-DIMENSIONAL IMMUNOBLOTTING

Global autoimmune profiling was developed as an unbiased approach to investigate the expression of autoantibodies against each protein making up the brain proteome. We initially evaluated the effectiveness of this strategy using 1-D immunoblotting. Specifically, rat brain proteome was fractionated on 1-D SDS-PAGE gels, transferred to PVDF membrane and then probed with immunoglobulins present in serum of control or TBI rats. This investigation confirmed that TBI-induced autoantibodies could, in fact, be identified by 1-D immunoblotting. Moreover, the reactive protein features can be mapped to replicate protein gels and identified proteomically.

Figure 5 depicts immunoblots of rat brain proteome probed with control or TBI serum. Equal volumes and concentrations of membrane bound (lanes 1 and 2) and soluble proteomes (lanes 3 and 4) of a naïve rat brain were fractionated on 10% polyacrylamide gels and either transferred to PVDF membranes or stained with Coomassie blue. Blots were probed with serum pooled from eight adult male naïve or eight adult male TBI rats (1:250 dilution). Reactive autoantibodies were visualized by horseradish peroxidase-labeled anti-rat IgG and enhanced chemiluminescence using a Fuji Image Reader LAS-3000 system and Multi Gauge V3.0 software. Immunoreactive features unique to the TBI blots were mapped to replicate Coomassie-stained protein gels and unique features were excised from the gel and identified by peptide mass finger printing. The results of this analysis included identification of alpha internexin, collapsin response mediator protein 2 (CRMP2) and the brain specific isoform of creatine kinase (CKBB) as candidate TBI biomarkers. Importantly, CKBB has been recognized as a potential TBI biomarker for

more than two decades, indicating the validity of autoimmune profiling as a strategy for identifying TBI biomarkers that are novel to the field. In this regard, alpha internexin and CRMP2 are completely novel to the field of TBI biomarkers. Similar experiments investigating IgM autoantibodies yielded similar results (see Fig. 7).

Based on these promising results attention was placed on increasing the resolving power of our experimental approach. Due to the limited resolution of 1-D gel electrophoresis, complex samples often result in bands of interest containing more than one protein. A solution to this problem is the use of 2-D fractionation on large-scale gels. This approach allows for the separation the brain proteome by both isoelectric point and molecular weight, thus effectively separating proteins with similar size or charge.
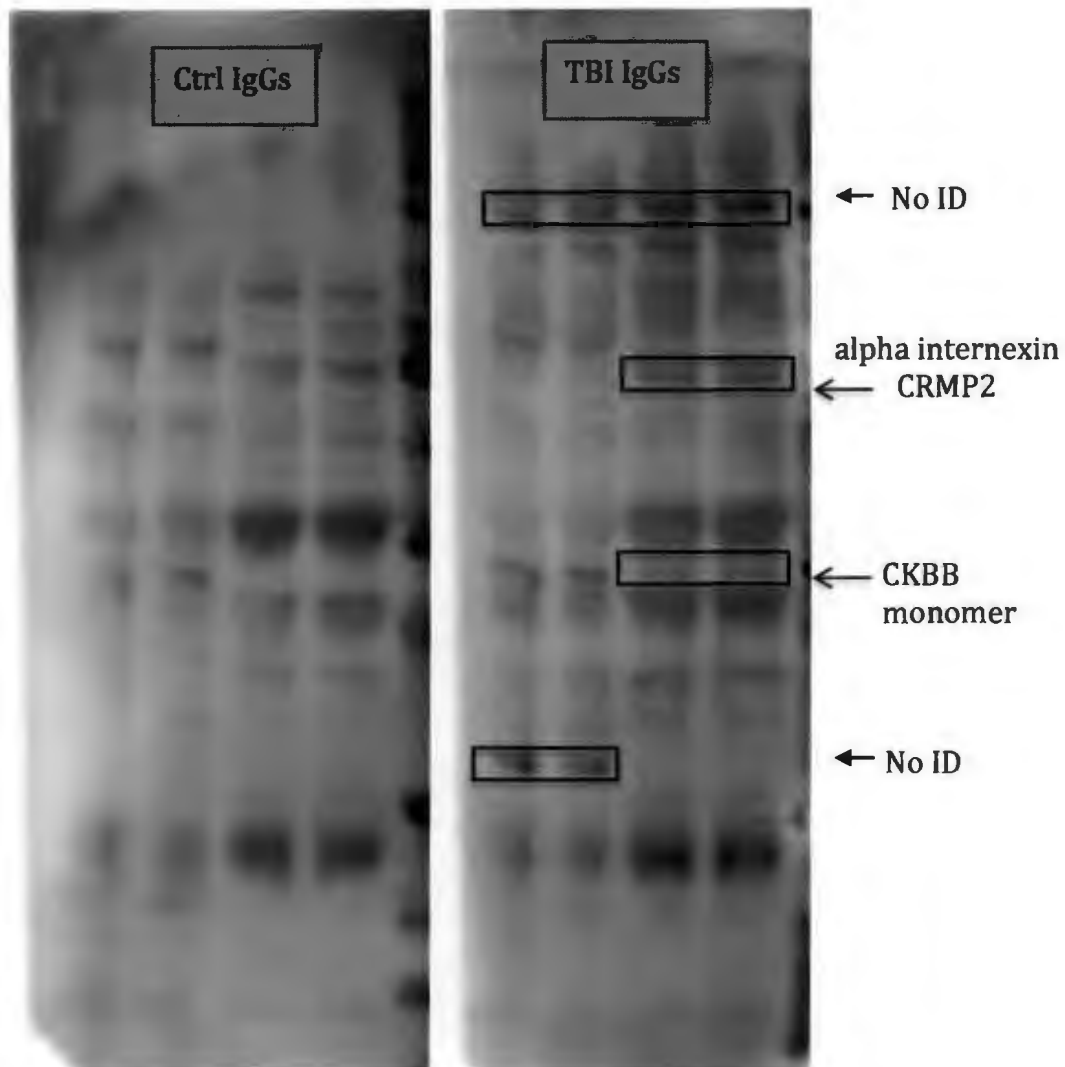
Figure 5. Autoimmune profiling of TBI-induced autoantibodies by 1-D gel electrophoresis and immunoblot analysis. The membrane bound (lanes 1 and 2) and soluble proteomes (lanes 3 and 4) of whole rat brain were fractionated on 10% polyacrylamide gels and transferred to PVDF. Blots were probed with serum pooled from eight naïve (left panel) or eight TBI (right panel) rats (1:250 dilution). Reactive autoantibodies were visualized by horseradish peroxidase-labeled anti-rat IgG or IgM and enhanced chemiluminescence. Reactive features that were unique to TBI (arrows) were mapped to replicate, Coomassie-stained protein gels and identified by peptide mass finger printing. No ID = no identification.

GLOBAL AUTOIMMUNE PROFILING OF TBI-INDUCED AUTOANTIBODIES BY 2-DIMENSIONAL IMMUNOBLOTTING

Based on the success of 1-D autoimmune profiling for the discovery of TBI-induced autoantibodies, a more intense search was carried out using 2-D gel electrophoresis and the largest gels commercially available. Soluble proteome of rat brain was first subjected to isoelectric focusing (1st dimension) and then molecular weight separation (2nd dimension). Next, the fractionated proteins were transferred to PVDF membranes and probed with serum pooled from eight naïve adult male Sprague Dawley rats or eight adult male TBI rats (CCI, 7 days, 1:250 dilution). Reactive autoantibodies were visualized by horseradish peroxidase labeled anti-rat IgG or IgM and enhanced chemiluminescence (Fig. 6). The control immunoblot (naïve) shows a characteristic pattern of IgG binding that reflects non-specific binding due to the relatively high concentration of serum (1:250 dilution) used to maximize the intensity of specific autoimmune signals. The primary focus of this investigation, however, was on immunologic signals that were newly revealed or greatly enhanced on TBI blots as compared to control blots. Boxes indicate areas on blots where differences between control and TBI were especially evident. Immunoreactive features unique to TBI were mapped to replicate silver stained protein gels. Unique protein features were excised from the gels and identified by peptide mass finger printing. In some cases, protein identifications were confirmed by tandem mass spectrometry performed at the W. M. Keck Biotechnology Resource Laboratory, Yale University.
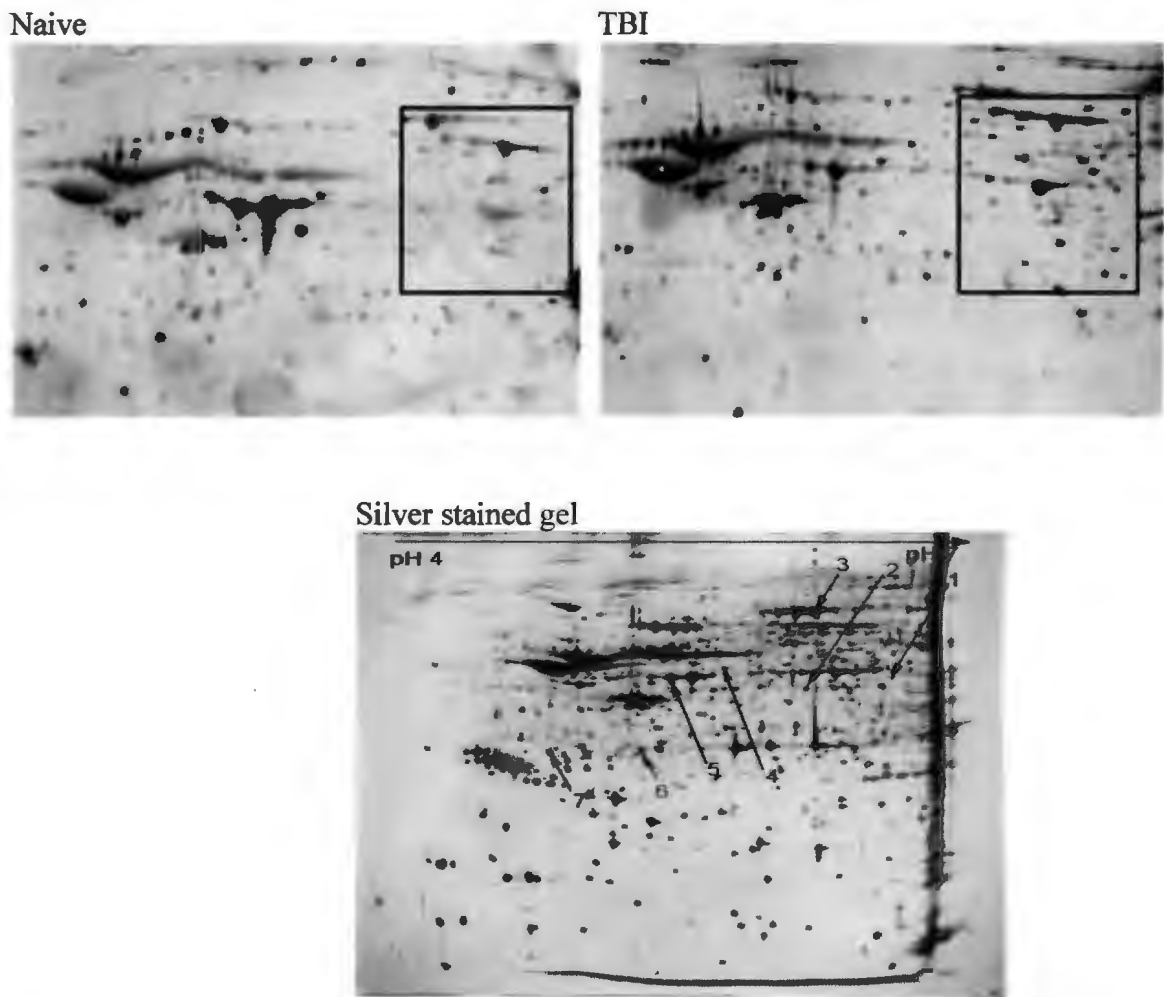
Figure 6. Autoimmune profiling of TBI-induced autoantibodies by 2-D gel electrophoresis and immunoblot analysis. The soluble proteome of whole rat brain (500 μg) was fractionated by isoelectric point (pH 4-7, 1st dimension) and molecular weight (2nd dimension), and then transferred to PVDF. The resulting immunoblots were probed with serum pooled from eight naïve (upper left panel) or eight TBI (upper right panel) rats (1:250 dilution). Reactive autoantibodies were visualized by horseradish-labeled anti-rat IgG or IgM and enhanced chemiluminescence. Boxes indicate areas on blots where differences between control and TBI were especially marked. Reactive features were mapped to replicate, silver stained protein gels (lower panel) and identified by peptide mass finger printing and/or tandem mass spectrometry. Protein identification were as follows: 1. TUC-4b; 2. dual specificity mitogen-activated protein kinase 1; 3. CRMP2; 4. neuronal pentraxin 1; 5. creatine kinase B-type; 6. mu-crystallin homolog; 7. annexin A5. The experiment presented here is representative of 14 separate runs analyzing different pools of control and TBI serum (autoantibodies) and involving 4 to 8 gels each.

CANDIDATE TBI BIOMARKERS IDENTIFIED BY GLOBAL AUTOIMMUNE PROFILING

A total of fourteen 2-D gel analyses were performed using pools of control and TBI serum prepared from different groups of rats. Each run consisted of 4-8 gels. After several iterations a number of candidate TBI biomarkers began to replicate, with both IgG and IgM screening. Proteins were selected as candidate TBI biomarkers based upon their repeated identification as targets for autoantibodies and by their reported localization and functions within the CNS. A composite Venn diagram of these identifications is presented below in Figure 7 (see Appendix II for a summary of all analyses).
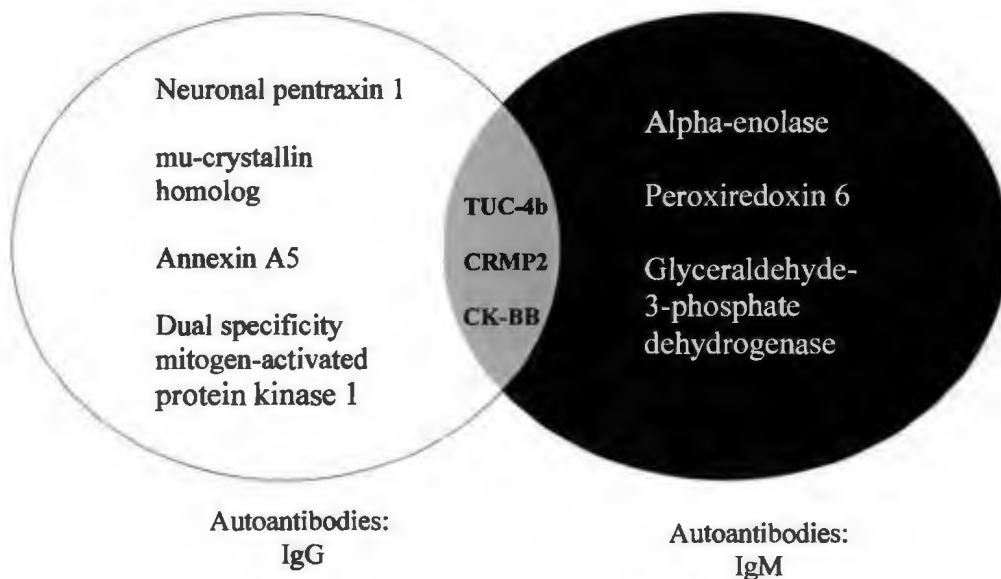
Figure 7. Venn diagram of candidate TBI biomarkers identified by global autoimmune profiling. Proteins identified by IgG autoantibodies are depicted on the left, proteins identified by IgM autoantibodies are depicted on the right and proteins identified by both IgG and IgM autoantibodies are depicted within the overlapping region in the center of the diagram.

A representative example of the TBI biomarker discovery process is presented in Figure 8 for the novel candidate, peroxiredoxin 6 (PRDX6). Also discussed is the subsequent characterization work performed for other newly discovered biomarker candidates. In the present project, the greatest success was achieved with the discovery and development of PRDX6. However, IEAs were similarly developed and used for the investigation of CKBB and CDK5 (CDK5 was discovered by protein microarray). Efforts to develop analytical tools for neuronal pentraxin 1, PCLO, CRMP2, and mu-crystallin homolog were met with limited success and not yield IEAs suitable for the analyses needed here. This was due to either the absence of appropriate antibodies, standard proteins or a lack of assay sensitivity.

AUTOIMMUNE PROFILING IDENTIFIES PRDX6 AS A CANDIDATE TBI BIOMARKER: A REPRESENTATIVE EXAMPLE FOR THE DISCOVERY PROCESS

The discovery and development of PRDX6 as a candidate TBI biomarker is presented here as an example of the specific steps involved in the process of autoimmune profiling and biomarker discovery. Figure 8 depicts the identification of PRDX6 as a protein reactive with autoantibodies induced by brain injury in rats. The rat brain proteome was fractionated on large scale 2-D gels, transferred to PVDF and then probed with immunoglobulins present in serum from control (panel A) or TBI (panel B) rats. As discussed above, the control immunoblot (panel A) shows a characteristic pattern of IgG binding that reflects the high concentration of serum (1:250 dilution) used to maximize the intensity of specific autoimmune signals. Most important to this investigation, however, were immunologic signals that distinguished TBI blots from control blots. One such prominent feature present on the TBI versus control blot (circled) was mapped to a

replicate silver stained protein gel (panel C) and identified by peptide mass finger printing (panel D). The protein was definitively identified with 77% sequence coverage as PRDX6: a 224 amino acid protein with a theoretical PI of 5.64 and a molecular weight of 24.8 kDa. The identification of PRDX6 was confirmed in separate experiments and additional samples analyzed independently by the W.M. Keck Biotechnology Resource Laboratory, Yale University (see Methods). Additionally, high titers of anti-PRDX6 autoantibodies were also detected in clinical plasma samples (collected at the National Institutes of Health) from three patients with profound yet undiagnosed neurological disorders (not shown). These observations extend the potential role of PRDX6 as a marker for neuropathology to humans.

Based upon the identification of PRDX6 as a candidate TBI-autoantigen, a sandwich IEA was established for measuring PRDX6 in human samples. This assay was based upon a matched pair of capture and primary monoclonal antibodies, each recognizing a separate epitope on the PRDX6 molecule. Panel E shows a representative standard curve for the assay utilizing recombinant human PRDX6 protein as standard (see Methods for details).
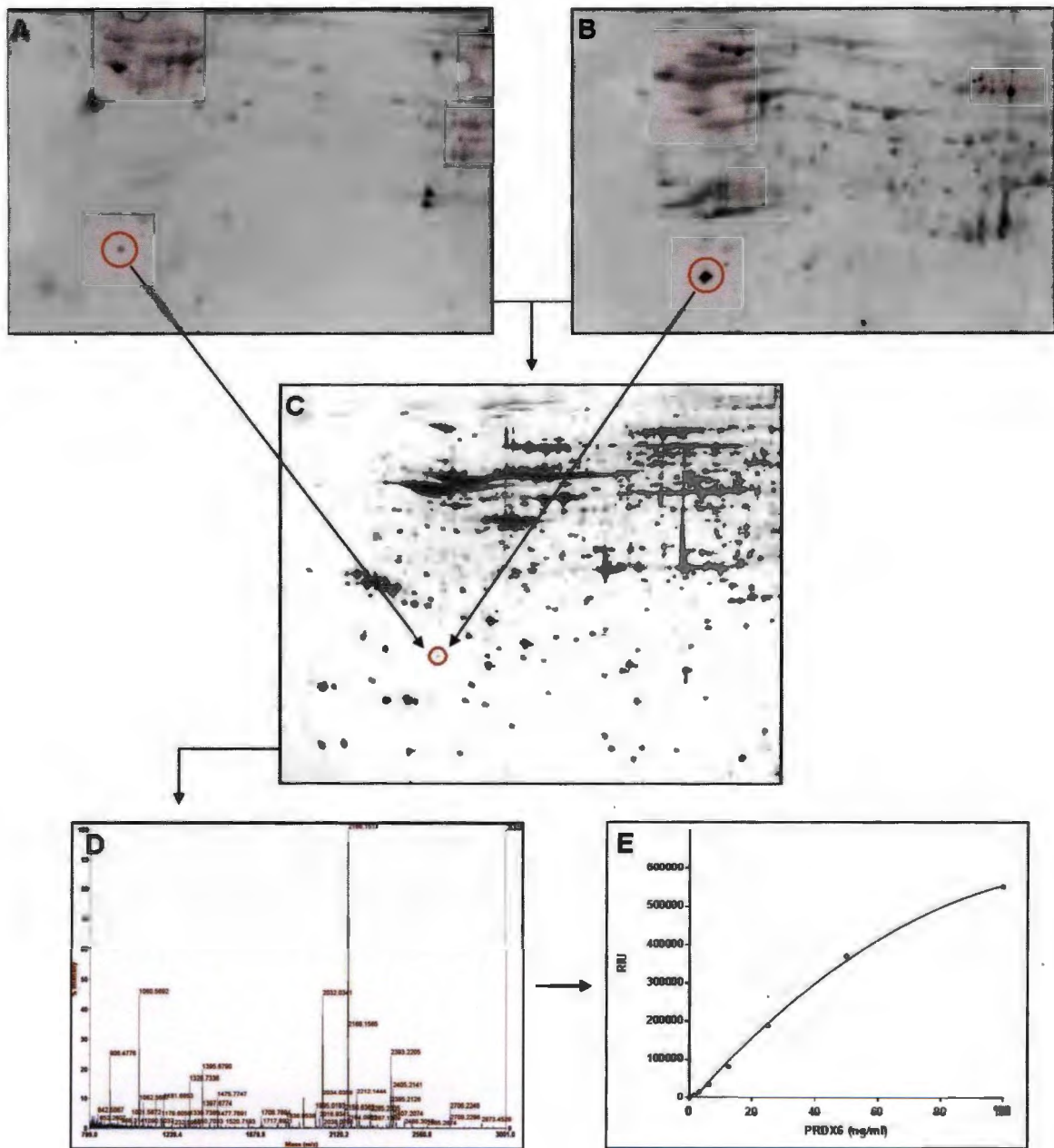
Figure 8. Discovery of PRDX6 as a candidate biomarker for brain injury. The rat brain proteome was fractionated by 2-D gel electrophoresis and transferred to PVDF. Blots were probed with serum from control and TBI rats (1:250), and visualized by enhanced chemiluminescence using pooled anti-rat IgG and IgM detection antibodies (panels A and B, respectively). A feature showing enhanced autoreactivity following TBI (circles) was mapped to a replicate protein gel (panel C) and identified by peptide mass finger printing as PRDX6 (panel D MALDI-TOF Spectra). Panel E presents a representative standard curve for the sandwich IEA developed to measure PRDX6 in human blood.

58

CHARACTERIZATION OF PRDX6 AS A CANDIDATE TBI BIOMARKER PROTEIN: 1-D IMMUNOBLOTTING DEMONSTRATES THE SPECIFICITY OF THE PRDX6 IEA

The specificity of the capture and primary antibodies was evaluated by immunoblot using recombinant human PRDX6 protein and extracts of human cerebral cortex and platelets (Fig. 9). Panel A shows a replicate silver stained gel that depicts the complexity of the brain and platelet samples. While the capture antibody was not compatible with immunoblotting under the conditions used here, the primary antibody exhibited remarkable specificity for authentic PRDX6 present in highly complex samples of human brain and platelets (panel B). The recombinant PRDX6 standard exhibited a higher molecular weight as compared to tissue PRDX6 due to presence of a histidine expression tag. Also, panel A reveals the large amount of carrier protein present in the commercial standard; the recombinant PRDX6 was barely evident (arrow) at this protein loading. Platelet samples making up the male and female pools were assayed individually for concentrations of PRDX6 and determined to be 500 ± 29 ng/mg and 507 ± 19 ng/mg soluble protein for males and females (N=8), respectively. The concentration of PRDX6 in the single human brain sample was approximately double that of platelets at 940 ng/mg soluble protein.
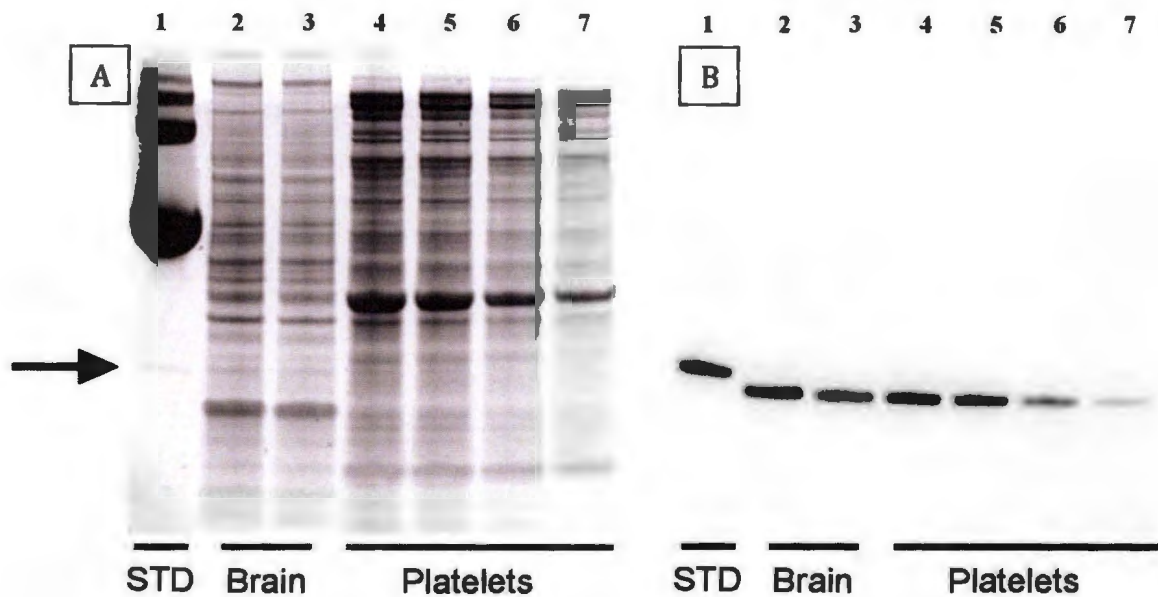
Figure 9. Immunoblot analysis of PRDX6 in extracts of human brain and platelets. Recombinant PRDX6 (200 ng, lane 1), human brain extract (20 μg, and 10 μg; lanes 2 and 3, respectively) and human platelet extract (20 μg, 10 μg, 5 μg and 2.5 μg; lanes 4-7, respectively) were analyzed by silver staining (panel A) and immunoblot and probed with anti-PRDX6 antibody (panel B).

CHARACTERIZATION OF PRDX6 AS A CANDIDATE TBI BIOMARKER PROTEIN: IMMUNOREACTIVE PRDX6 IN MATCHED HUMAN SERUM AND PLASMA

The performance characteristics of the PRDX6 IEAs were evaluated using different types of biological samples including serum and plasma, as well as extracts of human brain and platelets. Similar tests performed with rat samples revealed that the PRDX6 IEA does not cross-react with this species.

Figure 10 presents the mean values for PRDX6 in human serum and plasma from normal male and female volunteers. The samples were prepared as matched sets from the same blood draws (n=10); NaEDTA was used as anticoagulant for the preparation of plasma. The data presented represent two separate experiments (panels A and B) carried out on two different sets of matched plasma and serum samples (N=40). Levels of

60

PRDX6 were estimated using a standard curve that included an equivalent amount of either horse serum or chicken plasma (NaEDTA anticoagulant) to control for the non-specific effects of serum or plasma matrix, respectively. The presence of non-cross reactive (non-human) plasma or serum matrix increased nonspecific background signal by two- to three-fold over buffer alone, but did not interfere with the performance of recombinant PRDX6 protein standard in the IEA. Levels of PRDX6 in plasma were higher in females as compared to males ($p < 0.001$) in both experiments (168 ± 36 ng/mL vs. 65 ± 10 ng/mL and 178 ± 30 ng/mL vs. 43 ± 8 ng/mL, respectively). The process of coagulation dramatically reduced measured concentrations of PRDX6 in female blood samples ($p < 0.01$). A tendency for this phenomenon was also observed in male samples; however, the effect here was not significant due to the lower starting levels of PRDX6 in male plasma.
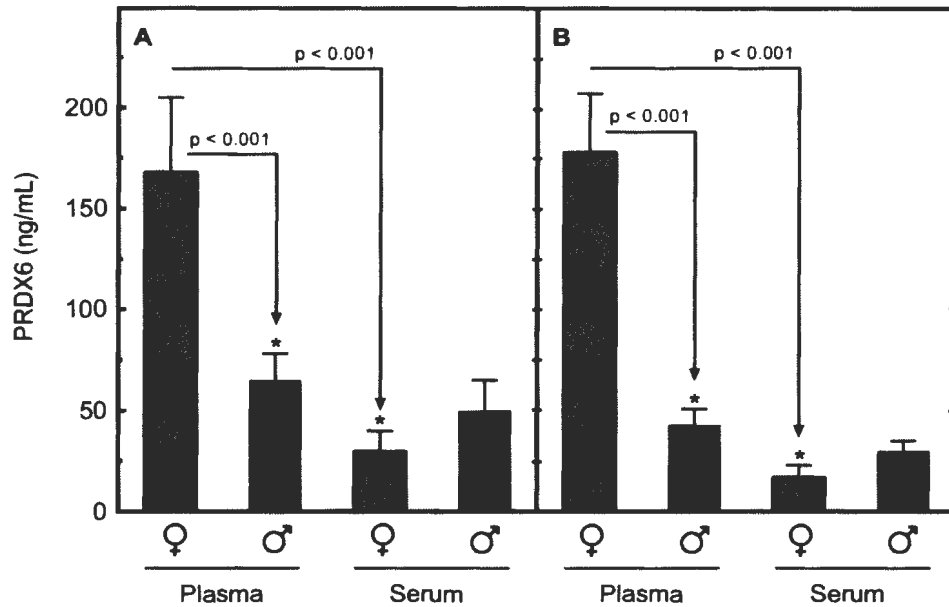
Figure 10. Comparison of levels of PRDX6 in human plasma and serum. Serum and plasma were prepared as matched sets from blood samples drawn from normal male and female volunteers (N=10 each). The experiment was replicated in a second independent cohort of the same size (panels A and B). Differences with statistical significance are shown by the arrows and corresponding p-values.

CHARACTERIZATION OF PRDX6 AS A CANDIDATE TBI BIOMARKER PROTEIN: IMMUNOHISTOCHEMISTRY

Immunohistochemistry on PRDX6 was performed to gain better insight into the neurobiology of this antioxidant enzyme. This preliminary study was performed in rat brain using an anti-PRDX6 antibody that recognizes rodent PRDX6 in fixed brain tissue. Brain expression of PRDX6 was examined in one naïve and one adult male CCI rat, 8 days post-injury. An analysis of cellular co-localization was carried out using anti-GFAP IHC to identify (Millipore), IBA-1 and ED-1 to identify quiescent and activated microglia respectively, and Neu N to identify neurons (see Methods section for details).

62

In all cases, a donkey anti-rabbit green fluorescence antibody, Alexa Fluor 488 secondary antibody, was used to visualize PRDX6, whereas a donkey anti-mouse red fluorescence antibody was used to visualize the cell-specific detection antibody. Secondary only controls carried out for each co-localization condition were all negative (not shown).

This study demonstrated that the expression of PRDX6 is predominantly in astrocytes, with little or no expression detected in microglia or neurons. A finding of particular note is the remarkable abundance of PRDX6 in astrocyte foot processes impinging on the walls of cerebral blood vessels (Fig. 11 and Fig. 12). Further, the expression of PRDX6 appeared to be up-regulated by TBI, creating a gradient of expression that was highest in the penumbra and lower in surrounding uninjured brain tissue (Fig. 13). Finally, the expression of PRDX6 was also detected in cell-like structures of uncharacteristic morphology located in the region of the penumbra. Based upon the IHC staining controls (see Methods section for details), these PRDX6-expressing structures appear to be necrotic astrocytes or possibly apoptotic remnants of astrocytes.
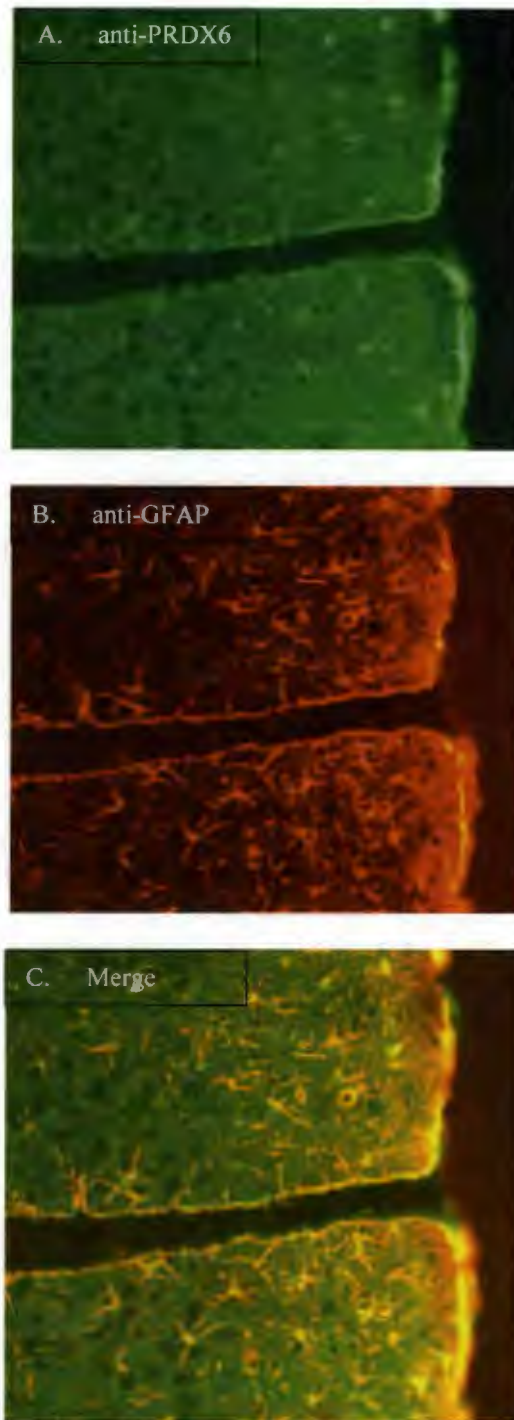
Figure 11. PRDX6 is highly expressed in astrocytes in rat cerebral cortex. The 40x
section includes a blood vessel sectioned along its axis to reveal its wall and
lumen. Panel A shows cells labeled by anti-PRDX6 antibodies. Panel B shows
cells reactive with the astrocyte marker protein, GFAP. Panel C shows the
merge of the green and red fluorescence to reveal the co-localization of PRDX6
and GFAP in astrocytes (yellow).
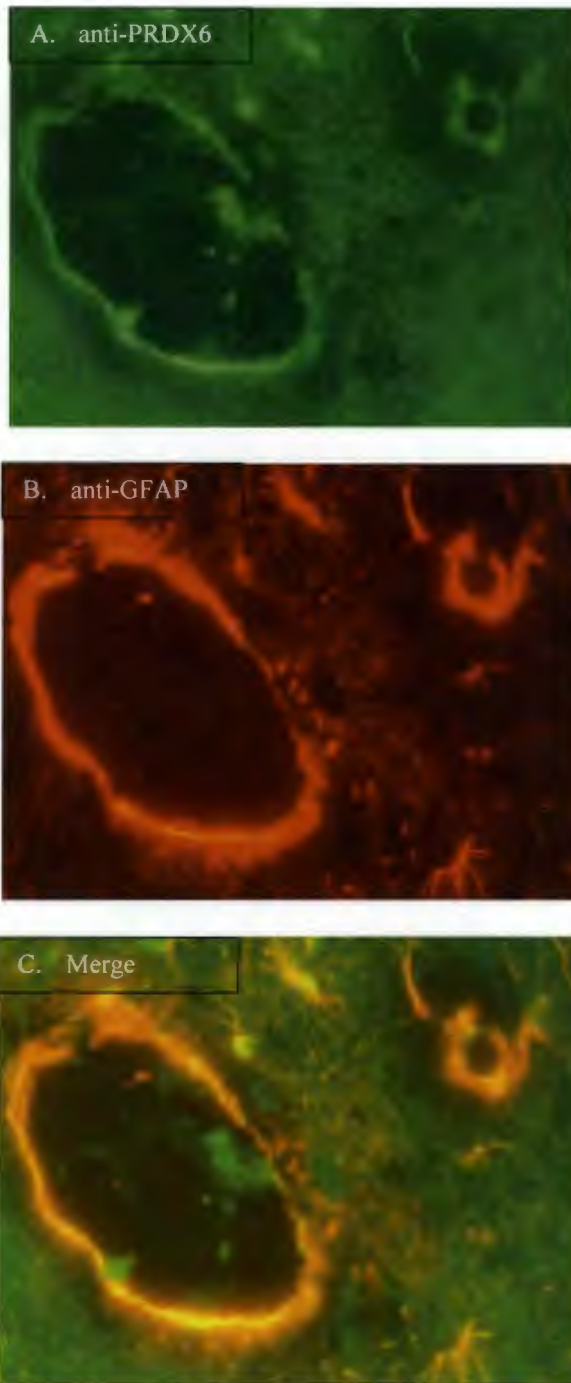
Figure 12. PRDX6 is highly expressed in astrocytes at the blood brain barrier in rat cerebral cortex. The 40x section includes two blood vessels cross-sectioned to reveal its wall and lumen, and in the larger vessel, a nucleated blood cell. Panel A shows cells labeled by anti-PRDX6 antibodies (green). Panel B shows cells reactive with the astrocyte marker protein GFAP (red). Panel C shows the merge of the green and red fluorescence to reveal the co-localization (yellow) of PRDX6 and GFAP in astrocytes with intense expression of PRDX6 at the brain-blood vessel interface.
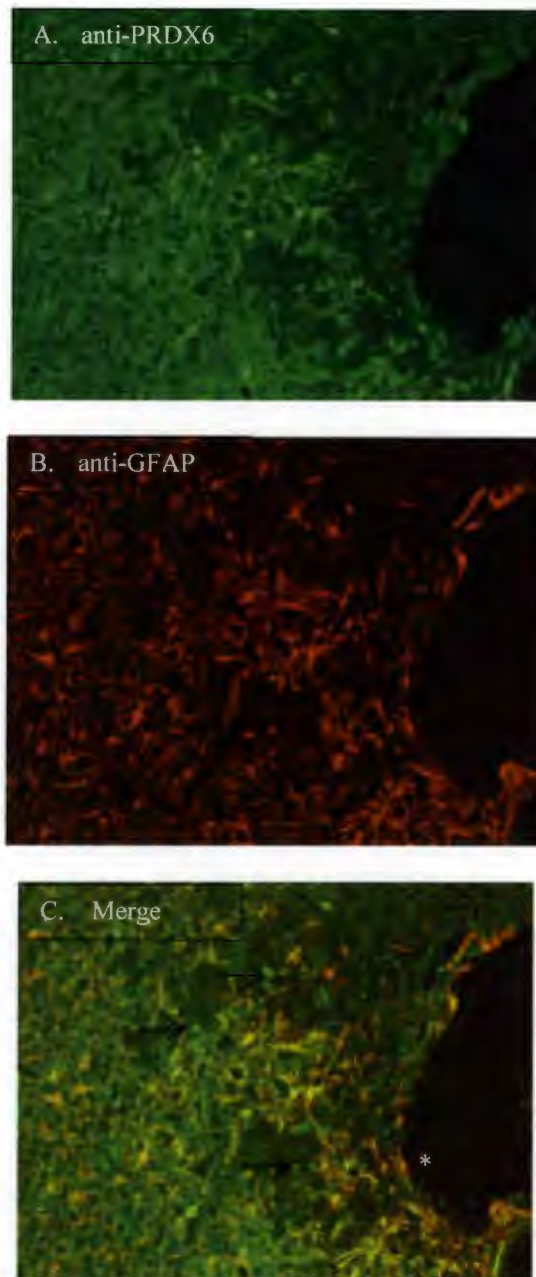
Figure 13. PRDX6 is highly expressed in astrocytes in rat cerebral cortex surrounding the penumbra. The sample was collected 8 days following TBI. The 10x section shows the lesion site on the right and includes a portion of the penumbra (*). Panel A shows cells labeled by anti-PRDX6 antibodies (green). Panel B shows cells reactive with the astrocyte marker protein, GFAP (red). Panel C shows the merge of the green and red fluorescence to reveal the co-localization (yellow) of PRDX6 and GFAP in astrocytes. There is an apparent gradient in PRDX6 expression from highest in the penumbra, as well as, an increased size of the PRDX6-expressing astrocytes in the penumbra. In addition, the presence of PRDX6 positive cells thought to be narcotic astrocytes are evident surrounding the lesion (arrows, panel C)

The remarkable abundance of PRDX6 in brain, its perivascular concentration and its apparent up-regulation in response to TBI all support the conclusion that PRDX6 will to be an informative biomarker for TBI.

CANDIDATE TBI BIOMARKERS IDENTIFIED BY AUTOIMMUNE PROFILING IN BOTH RODENTS AND HUMANS

Table 3 presents a list of the most promising candidate TBI biomarker proteins identified by global autoimmune profiling in rats or protein microarray profiling in humans. As noted above, the proteins listed here were selected on the basis of their repeated identification as targets for TBI-induced autoantibodies and by their reported functions and specificity in brain. This list has been formally filed in an invention disclosure document.

Table 3. Candidate TBI Biomarker Proteins Identified by Autoimmune Profiling.

1	Alpha internexin – 66kDa A class IV neuronal intermediate filament protein involved in morphogenesis of neurons. Primarily expressed in adult CNS
2	Beta-soluble NSF attachment protein (betaSNAP) – 33kDa Mediates vesicular transport and release in neurons. Brain specific expression
3	Collapsin response mediator protein (CRMP2) – 62kDa Neuronal receptor for semaphorin, involved in guidance of growth cone. Neuron specific expression
4	Creatine kinase B (CK-BB) – 42kDa Cytosolic enzyme that catalyzes the formation of high energy phosphocreatine Predominately expressed in brain
5	CRMP4 (TUC-4b) – 62kDa Neuronal receptor for semaphorin, involved in guidance of growth cone. Neuron specific expression

6	Cyclin-dependent kinase 5 (CDK5)* – 33kDa
	Involved specifically in neuronal processes: migration, cortical layering, and synaptic plasticity. Dysregulation is linked to neuropathological alterations: CRMP2 and tau hyperphosphorylation, neuronal and synaptic loss
	Highly expressed in mature neurons
7	Mu-crystallin homolog – 33kDa
	Binds thyroid hormone and catalyzes reduction of imine bonds in proteins
	Expressed in brain and lens of the eye
8	Neuronal pentraxin-1 – 47kDa
	Involved in synaptic remodeling. Known as the C-reactive protein of brain.
	Brain specific expression
9	Peroxiredoxin 6 – 25kDa
	Antioxidant enzyme that catalyzes the hydrolysis of H_2O_2
	Highly expressed in brain, also expressed in lung and kidney
10	Presynaptic cytomatrix protein (piccolo, PCLO)* - 552kDa
	Presynaptic cytoskeletal matrix protein that mediates the release of synaptic vesicles
	Neuron specific expression
11	RalA-binding protein 1 (RALBP1)* - 76kDa
	Interacts with GTP binding proteins to regulate receptor mediated endocytosis
	Widely expressed in many cell types
12	Regulator of G-protein signaling 8 (RGS8)* - 21kDa
	Inhibits GTPase signaling transduction
	Brain specific expression
	*Identified by protein microarray in humans, all others by immunoprofiling in rat

DEVELOPMENT OF IMMUNOSORBENT ELECTROCHEMILUMINESCENCE ASSAYS (IEA) FOR CREATINE KINASE BB AND CYCLIN-DEPENDENT KINASE 5

IEAs were successfully developed for creatine kinase BB and cyclin-dependent kinase 5 following the approaches detailed for PRDX6 above (noted above; see METHODS section for details). Both assays were used for the analysis of human (Table 7 and Figure 18 – CDK5 and CKBB not shown) and rodent samples (not shown). As noted above, dedicated efforts to develop assays for neuronal pentraxin 1, CRMP2, mu

68

crystallin homolog and presynaptic cytomatrix protein were not successful due to the lack of suitable antibodies available commercially. We did not attempt to develop assays for the other candidates listed in Table 3 due to the limitations of time and/or reagents.

APPROACHES FOR THE ANALYSIS OF CANDIDATE BIOMARKERS IN HUMAN PATIENT SAMPLES

The analysis of human samples was designed to identify a biomarker signature consisting of a profile of proteins that would effectively differentiate the spectrum of TBI severity spanning from no injury, to mild/moderate injury, to severe injury. These analyses involved the use of a multiplex platform (for measuring 6 candidates simultaneously) and singleplex analyses. The analytes measured by the multiplex platform were: S100b, BDNF, NSE, MCP1/CCL2, ICAM-5 and GFAP (see Appendix I). Singleplex assays were used for the measurement of PRDX6, CDK5.

ANALYSIS OF CANDIDATE BIOMARKERS IN HUMAN PATIENTS EXPERIENCING MILD TO MODERATE TBI

This study determined the response pattern of a panel of candidate biomarkers in 154 TBI adult patients admitted into local emergency departments with apparent brain injury. The majority of the patients in this study were admitted into Suburban Hospital, Bethesda, MD. The mechanisms of injury were mainly divided among injuries due to falls (54%), direct head impact (27%) and acceleration/deceleration injuries (mostly automobile accidents, 12%). The average Glasgow Coma Scale score at the time of admission was above 14.5, consistent with mild TBI. Clinical data also included information concerning loss of consciousness, post-traumatic amnesia, computed axial tomography (CAT or CT) scan and magnetic resonance imaging (MRI). An analysis of

69

the CT and MRI data revealed that 30%, 39%, 24% of the TBI patients presented with CT, MRI or CT and MRI imaging abnormalities, a feature consistent with the diagnosis of moderate TBI. Nevertheless, these same imaging positive patients had normal or near-normal Glasgow Coma Scale scores, and loss of consciousness and post-traumatic amnesia intervals consistent with mild TBI. Together, these observations illuminate the difficulty that exists in making a definitive diagnosis of mild TBI based upon conventional modalities for assessment.

The clinical component of this study was designed and directed by Dr. Lawrence Latour with the primary objective of evaluating the limits of current imaging technology in diagnosing mild TBI. Accordingly, blood samples were collected at the time of admission into an emergency department and then again at a time ranging between two and seven days after the first sample collection. The variation in the timing for the second blood sample reflects the clinical schedule for neuroimaging. Commercially purchased control samples were collected from normal volunteers (76% Caucasian) ranging in age from 19-50, and with a mean and median age of 25 and 24 respectively. These samples were considered most relevant to our research design compared samples from other emergency room patients admitted with non-TBI injuries. It would be difficult to establish baseline values for our candidate biomarkers in non-TBI injured patients, considering that an emergency room admission by its very nature disqualifies those patients as healthy controls.

A listing of the available patient demographics and clinical data is presented below in Table 4. A complete listing of all clinical variables collected is found in

Appendix III. Controls listed in Table 4 are a representative subset and those used in the data analysis model depicted in Figure 16.

Table 4. Demographic characteristics and clinical variables for patients with mild TBI

		TBI N = 154	Controls N = 30
Age			
	Mean, y (SD)	47 (19)	25 (5)
	Median	45.8	24
	Range	19-91	19-50
Gender (%)			
	Male	103 (67)	15 (50)
	Female	43 (28)	15 (50)
	Unknown	8 (5)	0 (0)
Race (%)			
	Caucasian	103 (67)	23 (76)
	Non-Caucasian	30 (19)	7 (24)
	Unknown	21 (14)	0 (0)
Education (%)			
	< Grade 12	4 (3)	
	High School / equivalent /Associates	70 (45)	
	Bachelor's degree	27 (17)	
	PhD/Professional	30 (19)	
	Unknown	23 (15)	30 (100)
Mechanism of Injury (%)			
	Acceleration/deceleration	18 (12)	0
	Fall	83 (54)	0
	Direct impact	43 (27)	0
	Unknown	10 (6)	0
Glasgow Coma Scale score in ED (%)			
	< 9	3 (2)	0
	9 - 12	3 (2)	0
	≥ 13	132 (86)	30 (100)
	Unknown	16 (10)	0
Loss of Consciousness (%)			
	Yes	69 (45)	0
	No	58 (37)	30 (100)
	Unknown	27 (18)	0

71

Post-traumatic amnesia (%)			
	Yes	83 (54)	0
	No	67 (43)	30 (100)
	Unknown	4 (3)	0
Imaging - CT (%)			
	CT-Scalp_Hematoma	34 (22)	0
	CT-Skull_Fracture	1 (0.6)	0
	CT-Subdural_Hematoma_Acute	16 (10)	0
	CT-Subarachnoid_Hemorrhage	24 (16)	0
	CT-Contusion	11 (7)	0
	CT-Intracerebral_Hemorrhage	10 (6)	0
	CT-Diffuse Axonal Injury	0 (0)	0
	CT-Intraventricular_Hemorrhage	4 (3)	0
Imaging - MRI (%)			
	MRI-Scalp_Hematoma	24 (16)	0
	MRI-Epidural_Hematoma	0 (0)	0
	MRI-Subdural_Hematoma_Acute	21 (14)	0
	MRI-Subarachnoid_Hemorrhage	23 (15)	0
	MRI-Contusion	19 (12)	0
	MRI-Intracerebral_Hemorrhage	20 (13)	0
	MRI- Diffuse Axonal Injury	10 (6)	0
	MRI-Intraventricular_Hemorrhage	9 (6)	0
Admitted to Hospital (%)		100 (65)	0
	Unknown	32 (20)	
Neurobehavorial symptom inventory score	·		N/A
22 symptoms scoring 0-4	Mean	0.75	
Extended Outcome 30-day Post-injury			N/A
Satisfaction with life scale (1-35) (n=26)	Mean	23	
Glasgow outcome scale extended (1-8) (n=59)	Mean	6.5	
Extended Outcome 90-day Post-injury			N/A
Satisfaction with life scale (1-35) (n=26)	Mean	24	
Glasgow outcome scale extended (1-8) (n=61)	Mean	7	

EFFECTS OF MILD TO MODERATE TBI ON PLASMA LEVELS OF CANDIDATE BIOMARKERS PROTEINS

The patient samples were analyzed as two cohorts of approximately equal size. Table 5 presents the mean plasma levels for all biomarkers at all time points for the 154 TBI patients and 30 commercially purchased controls making up this study. All controls were assayed with each TBI cohort with equivalent results. Values that are statistically different from control values are indicated by specific p-values.

Table 5. Mean plasma values of candidate TBI biomarker proteins in patients with mild to moderate TBI and controls.

Condition	ng/ml	BDNF	GFAP	ICAM-5	MCP1/CCL2	NSE	S100b	PRDX6
Control	Mean	2.78	<0.30	0.90	0.11	29.95	0.15	78.20
	SEM	0.56	-	0.06	0.01	6.22	0.03	17.51
	Mean	9.08	<0.30	0.92	0.17	55.50	0.72	387.9
Baseline	SEM	0.58	-	0.02	0.01	2.83	0.13	14.95
	p =	<0.0001	-	NS	<0.001	<0.0001	<0.03	<0.0001
	Mean	9.41	<0.30	0.90	0.17	67.34	0.62	430.8
2-7 Days	SEM	0.64	-	0.02	0.01	3.32	0.12	15.81
	p =	<0.0001	-	NS	<0.001	<0.0001	<0.03	<0.0001

Figure 14 presents additional information on the effects of mild to moderate TBI on plasma levels of PRDX6. Data shown are for male and female patients at the time of admission to an emergency department and at a second time ranging from 2 to 7 days post-injury. As depicted in the controls, plasma levels of PRX6 tended to be higher in females, as compared to males and levels in both males and females at admission were approximately 3-fold higher than control values. Accordingly, PRDX6 appears to be a sensitive indicator of mild to moderate TBI in both genders.
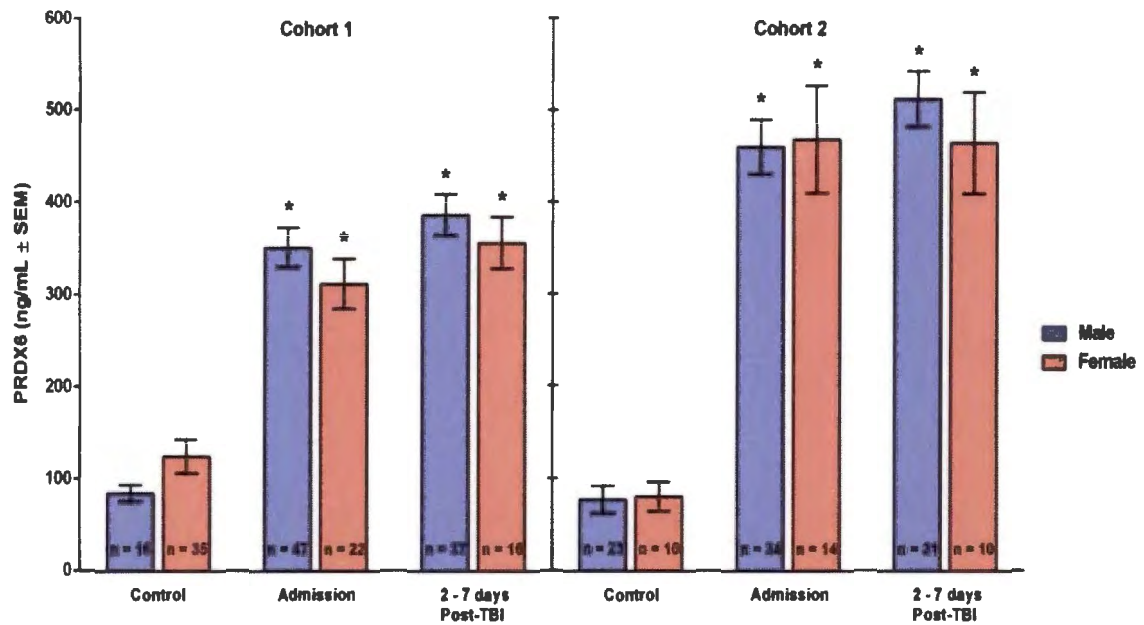
Figure 14. Comparison of levels of PRDX6 in human plasma from control and TBI patients at the time of admission and at 2-7 days post-injury. The experiment was replicated in a second cohort of similar size (panels Cohort 1 and 2). Bars reflect mean ± standard error. Sample sizes are listed within bar. * p < 0.0001 as compared to control values.

Figure 15 shows the time course for the fold-changes in plasma levels of seven candidate TBI biomarker proteins. Plotting data as a fold-change standardizes for the wide differences that exist in the absolute concentrations of the biomarkers in plasma. While the duration between the first and second samples was variable due to the study's design (see above), time-related increases in plasma levels were observed for five of the seven candidate biomarker proteins: BDNF, MCP1/CCL2, NSE, S100b, and PRDX6. Levels of GFAP were below the level of quantification for all time points and thus, no changes were detected under the conditions of this study.
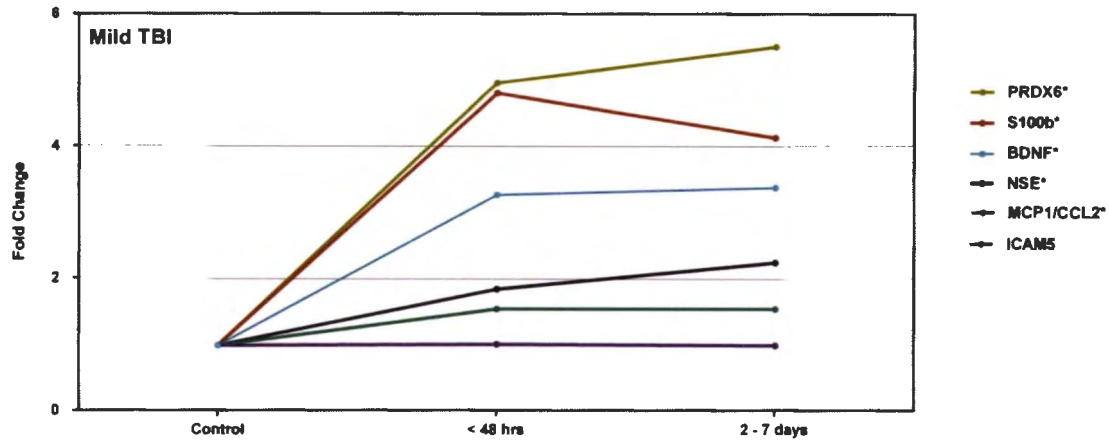
Figure 15. Effects of mild to moderate TBI on plasma levels of candidate biomarker protein expressed as fold-changes from controls values. Plotted are the values obtained within 48 hours of injury and again at 2 to 7 days post mild TBI. Graph lines for ICAM-5 and GFAP closely overlap. *Changes significantly different from control (see Table 4 for p-values)

FURTHER ANALYSIS OF PLASMA LEVELS OF CANDIDATE TBI BIOMARKERS IN PATIENTS WITH MILD TO MODERATE TBI

Data from the present study on mild to moderate TBI were further analyzed as depicted by the data analysis model presented in Figure 16. The examination was undertaken utilizing 7 dependent variables against 1, two-level (control:injured) independent variable. Multivariate analysis of variance (MANOVA) was used to minimize type I errors. It was recognized that the sample sizes were unequal, contained few outliers and displayed a skewed data distribution. The Box text and Levene's test which measure quality of covariance and variance respectively were both violated. After taking all of these conditions into account and considering the large sample size, a method I, type 3 sum of squares model design was used to keep all cells equally important. To further address the violation of statistical assumptions, data was analyzed

by the following alternative means: analysis of variance, analysis of covariance, type II sum of squares, and transformation of data (log). Appendix IV reports the Pillai's trace statistics for all calculations undertaken in the dissertation. Despite the uneven sample sizes, the "n" was sufficiently large in both studies that the results were still robust to violations of the statistical assumptions (116). Therefore, a MANOVA analysis was utilized to determine how the demographic variables of age, race, gender and level of education might be related to biomarker responses. A similar analysis was performed to examine how the presence of abnormal medical imaging or Glasgow Coma Scale score might relate to biomarker responses.

Figure 16. Data analysis model for the clinical and demographic data of the mild to moderate TBI study.

When co-varying for gender, race, age, and education, there was no overall difference between males and females and no differences with regard to race and

76

education. With regards to age, younger patients (< 45 yrs) had modestly lower levels of MCP1/CCL2 at admission as compared to levels measured in older (> 45 yrs) individuals (p > 0.05). None of the other biomarkers showed this pattern. Regarding the two clinical variables examined, we could not differentiate between levels of admission Glasgow Coma Scale or CT/MRI imaging positive results and changes in the levels of plasma biomarkers. Because the clinical variables were analyzed as nominal/dichotomous variables, and multiple dependent variables were considered a correlation analysis was not appropriate. In regards to the mild to moderate brain injury and biomarker response it was found that in every case the overall multivariate model was significant for each time point with an effect size greater than 0.14 and a power of 1.0.

ANALYSIS OF CANDIDATE BIOMARKERS IN HUMAN PATIENTS EXPERIENCING MODERATE TO SEVERE TBI

A study of moderate to severe TBI was conducted in collaboration with Dr. Shawn Rhind and his colleagues in the Defence Research and Development Canada, the Canadian counterpart to the Department of Defense. This study involved a total of 106 patients who were admitted with isolated head injuries and diagnosed with moderate to severe TBI. Plasma samples were obtained at admission and 6, 12, 24 hours post-injury. Glasgow Coma Scale scores on admission were all below 12 (range = 3-12; mean = 6; median = 6) and 26 of 106 patients died within the 24 hours following admission.

DEMOGRAPHIC DATA OF THE MODERATE TO SEVERE TBI PATIENTS

Table 6 lists the demographic and clinical data available for the subjects involved in this ongoing study. The 44 control samples were provided by our collaborator. They were described as non-trauma, non-post-traumatic stress disorder military personnel. The demographic and clinical data available from this study are currently limited as compared to the data recorded in the mild to moderate TBI study (discussed above). Accordingly, an in-depth analysis of these variables could not be undertaken here.

Table 6. Demographic characteristics and clinical variables for patients with moderate to severe TBI study.

		TBI	Controls
		Total, N = 106	Total, N = 44
Age			
	Mean, y (SD)	47 (21)	
	Median	45.5	
	Range	16-96	
	Unknown	0	44 (100)
Gender (%)			
	Male	85 (80)	
	Female	21 (20)	
	Unknown	0	44 (100)
Glasgow Coma Scale score in Emergency Department (%)			
	< 9	75 (71)	0
	9 - 12	28 (26)	0
	≥ 13	0 (0)	44 (100)
	Unknown	3 (3)	0
Marshall Score (%)*			
	I	15 (14)	0
	II	51 (48)	0
	III	9 (8)	0
	IV	18 (17)	0
	V	9 (8)	0
	VI	0	0
	Unknown	4 (4)	0
Surgery in first 24 hours (%)**			
	Yes	28 (26)	0
	No	78 (74)	0
	Unknown	0	0
Dead (%)		26 (24)	0
Glasgow outcome scale extended at Hospital Discharge(1-8) (n=27)*	Mean	3.2	0

*A rating scale with 6 categories, used to predict both the risk of increased intra-cranial pressure and outcome in adults (Category I = diffuse injury, no visible pathology-Category 6 = major CT abnormality (70).

** A description of the surgeries performed is presented in Appendix IV

*** A rating scale with 8 categories used to measure outcome and clinical status 6 months after injury. (1 = severe disability and poor outcome - 8 = highly functional and good outcome (138).

EFFECTS OF MODERATE TO SEVERE TBI ON PLASMA LEVELS OF CANDIDATE BIOMARKER PROTEINS

The patient samples were obtained as two cohorts of approximately equal size.

Data from all the subjects at the individual time points was averaged prior to analysis.

Statistical analysis (MANOVA) was similar to that utilized in the mild to moderate study.

Appendix IV reports the Pillai's trace statistics for all calculations undertaken in the

dissertation. Table 7 presents the mean plasma levels for all biomarkers at all time points

for TBI patients and controls making up this study. Values that are statistically different

from control values are indicated by specific p-values.

Table 7. Plasma levels of candidate TBI biomarker proteins in patients with severe TBI.

Condition	ng/mL	BDNF	GFAP	ICAM-5	MCP1/ CCL2	NSE	S100b	PRDX6 Cohort 1 only	CDK5 Cohort 1 only
Control	Mean	1.18	<0.30	1.37	0.13	10.53	0.29	144.54	24.79
	SEM	0.22	-	0.08	0.01	0.89	0.03	24.20	15.04
	Mean	4.53	3.84	1.10	0.39	119.8	2.46	762.87	<6.80
Adm	SEM	0.54	1.49	0.14	0.05	9.95	0.58	85.45	-
	p =	<0.001	-	<0.08	<0.001	<0.001	<0.001	<0.001	-
	Mean	3.98	0.91	1.02	0.29	110.8	0.57	510.52	<6.80
6 hrs	SEM	0.41	0.15	0.08	0.05	9.28	0.09	53.15	-
	p =	<0.001	-	<0.001	<0.001	<0.001	<0.002	<0.001	-
	Mean	3.26	0.86	0.96	0.24	100.4	0.59	413.18	<6.80
12 hrs	SEM	0.43	0.14	0.07	0.03	9.26	0.12	43.53	-
	p =	<0.001	-	<0.001	<0.001	<0.001	<0.01	<0.001	-
	Mean	2.30	0.69	0.99	0.25	69.22	0.58	280.01	<6.80
24 hrs	SEM	0.25	0.06	0.08	0.03	7.35	0.17	44.44	-
	p =	<0.001	-	<0.001	<0.005	<0.001	<0.07	<0.006	-

Figure 17 presents the effects of moderate to severe TBI on plasma levels in

cohort 1 of PRDX6. As shown here, at the time of admission circulating levels of PRDX6

were greater than 5-fold of control values. This increase in plasma PRDX6 exceeded the

4.9 fold increase observed in the response to mild to moderate TBI (Fig. 15 and Table 5).

Plasma levels of PRDX6 progressively declined over the next 6, 12, and 24 hours, but

were still significantly elevated over controls at the 24 hour time point.
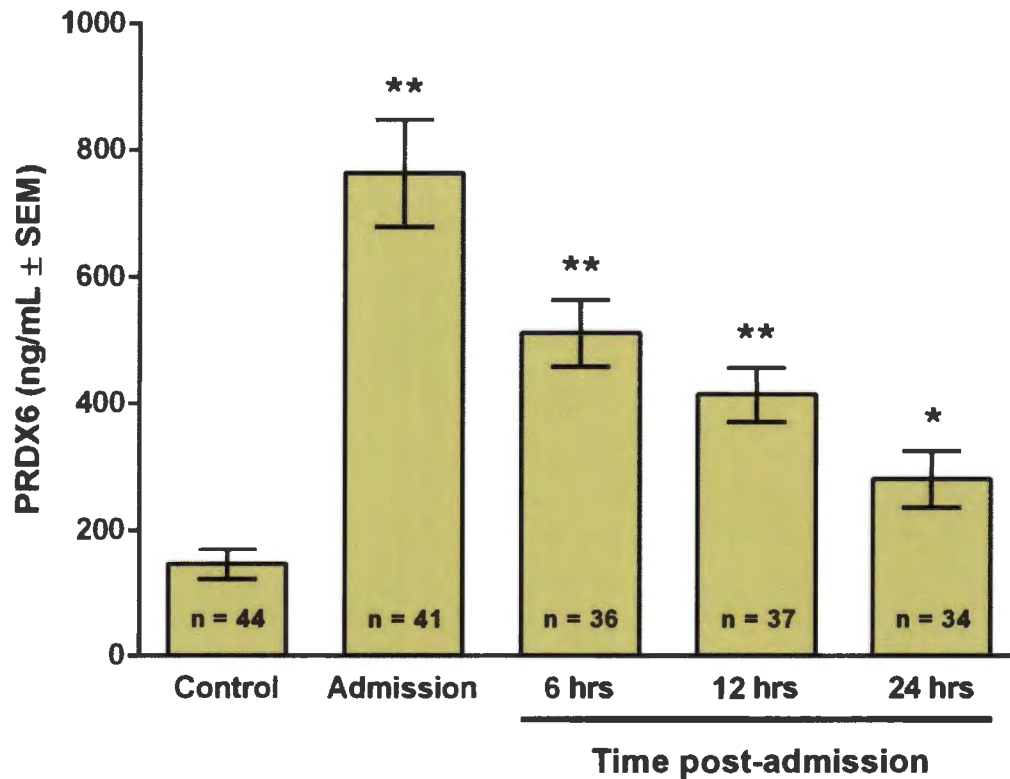
Figure 17. Time course for changes in plasma levels of PRDX6 in cohort 1 following
moderate to severe TBI. Bars reflect mean ± standard error. Sample size listed
within bar. ** p <0.0001, * p < 0.001.

Figure 18 shows the time course for the fold-changes in plasma levels of eight

candidate TBI biomarker proteins. Time-related increases in plasma levels were observed

for five of the eight candidate biomarker proteins: PRDX6, S100b, BDNF, NSE, and

MCP1/CCL2. Levels of ICAM-5 were not appreciably altered under the conditions of

this study. While the mean levels of GFAP in the TBI group rose into the detectable

range following moderate to severe TBI, a fold change could not be calculated because control values were below the limit of detection. Intriguingly, plasma levels of CDK5 were reduced in patients with moderate to severe TBI; however, this response could not be quantitated due to the low basal levels of plasma CDK5 in controls and the reduction in these low levels to values below the limit of assay quantification following TBI.
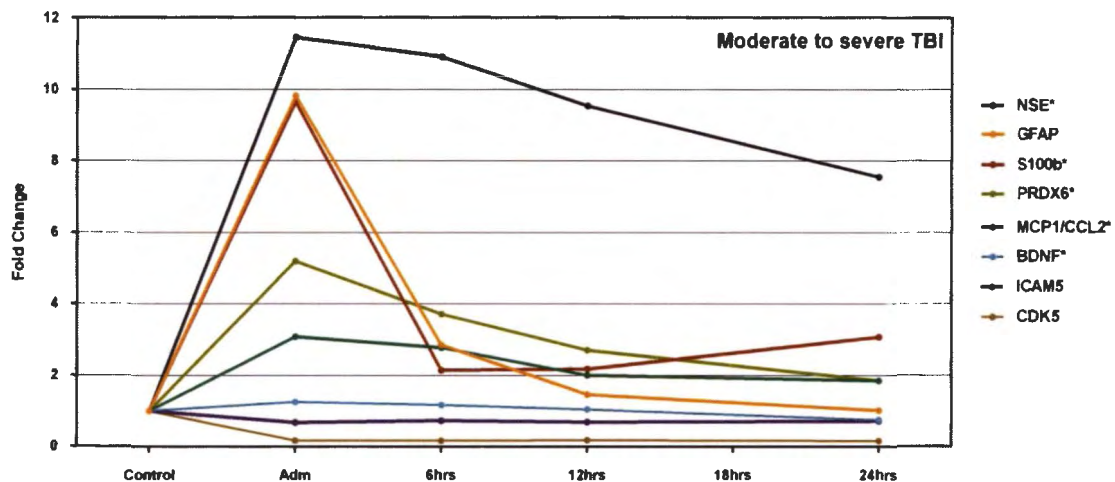
Figure 18. Effects of moderate to severe TBI on plasma levels of candidate biomarker proteins expressed as fold-changes from control values.

FORMULATION OF A TBI ASSESSMENT SCORE BASED UPON THE PROFILE OF BIOMARKER RESPONSES TO TBI

The distinctive profiles observed in plasma levels of biomarker proteins following TBI suggested that these patterns might contribute to formulation of a biomarker signature for the diagnosis of TBI. To explore this possibility, fold changes in the levels of each biomarker were calculated for samples collected at the time of hospital admission, as compared to control values. Table 8 presents the data from Table 5 for the study focusing on patients with mild to moderate TBI at the time of admission.

82

Table 8. Plasma values and fold changes of candidate TBI biomarker proteins in patients with mild to moderate TBI.

	BDNF	GFAP*	ICAM-5	MCP1/ CCL2	NSE	S100b	PRDX6
Control	2.78 ± 0.56	<0.30	0.90 ± 0.06	0.11 ± 0.01	29.95 ± 6.22	0.15 ± 0.03	78 ± 17.51
TBI Admission	9.08 ± 0.58	<0.30	0.92 ± 0.02	0.17 ± 0.01	55.50 ± 2.83	0.72 ± 0.13	388 ± 14.95
Fold Change	3	?	No Δ	2	2	5	5

*GFAP levels were beneath the level of detection in both control and TBI group.

A similar analysis was carried out for the data from patients diagnosed with moderate to severe TBI due to isolated head injury. Table 9 presents mean plasma levels and fold-changes for plasma levels of biomarker proteins in patients with moderate to severe TBI. In cases where changes were observed, these were all greater than those observed in response to mild TBI. While the mean levels of GFAP in the moderate to severe TBI group rose into the detectable range following injury, a fold-change could not be calculated because most of the control values (75%) were below the limit of quantification (0.3 ng/mL). Moreover, the increase in plasma concentrations of GFAP to a mean of 3.6 ± 1.1 ng/mL (median 0.8 ng/mL) measured in the injured patients reflects very high values in only 6 of 91 individuals who were disproportionally responsive as compared to the other 85 individuals in the group. In these highly responsive individuals, plasma values of GFAP ranged from 24 to 55 ng/mL (mean ± SEM: 40 ± 5 ng/mL). Accordingly, it is not possible to calculate a fold-change value for GFAP in response to TBI. However, it should be noted in that within individual patients a dramatic increase in

plasma GFAP following TBI may be relevant to the diagnosis and assessment of their

particular brain injury.

Table 9. Mean plasma values of candidate TBI biomarker proteins in moderate to severe
TBI patients and their respective fold changes compared to controls.

	BDNF	GFAP**	ICAM-5	MCP1/CCL2	NSE	S100b	PRDX6*
Control	1.18 ± 0.22	< 0.30 -	1.37 ± 0.08	0.13 ± 0.01	10 ± 0.89	0.29 ± 0.03	145 ± 24
TBI Admission	4.53 ± 0.54	3.84 ± 1.49	1.10 ± 0.14	0.39 ± 0.05	120 ± 10	2.46 ± 0.58	763 ± 85
Fold Change	4	?	?	3	11	9	5

* PRDX6 data represents patients from Cohort 1 only. **No fold change could be
calculated for GFAP because approximately 75% of the data for control values were
beneath the level of quantification. This is in contrast to the TBI patients where, at
admission, plasma GFAP values were all greater than the assay limit of quantification
(0.3 ng/mL).

TBI ASSESSMENT SCORE

On the basis of these findings, we propose that a clinically relevant TBI

Assessment Score can be based upon the fold changes observed in 5 of the biomarker

proteins studied here. Table 10 shows the formulation of this score, which is simply the

summation of the fold-changes observed in plasma levels of PRDX6, NSE, S100b,

BDNF, and MCP1/CCL2. Because control levels are unchanged for these biomarkers,

they each have been assigned a value of one, for a summation score of five. In the case of

mild TBI, we calculated a summation score of 17 for the candidate biomarkers listed in

Table 10. In the case of moderate to severe TBI the summation score was 32. Calculated

84

in this fashion, the TBI Assessment Score clearly distinguishes mild TBI from controls and from moderate to severe TBI.

Table 10. Formulation of a TBI Assessment Score.

Protein	Control	Mild to Moderate	Moderate to Severe
BDNF	1	3	4
MCP1/CCL2	1	2	3
NSE	1	2	11
S100b	1	5	9
PRDX6	1	5	5
TBI Score	5	17	32

It is proposed that this strategy of multivariate analysis can be further developed for the improved diagnosis of mild TBI. The present data demonstrate the five biomarkers studied here can be used to establish a meaningful signature that readily identifies mild TBI with an objective and quantifiable assessment score. As depicted in Figure 19, this TBI Assessment Score complements and extends that of the Glasgow Coma Scale (see Appendix V), which was originally designed for documenting states of consciousness, and therefore pertains best to conditions of moderate and severe TBI (117). The benefit of the TBI assessment score proposed here is its ability to aid in the diagnosis of mild TBI. In addition to the increased diagnostic sensitivity, the TBI Assessment Score has a wider dynamic range than the Glasgow Coma Scale. Because the TBI Assessment Score is based upon definitive measures of circulating biomarkers, it is an objective assessment that is easily standardized across clinical settings.

TBI Assessment Score
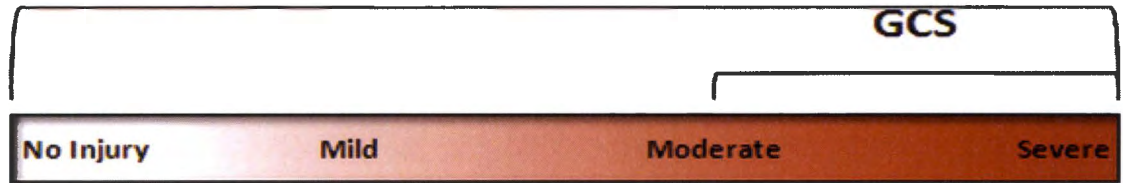
Figure 19. The Glasgow Coma Scale was designed to assess levels of consciousness. Accordingly, its clinical use focuses on the more severe forms of TBI. The TBI Assessment Score (TBI Score) proposed here has a wide dynamic range of sensitivity and can be used to assess the entire spectrum of TBI.

Chapter 5: DISCUSSION

The studies presented in this dissertation focused on the discovery of novel TBI biomarkers and the development of assessment tools for evaluating mild TBI. It is widely recognized that the accurate diagnosis and assessment of TBI, especially mild TBI, is critically important to the short and long-term management of brain injury. However, despite significant scientific effort regarding the mechanisms and neuropathology of TBI, no biomarkers have been validated for diagnosing mild TBI, assessing its underlying mechanisms or identifying effective therapeutic targets. Importantly, there is little information regarding biomarkers that may be potentially useful in identifying the subset of TBI patients most likely to develop persistent post-concussive symptoms and disabling cognitive and neuropsychiatric disorders. This dissertation project was designed to address the challenge of the diagnosis of mild TBI by identifying new biomarkers.

The most important outcome of this project is the demonstration of how a plasma profile of five biomarker responses can be interpreted to create an assessment score that identifies mild TBI. This TBI Assessment Score is based upon fold changes in plasma levels of both novel and recognized biomarker proteins measured in humans experiencing mild to moderate TBI versus moderate to severe TBI. This score offers a long sought solution to the need for a sensitive and objective tool for diagnosing mild TBI in adult patients.

The ability to diagnose and assess mild TBI is critically important to proper management. Missed diagnosis of mild TBI can deny appropriate care, including active measures to protect against the risk of a repeated injury. Incorrect diagnosis of mild TBI can trigger inappropriate treatment, adding additional stress to an already overburdened

healthcare system. Furthermore, as potential pharmacological interventions and other treatment modalities become available, the ability to accurately diagnose mild TBI will become even more important for effective clinical care.

The TBI Assessment Score discussed here offers a new approach for evaluating TBI by identifying a biomarker signature for structural changes, pathologic processes and compensatory responses as reflected in a diverse panel of protein biomarker responses. For example, a PRDX6 response is thought to reflect the degree of oxidative stress (81; 94; 114; 126), whereas NSE and GFAP responses reflect neuronal and glial cell death, respectively (13; 139; 141). Similarly, plasma responses in MCP1/CCL2 reflect the degree of inflammation and immune system activation in response to TBI (31; 67; 68). A response in plasma BDNF may reflect the activation of intrinsic compensatory mechanisms designed to rescue injured neurons (7; 11; 100). Plasma concentrations of ICAM-5 were unaffected by TBI under the conditions reported here. Nevertheless, ICAM-5 is diagnostic in epilepsy (142). It follows, therefore, that ICAM-5 may serve in differentiating underlying neuropathologies that are separate and distinct from TBI (37; 62; 71; 82; 122; 125). Finally, CDK5 was discovered here as a candidate biomarker and shown to actually decline in plasma following TBI (see Fig. 18). The biologic basis for this response is unclear at present but may involve compensatory repair mechanisms designed to limit the phosphorylation of CDK5 substrates, including Tau and CRMP2 (17; 20; 21; 23; 28-30; 42; 47; 65; 72). Overall, the findings presented here demonstrate that a panel of biomarker proteins can provide informative insights into the nature and extent of a brain injury. To our knowledge, this is the first such demonstration.

This investigation focused on a total of nine candidate TBI biomarkers. Five of these are well-recognized in the TBI field and have been studied in a number of clinical investigations. These are BDNF, GFAP, NSE, S100b and CKBB (Table 1). One biomarker, MCP1/CCL2 is recognized in the context of inflammation (25), and the remaining three are novel to TBI: PRDX6, ICAM-5 and CDK5 (Table 3). Ultimately, five of the nine candidates were used to formulate the TBI Assessment Score: NSE, S100b, BDNF, MCP1/CCL2 and PRDX6. Plasma levels of GFAP were below the level of quantification in controls and widely variable in TBI patients. Because of this, it was not possible to calculate a fold-increase for GFAP and as such, this marker could not be used in the arithmetic calculation of the TBI score. It is possible, however, to assign a value to a high level of plasma GFAP following TBI and factor this value into an aggregate TBI assessment score. Due to the small number of patients that exhibited markedly elevated levels of plasma GFAP post-TBI, this calculation was not done here. It will be important to determine if a dramatic GFAP response at the time of injury is predictive of future pathologies. If so, then the scoring of an acute GFAP response will have meaningful relevance to the progression of TBI pathology.

The present findings indicate that plasma levels of a novel biomarker, PRDX6, vary in time following TBI, peaking acutely but remaining elevated above control levels for a substantial time post-injury. If plasma levels of PRDX6, indeed reflect the existence of an oxidative state, then this oxidative condition persists for an extended period following the initial injury.

The modest difference observed in baseline levels of plasma PRDX6 between the commercially purchased controls used for the mild to moderate TBI study (Study I)

89

versus the control group for the moderate to severe TBI study (Study II) (78 ± 18 ng/mL vs. 144 ± 24 ng/mL) may be due to several possibilities including differences in demographics and also variables related to sample preparation. In contrast to the control group for Study I, the no-trauma control group of Study II was military personnel who were demographically matched to the TBI population of that study. Regarding sample preparation, we have observed that levels of PRDX6 are lower in serum as compared to plasma. Accordingly, differences in sample preparation may also be a relevant factor underlying the difference in control levels of PRDX6 measured here. It is important to note that the control and TBI samples for Study II were collected and prepared under the same conditions and therefore, the marked differences observed between the control and TBI groups of this study cannot be due to differences in sample preparation. This same rationale applies to Study I where control levels of plasma PRDX6 were similar to those of Study II and the overall magnitude of the differences between control and TBI levels of plasma PRDX6 were consistently dramatic.

In isolation, none of the recognized TBI markers has proven universally informative in the diagnosis of mild TBI. The data presented here, however, suggest that a multivariate analysis of the responses, taken in conjunction with those of other novel biomarkers, can result in a useful score for assessing TBI. It is expected that this assessment tool will be refined with the inclusion of additional newly discovered candidates having high sensitivity and specificity for TBI. Thus, while the specific proteins making up the TBI score will almost certainly change, the concept of a comprehensive, multivariate biomarker signature will be central to an effective TBI diagnostic score. Additionally, the clinical usefulness of this assessment score will be

enhanced by the consideration of relevant clinical information including neuropsychological findings, patient history and other clinical data that will help to discriminate between different types of brain injury.

The present findings indicate that brain injury activates the immune system to produce autoantibodies against specific brain proteins. We proposed that this autoimmune response serves as a pathway for the discovery of novel TBI biomarkers, and may itself constitute a biomarker signature as well as a potential mechanism for the long-term effects of TBI. These consequences may include the development of persistent post-concussive symptoms and potentially long-lasting effects such as chronic traumatic encephalopathy. Accordingly, knowledge of the autoimmune response to brain injury not only serves the discovery of relevant biomarker proteins but may also guide the development of novel immune-based therapies for treating TBI and alleviating the chronic consequences of neurotrauma. In this regard it may prove important to determine the frequency of the anti-PRDX6 response through TBI cohorts and thus begin assessment of the potential consequences of an anti-PRDX6 response to recovery.

There is recent precedent that head trauma can elicit an autoimmune response. Marchi and coworkers reported in collegiate football players that repeated subconcussive hits to the head resulted in the formation of autoantibodies against S100b (69). Additionally, serum titers of anti-S100b antibodies were proportional to the number and severity of the hits experienced. The authors speculate that the autoimmune response was due to repetitive disruption of the blood-brain barrier and subsequent immune activation. This is the first report in humans of a CNS autoimmune response resulting from head

trauma. Importantly, the response occurred in the absence of any objective measure of even mild TBI.

There are many clinical examples of autoimmune processes mediating neuropathology. These include multiple sclerosis, myasthenia gravis, systemic lupus erythematosus, Guillain Barré syndrome, neuromyelitis optica, Stiff-Person syndrome, paraneoplastic neurological syndromes, Lambert-Eaton myasthenic syndrome, neuromyotonia, autoimmune dysautonomia and polyneuropathies (26; 57). Further, it has been proposed that autoimmune mechanisms may contribute to the neuropathology of Alzheimer's and Parkinson's diseases (14; 45; 78). One common denominator in all of these pathologies is the fundamental principle of autoimmune disease, where the fine line between immune tolerance and autoimmunity is crossed.

The research approach developed here is novel to the TBI field and has already resulted in a significant body of evidence demonstrating its potential for success. The approach is based upon the hypothesis that the autoimmune response to brain injury can reveal novel autoantibodies and brain-specific proteins that may serve in the diagnosis, understanding and treatment of TBI. Specifically, the present studies have identified PRDX6 and CDK5 as candidate TBI biomarkers, and measures of their levels in blood were shown to be informative for TBI in humans (Figs. 15, 18). This investigative approach also identified the brain specific isoform of creatine kinase (CKBB), an established biomarker for TBI (6; 19; 59; 61; 92; 111; 120; 121; 137). The ability of autoimmune profiling to identify recognized biomarkers for TBI establishes confidence that the novel candidates revealed by this approach may prove to be clinically meaningful. In this regard, a panel of twelve candidates has been identified (Table 3) for

further development as TBI biomarkers. Importantly, these proteins have generally escaped notice by the conventional approaches for TBI biomarker discovery and thus represent completely novel candidates.

The traditional approach to biomarker discovery has followed a very different approach to that described here for autoimmune profiling. Much of that work has involved the selection of likely candidates based on deductive reasoning. If the protein was known to be brain-specific, and was shown to produce a distinct peptide signature when digested with proteases known to be activated by TBI, then that protein and its fragments were pursued as candidate TBI biomarkers. In this manner, the traditional approach is completely biased to the specific protein selected for investigation. While this strategy has resulted in a large number of potential biomarkers, none of these candidates have proven useful in the diagnosis of mild TBI when studied alone. Accordingly, the new approach of autoimmune profiling was investigated here as an unbiased approach for biomarker discovery.

Autoimmune profiling was the central strategy for discovery used in this dissertation. This was carried out by either a proteome-wide approach, referred to as global autoimmune profiling, or by a more focused, protein microarray-based profiling. Major strengths of the global approach are that it is specific, sensitive and (most important to the identification of novel biomarker candidates) unbiased, eschewing *a priori* assumptions concerning the identity of potential TBI biomarker candidates. Accordingly, global autoimmune profiling holds the potential for identifying completely novel biomarkers for TBI through the objective investigation of the entire brain proteome. This is in marked contrast to conventional approaches, which are biased to the

specific candidates selected for investigation (see above). Limitations of the global approach to autoimmune profiling include its technical complexity, low throughput and high expense. The second approach used here involved autoimmune profiling by protein microarray. Though intrinsically biased to the proteins printed on the array, the platform used here consisted of over 9,000 human proteins that included a large number relevant to the nervous system. Strengths for the protein microarray approach for autoimmune profiling include its sensitivity, specificity and ease of use. The major limitations of this approach are its focus on only the proteins arrayed, as well as its considerable expense.

The findings from the protein microarray analyses confirm that, in humans, TBI induces an autoimmune response targeting brain proteins. Autoantibodies to 43 unique proteins were up-regulated at 30 days post-injury as compared to baseline conditions. No proteins were observed to be down-regulated 30 days post-injury. The representation of proteins specific to brain in the 43 TBI targets was 40%, greatly exceeding the representation of brain-centric proteins across the entire array (~1%). Accordingly, the human autoimmune response to TBI is clearly focused on proteins of CNS origin.

The significance of these findings is supported by the recent reports of Nagele and co-workers, who demonstrated the effectiveness of the protein microarray platform for identifying autoantigens relevant in Alzheimer's and Parkinson's diseases (45; 78). Specifically, they identified 10 autoantibody biomarkers that effectively differentiated Alzheimer's disease from non-demented, age-matched controls with a sensitivity of 96% and specificity of 93%. Similarly, they identified a panel of autoantibody biomarkers that differentiated Parkinson's disease from age-matched controls with a sensitivity and specificity of 93% and 100%, respectfully. Moreover, the autoimmune profiles of

Alzheimer's and Parkinson's disease patients were clearly distinguishable from each other and from that of patients with a diagnosis of breast cancer or multiple sclerosis. Together, these results demonstrate the significant potential and power of the protein microarray for immune response biomarker profiling.

The findings presented here demonstrate clear differences in the proteins identified by protein microarray and immunoblot approaches for autoimmune profiling. It is believed that these differences have several possible causes. First, controlled cortical impact in rodents is more defined and specific to an isolated brain injury as compared to the more generalized trauma experienced by the patients that were analyzed by protein microarray. As such, different immune responses may be elicited by the different conditions. Second, there are intrinsic differences between the two detection modes: whereas immunoblotting interrogates proteins that are fully denatured, the protein microarray interrogates proteins that are not denatured. Accordingly, different epitopes may be presented for immune recognition by the two techniques.

Identifications from the protein microarray are based upon the addressable locations of the features on the array, whereas autoantigens revealed by immunoblotting are identified proteomically. Peptide mass fingerprinting is most effective for proteins having higher molecular weight and greater abundance, and thus may miss smaller and low-abundance proteins. In these cases, the protein microarray may be a better discovery tool. Conversely, the protein microarray is limited specifically to the proteins printed on the array. Considering the difference in species, injury mechanisms, sample timing post-injury and detection mode, the protein microarray and immuno-based methods could well be expected to identify different autoantibodies and their respective protein antigens.

95

Another consideration for the findings reported here pertains to the small sample size analyzed by protein microarray. While a within-subject comparison involving 10 individuals is considered to be a very reasonable preliminary study, findings from such studies are generally used to set the stage for much larger studies involving hundreds of subjects and costing hundreds of thousands of dollars. Such studies are most often conducted by large, well-funded pharmaceutical companies. An endeavor of this scope was not feasible here due to the costs involved. Nevertheless, the present protein microarray study is considered to be highly successful and to have produced findings that merit extensive follow-up.

Additional considerations for the findings presented here pertain to the possibility of identifying false positives and false negatives. This consideration applies to both the microarray and immunoblot approaches. Immunoglobulins may nonspecifically bind to immobilized proteins through simple protein–protein interactions, thus creating a signal that is immunologically meaningless. False positives may also result as artifacts from the expression system used to generate proteins for the protein microarray. For example, the expression may introduce unnatural post-translational modifications that are "immunologically sticky." Conversely, such modifications could result in false negatives by masking a natural epitope. The natural epitope of a protein could also be masked by the conformation of the protein immobilized on a solid substrate, either a glass microarray slide or PVDF membrane.

The present investigation has identified candidate biomarker proteins and their respective autoantibodies, both of which may be relevant to the diagnosis and understanding of TBI. Accordingly, it is important to confirm or validate both of the

discoveries by independent methods. The best approach for validating biomarker proteins is through the development of sensitive, specific assays for these proteins and demonstrating that they are, in fact, informative for the condition of TBI. This was done here for PRDX6 and CDK5 in humans and CKBB in rodents. Efforts to develop assays for several other candidates, including neuronal pentraxin 1, piccolo, mu crystallin, alpha internexin and CRMP2, were not successful due to the lack of suitable antibodies. Several approaches may be taken to validate autoantibodies thought to be important in TBI. One involves the Luminex-based assay in which target proteins are immobilized on microscopic beads and then probed with experimental samples containing autoantibodies (55). Another approach for validating autoantibodies is the Luciferase Immunoprecipitation System (LIPS) assay (16). LIPS analysis involves cloning target proteins in conjunction with a luciferase reporter. Immunoprecipitation of the fusion protein by the autoantibodies and detection by luminescence constitute the readout of the LIPS assay. A third approach for validating autoantibodies involves the immunosorbent electrochemiluminescence platform used in IEA assays. In this case, proteins are immobilized on the plate and used to capture autoantibodies in experimental samples. One or more of these three approaches can be used to further characterize and validate an autoimmune response to TBI.

FUTURE CONSIDERATIONS AND FUTURE DIRECTIONS

There are several other considerations that are relevant to the interpretation of the findings presented here and the diagnosis of TBI. First, to the best of our knowledge, none of the proteins under consideration as TBI biomarkers (both here and by other labs) are strictly unique to the central nervous system. Accordingly, the concept of a brain–

97

specific response must be qualified when discussing TBI and should include the potential contribution of poly-trauma to a biomarker signature. Second, in view of the statistic that nearly 1/3 of all traumas are associated with alcohol consumption, it is important to recognize the impact that alcohol has on the diagnosis of TBI. Alcohol intoxication compromises the value of neuropsychiatric testing normally performed as part of the TBI assessment. The effect, if any, of alcohol consumption on blood levels of specific biomarkers has yet to be determined. Third, demographic differences including age, gender and genetic background as well as concurrent and past medical conditions, (especially a history of recurrent head injury) may all influence measures of TBI biomarkers. Fourth, different mechanisms of neurological injury may result in different biomarker responses. This may be the case for TBI due to its highly varied injury types that include penetrating injury, acceleration/deceleration injury, falls, and head striking object/object striking head. Fifth, due to the heterogeneous nature of the human condition, longitudinal studies are required for the most meaningful assessment of biomarker responses in TBI. In this regard, military service members offer a unique study population where pre-deployment blood samples are routinely collected and thus are available for evaluating the entire spectrum of deployment experiences including the stress of arriving in theater, combat operations and post-deployment reintegration. In the event of a TBI, sequential sampling provides an excellent opportunity for following biomarker responses post-injury. Sixth, validation of the biomarkers discovered here was hindered by the lack of commercially available antibodies and protein standards. Accordingly, development of specific monoclonal antibodies and protein standards is necessary to advance the development of a number of our TBI biomarker candidates.

Seventh, it is important to pursue the role that disruption in the BBB has in the autoimmune response to TBI. Specifically, it is important to determine if disruption of the BBB is necessary for the generation of autoantibodies following TBI and further, the extent to which pharmacological or inflammatory disruptions of the BBB may produce autoimmune responses similar to those of TBI. Finally, this work brings forward an intriguing concept concerning the role brain-centric autoantibodies have in the long-term consequences of TBI. Autoimmune-based neuropathologies could be evaluated in models examining the effects of aggressive immunosuppression on the recovery of behavioral and motor functions following TBI.

In summary and conclusion, this research has two major outcomes. First, it has demonstrated that autoimmune profiling can be used to identify novel biomarkers for TBI. Importantly, the candidate biomarkers identified by this approach are unique and have not been detected by conventional strategies for TBI biomarker discovery. The second major outcome from this investigation is the demonstration that a profile of biomarker responses can be used to formulate a diagnostic score that is sensitive for the detection of mild TBI. It is proposed that this concept of a multivariate TBI Assessment Score will be refined with more sensitive and specific biomarkers that will effectively define the entire spectrum of TBI. Finally, an additional important aspect of this research is the identification of specific TBI-induced autoantibodies. The presence of these molecules introduces new mechanisms through which the immune system may contribute to the long-term negative consequences of TBI. Understanding the details of the autoimmune response to TBI will guide treatments designed to regulate the immune

response to TBI, and thereby optimize neuroregeneration and restoration of functional circuits.

APPENDIX I

A multiplex analytical platform for six candidate TBI biomarkers (TBI 6-Plex) was established on SECTOR® Imager 6000 reader plates (Meso Scale Discovery, Gaithersburg, MD) in the following three steps. First, two-antibody immunosorbent electrochemiluminescence assays (IEA) were established and characterized for each of the analytes in singleplex. This involved identification of optimal antibody pairs, protein standards and assay conditions, including buffer compositions, incubation times, blocking reagents and matrix controls. Limits of detection and quantitation were determined, as well as the detection of known amounts of calibrant protein added into human serum and plasma. Second, each singleplex IEA was then used to analyze all of the normal samples for which data are presented here. Third, each characterized assay was then assembled in multiplex on SECTOR® Imager 6000 reader plates and all samples were reanalyzed with this platform. Data from the single plex and multiplex analyses revealed that each IEA performed equivalently in both configurations.

ESTABLISHING SINGLEPLEX ASSAYS

Commercially available antibodies and calibrant proteins used for the TBI 6-Plex platform are listed in Table 11. Between eight and fourteen monoclonal or polyclonal antibodies were evaluated for each of the six analytes. These were screened for compatibility and the best working pairs were selected for IEA optimization. Assays were developed using standard bind electrochemiluminescence microtiter plates of Meso Scale Discovery, LLC (Gaithersburg, MD). Wells were coated overnight at 4°C with the

capture antibodies listed in Table 11 (2 μg/mL diluted in phosphate buffered saline (PBS), 25 μL/well). Wells were emptied and then blocked for two hours with 5% fetal bovine serum in PBS (PBS-5% FBS). Wells were washed 3X with PBS containing 0.05% Tween-20 (PBS-T) and samples were introduced into the wells in a total volume of 100 μL consisting of 25 μL human sample, 75 μL PBS-5% FBS. Standard curves were prepared similarly in buffer containing 25 μL of an appropriate matrix. Chicken plasma was used to control for non-specific effects of human plasma and heat inactivated horse serum was similarly used to control for the matrix effects of human serum (see below). Plates were incubated for three hours, washed and then incubated for one hour with detection antibody. All detection antibodies were derivatized with electrochemiluminescent Sulpho-tag NHS-ester R91AN-1 using SULFO-TAG reagent and procedures provided by Meso Scale Discovery. Plates were washed, treated with the addition of MSD Read Buffer (Meso Scale Discovery; catalog# R92TC; 150 μL/well), and electrochemiluminescence was measured using a SECTOR® Imager 6000 instrument (Meso Scale Discovery). All incubations were carried out at room temperature with the exception of that for the capture antibody, which was carried out at 4°C.

Table 11. Reagents used to develop the TBI 6-plex assay platform

		BDNF	S100b	NSE	GFAP	MCP1/CCL2	ICAM-5
Capture Antibody	Vendor	R&D	Sigma	R&D	Genway	R&D	R&D
	Cat #	MAB 848	S2532	MAB 5169	20-272-190050	MAB 679	MAB 1950
	Species	Mouse	Mouse Ascites IgG1	Mouse IgG2B	Mouse IgG2b	Mouse IgG2B	Mouse IgG2A
	Form	Lypho. PBS, 5% Treh	Liquid ascites with NaN3	Lypho. PBS, NaCl 5% Treh	Liquid PBS 0.1% Azide	Lypho. PBS, 5% Treh	Lypho. PBS, 5% Treh
	Purification	Protein A or G	Not listed	Protein A or G	Protein G	Protein A or G	Protein G
Calibrant	Vendor	R&D	Sigma	Abnova	Calbiochem (EMD)	R&D	R&D
	Cat #	248BD005	S6677	H00002026-P01	345996	279-MC-010	1950-M5
	Species	reHuman	Bovine brain	reHuman	Human brain	reHuman	reHuman
	Form	Lypho. NaCitrate, NaCl, BSA	Lypho. Powder	Liquid, Tris glutathione, pHB	Lypho. Urea, NaPbos. & Bicarb.	Lypho. PBS, BSA	Lypho. PBS
	Purification						
Detection Antibody	Vendor	R&D	Genway	R&D	DAKO	R&D	R&D
	Cat #	MAB 648	18-272-198528	AF5169	Z0334	AF-279-NA	AF1950
	Species	Mouse	Rabbit Immunoglob	Sheep IgG	Rabbit Immunoglob	Goat IgG	Goat IgG
	Form	Lypho. PBS, 5% Treh	Liquid with NaN3	Liquid, PBS	Liquid NaCl NaN3	Lypho. PBS, 5% Treh	Liquid, PBs
	Purification	Protein A		Antigen Affinity Pur	Adsorbed with Hu & Cow serum proteins	Antigen Affinity Pur	Antigen Affinity Pur

Lypho: Lypholized; Treh: Trehalose; MAB: Monoclonal antibody; PBS: Phosphate buffered saline; BSA: Bovine serum albumin; Re: Recombinant; Pur: Purified

SELECTION OF MATRIX

Standard curves were performed with and without chicken plasma or horse serum to correct for non-specific matrix effects of the two sample types, plasma *versus* serum. These control matrices were selected from a panel of serums (cow, donkey, goat, guinea pig, horse, pig, rabbit; all obtained from Innovative Research) based upon their ability to replicate the behavior of human samples in each IEA. Comparisons involved considerations of the performance of matrix and human samples, each spiked with known amounts of standard (calibrant) protein, as well as the performance of varying volumes of sample incorporated into each IEA assay (0 – 100 uL; matrix or human sample). Selections were based upon the matrix that: (1) exhibited an estimated background equivalent to that of the corresponding human sample, (2) produced the same low

103

background IEA signal regardless of the volume of matrix assayed, and (3) resulted in standard curves that matched those of the corresponding human sample containing equal amounts of calibrant.

SAMPLES AND SAMPLE PREPARATIONS

Once the performance characteristic of each singleplex assay was optimized, these were then used to analyze serum and plasma samples collected as matched sets from normal adult (19-50 y/o) Caucasian (76%) males and females (Innovative Research). Plasmas were prepared using sodium ethylenediaminetetraacedic acid (NaEDTA) anticoagulant. Similar analyses were performed on extracts of platelets prepared from blood of normal male and female donors (19-50 y/o; Caucasian (76%); Innovative Research) and of human cerebral cortex (male; 52 y/o; African American; cause of death was atherosclerotic cardiovascular disease; postmortem interval was 2 hrs; neuropathologic evaluation revealed brain to be normal; obtained from the Brain and Tissue Bank for Developmental Disorders of the National Institute of Child Health and Human Development, University of Maryland, Baltimore, MD). Platelet rich plasma (~60 mL), prepared from 450 mL whole blood, was combined with an equal volume of Tyrode's solution (137 mM NaCl, 2.7 mM KCl, 1 mM $MgCl_2$. 1.8 mM $CaCl_2$. 0.2 mM Na_2HPO_4. 12 mM $NaHCO_3$. 5.5 mM D-glucose) containing prostacyclin (100 ng/mL; Sigma-Aldrich, St. Louis, MO) and centrifuged at 1800xG for 15 min at 15°C. The washed platelets were resuspended in 30 mL Tyrode's/prostacyclin solution containing protease inhibitors (1X complete protease inhibitor cocktail, Roche, Indianapolis, IN) and evaluated microscopically for purity (>99% routinely) and condition (spherical with few or no signs of activation) and aliquoted for storage at -80°C. Platelet extracts were

prepared by freeze/thawing times three with sonication. Platelet extracts were then centrifuged at 14,000 x g for 10 min (4°C) and supernatants assayed for total protein (BCA: = 13.2 mg /mL). Extracts were diluted with phosphate buffered saline containing 1% BSA and incorporated into the singleplex IEA assays. A homogenate of soluble protein from human cerebral cortex was prepared from a wedge of tissue (~5 gm) spanning all layers of the cortex. The tissue was thawed and homogenized by Polytron (3X 10 seconds, setting 6-7) in 10 volumes/gm in 0.25 M sucrose, 20 mM TES mM, 1 mM EDTA, 0.6 M KCL, pH 7.0 containing protease inhibitors. The resulting homogenate was subjected to Potter-Elvehjem (glass/Teflon) homogenization (five down/up strokes) and centrifuged at 4,900 x g (4°C, 15 min) to remove cellular debris. The resulting supernatant was centrifuged at 150,000 x g (4°C, 60 min). The supernatant was assayed for total protein (BCA; 2.7 mg /mL) and aliquoted for storage at -80°C. Pediatric plasma samples were prepared with sodium citrate anticoagulant and stored at -80°C until assays.

Establishing the Multiplex Platform

The six singleplex assays were assembled together in multiplex format using the proprietary printing service of Meso Scale Discovery (MSD). Each of the capture antibodies (Table 11) were provided to MSD for printing at addressable locations in the wells of standard bind MSD multiplex assay plates. Stock solutions of protein standards (30 X) and SULPHO-Tagged primary antibodies (10X) were prepared in PBS-1% BSA and stored at -80°C as single use aliquots. The standard protocol for performing the multiplex assay is as follows. Plates were hydrated for 60 min at room temperature with 25 μL PBS 1%BSA containing immunoglobulin blockers (goat IgG 0.1% , Kerrville, TX,

mouse IgG 0.02% and rabbit IgG 0.1%, Rockland, Gilbertsville, PA). Samples were

diluted in an equal volume of PBS-1% BSA and added directly into the wells in a volume

of 25 μL. Plates were shaken at room temperature for 2 hrs and then incubated at 4°C

overnight. Wells were washed 3X with PBS/-TBST and then incubated for 1 h with the

blended SULPHO-Tagged primary antibodies (Table 11) diluted to 2 ug /mL each in

PBS-1% BSA (25 μl/well). S-100b was also printed in a basic buffer 10 mM sodium

bicarbonate, pH 9.2) on the basis of benefits gained in a similar assay format. Ultimately,

printing under basic conditions was shown to offer no particular benefit under the

conditions of the multiplex IEA for S-100b. The plates were then wash 3X with PBS-1%

BSA, developed with the addition of MSD Read Buffer (150 μL/well) and read in a

SECTOR Imager 6000 Reader (MSD).

STATISTICS

Lower limits of detection and lower limits of quantitation were defined for each

assay as 3 times and 10 times the standard deviation of the averaged blank well for each

assay, respectively (n=10 for three replicate experiments). Gender differences in plasma,

serum and platelet level for the candidate biomarkers were identified using the Student's t

test; $p < 0.05$.

MULTIPLEX IEA PPERFORMANCE

Table 12 presents the values for the lower level of detection and quantitation for

each of the six assays, working in multiplex. Assay performance characteristics were

equivalent for the assays working in singleplex or multiplex.

Table 12. Matrix effect on LOQ and LOD

Table 2. Effects of sample matrix on the lower limits of quantitation and detection (LOQ/LOD) of TBI biomarkers.

	Buffer only LOQ/LOD	Plasma Matrix LOQ/LOD	Serum Matrix LOQ/LOD
BDNF	0.17/0.08	0.06/0.03	0.011/0.004
S100b	0.06/0.02	0.39/0.13	0.038/0.019
NSE	0.24/0.07	0.87/0.28	0.025/0.019
GFAP	0.26/0.20	0.27/0.21	0.139/0.051
MCP1/CCL2	0.003/0.002	0.015/0.015	0.003/0.003
ICAM-5	0.21/0.12	0.51/0.42	0.726/0.211

Values: ng/mL
n = 6 replicates per standard curve concentration

LOQ: The biomarker concentration represented by the mean signal for zero concentration plus 10 times the standard deviation of this mean.
LOD: The biomarker concentration represented by the mean signal for zero concentration plus 3 times the standard deviation of this mean.

Data are representative of three replicate experiments.

Table 13 presents the mean values for each candidate biomarker measured in serum, plasma and platelets from normal, male and female volunteers (Caucasian (76%); age 19 – 50 y/o). Serum and plasma samples were prepared as matched sets from the same blood draws. Platelets were collected from separate male and female donors. Values for brain are for a single sample of cortex as described above under **Samples and sample preparations**.

Table 13. Plasma and serum levels of candidate TBI biomarkers

Table β. Levels of candidate TBI biomarkers in serum, plasma and platelets of normal adult males and females.

Biomarker	Male (ng/ml)		(ng/mg)	Female (ng/ml)		(ng/mg)	
	Serum	Plasma	Platelets	Serum	Plasma	Platelets	Brain
GFAP	0.83 ± 0.18	0.84 ± 0.13	0.21 ± 0.02	0.65 ± 0.11	0.82 ± 0.10	0.14 ± 0.01	10,612
BDNF	4.08 ± 0.41	2.45 ± 0.72	5.9 ± 0.62	4.32 ± 0.58	3.39 ± 0.94	6.69 ± 0.67	1.50
MCP-1	0.22 ± 0.02	0.07 ± 0.01	.015 ± 0.001	0.21 ± 0.03	0.10 ± 0.02	.014 ± 0.001	0.03
ICAM-5	0.24 ± 0.03	0.86 ± 0.07	0.14 ± 0.01	0.35 ± 0.08	0.86 ± 0.14	0.21 ± 0.01	24.11
NSE	4.24 ± 0.70	10.17 ± 2.21	140.7 ± 18.5	2.85 ± 0.43	39.69 ± 10.75	110.46 ± 13.13	22,786
S100B	0.36 ± 0.10	0.44 ± 0.12	0.17 ± 0.05	0.25 ± 0.06	0.29 ± 0.06	0.14 ± 0.05	2,042

Platelet and brain extracts were diluted in PBS 1% BSA and were evaluated with standard curves in which calibrant proteins were diluted similarly. Serum and plasma samples were analyzed together in the same assays and values calculated from standard curves that contained the same amounts of sample matrix, either heat inactivated horse serum or chicken plasma (NaEDTA anticoagulant), to control for the non-specific effects of the two sample types. The presence of plasma or serum matrix altered the lower limits of detection and quantitation of each assay as presented in Table 12. Levels of GFAP, BDNF and S-100b in plasma and serum were statistically the same and there were no differences between males and females. Levels of CCL2/MCP-1 in serum were approximately 2-fold higher that those observed in plasma, for both males and females; levels of CCL2/MCP-1 in serum and plasma did not differ by gender. Conversely, in both males and females, levels of ICAM-5 and NSE observed in plasma were significantly higher in plasma as compared to serum. This difference was most dramatic in females where average plasma levels of NSE exceeded those of serum by approximately 13-fold (2.85 ng/mL *vs* 39.69 ng/mL). While there were no gender differences in circulating levels of ICAM-5, average plasma levels of NSE were nearly 4-fold higher in females as

compared to males 10.17 ng/mL vs 39.69 ng/mL). Serum levels of NSE tended to be lower in females as compared to males; this difference was not statistically significant. While platelet levels of individual biomarkers did not differ between males and females, absolute concentrations ranged dramatically from virtually non-detectable for GFAP, CCL2/MCP-1, ICAM-5 and S100b (>0.2 ng/mg protein) to approximately 6 ng/mg protein for BDNF and over 100 ng/mg protein for NSE. Intriguingly, levels of BDNF in platelets exceeded those of our single human brain sample by approximately 6-fold, whereas, levels of GFAP, ICAM-5, NSE and S100b were markedly lower in platelets as compared to brain tissue. Levels of the proinflammatory mediator, CCL2/MCP-1, were essentially non-detectable in both platelets and brain extracts.

APPENDIX II

Table 14. Protein identifications from rat based 2-D gel electrophoresis and autoimmune profiling.

Global Autoimmune Profiling in Rodent — 2 — 3 — >3

Rat Proteins 11-31-2012

Protein	MW	PI	Accession#	IgG #1	IgG #2	IgG #3	IgG #4	IgG #5	IgG #6	IgG #7	IgM #8	IgM #11	IgG #17	IgM #19	IgM/IgG #20	IgM/IgG #21	IgM #22
14-3-3 protein beta/alpha	28055	4.8	P35213						X								
14-3-3 protein gamma	28303	4.8	P61983						X								
3-mercaptopyruvate sulfurtransferase	33023	6.1	Q99J99			X											
4-aminobutyrate aminotransferase, mitochondrial	56418											X					
60 kDa heat shock protein, mitochondrial	60956	5.9	P63039						X								
Aconitate hydratase Mitochondrial	85434	7.9								X					X		
Actin, cytoplasmic 1	41737	5.3	P60709	X	X			X	X	X				X			
actin, alpha skeletal muscle	42024	5.4												X			
actin-related protein 2/3 complex subunit 2	34326												X				
adaptin ear-binding coat-associated	29774											X					
adaptin ear-binding coat-associated protein 1	29774											X					
alcohol dehydrogenase[NADP+]	36483												X			X	
aldose reductase	35774											X					
aldose reductase	35774	6.8											X				
Alpha-enolase	47128	6.2	P04764		X			X							X		
Alpha-internexin	55391	5.3	Q16352					X									
Alpha-soluble NSF attachment protein											X						
Annexin A3	36364	6	P14669			X											
Annexin A5	35745	4.9	P14668														X
Aspartate aminotransferase cytoplasmic	46429	6.7							X						X		
Aspartate aminotransferase Mitochondrial	47315	9.1													X		
beta-soluble NSF attachment protein	33535											X					
Beta-synuclein	14504	4.5	Q63754														X
big tau	71731											X					
calponin-3	36412											X					
carbonic anhydrase 2	29096												X				
cathepsin D	44594												X				
CB1 cannabinoid receptor-interacting protein 1	18647											X					
Ckb protein	45220												X				
COP9 signalosome complex subunit 4	46261	5.6											X				
Creatine kinase b (Ckb) protein	45220											X					
Creatine kinase	42699											X					
Creatine kinase B-type	42726	5.4	P07335	X					X								
Creatine kinase U-type Mitochondrial	47004	8.4												X			
Creatine kinase U-type Mitochondrial precursor	46932																
Delta(3,4)-Delta(2,4)-dienoyl-CoA isomerase, mitochondrial	36148											X					
Desmoplakin isoform 2	332187											X					
Dihydropyrimidinase-related protein (CRMP)	62239												X				
Dihydropyrimidinase-related protein (CRMP)	61356											X					
Dihydropyrimidinase-related protein 2	62294	6	Q16555		X			X									
Dihydropyrimidinase-related protein 2	62239												X				
Dihydropyrimidinase-related protein 2	62278	6	P47942													X	
Dystrobrevin beta	73879	8.9	P84060													X	
electron transfer flavoprotein subunit alpha, mitochondrial precursor	34929											X					
Elongation factor 1-gamma	50061	6.3	Q68FR6		X												
Elongation factor 1-alpha 2	50455	9.1	P62632													X	
Endophilin-A2	35964	5.4	O35964		X												
endoplasmic reticulum resident protein 29 precursor	28557											X					
Eno1 protein	51223	6.6											X				
Fatty acid-binding protein, brain	14864	5.5	P55051														X
F-actin-capping Protein subunit alpha-1	32889											X					
F-actin-capping protein subunit alpha-2	32947											X					
F-actin-capping Protein subunit beta											X						
Fructose-bisphosphate aldolase A	39352	8.3	P05065						X						X		
Fructose-bisphosphate aldolase C	39284	6.7								X							
Gamma-enolase	47141	5	P07323				X										

Protein	MW	pI	Accession															
Glial fibrillary acidic protein (GFAP)	49881	5.4	P14136			X	X											
Glucose-6-phosphate 1-dehydrogenase	59376	6	P05370	X														
Glutamine synthetase	42268	6.6	P09606									X	X					
Glutamyl aminopeptidase	107996	5.2	P50123														X	
glutaredoxin-3	37825									X								
Glutathione S-transferase omega-1	27651									X	X							
glyceraldehyde 3-phosphate-dehydrogenase	35813	7.9									X	X						
glyceraldehyde 3-phosphate-dehydrogenase	35771										X	X						
glyceraldehyde 3-phosphate-dehydrogenase-like	35760										X	X						
Heat shock 70 kDa protein 1A/1B	70053	5.5	P08107						X									
Heat shock 70 kDa protein 1B	70142										X							
Heat shock 70kDa protein 1-like	70376	5.8	P34931						X									
Heat shock cognate 71 kDa protein	70899	5.4	P11142						X									
Heat shock cognate 71 kDa protein	70872	5.4	P63018	X	X				X		X							
Heat shock cognate 71 kDa protein	70805	5.2	P19378				X											
Heat shock cognate 71 kDa protein	70827										X							
Heterogeneous nuclear ribonucleoproteins A2/B1 isoform A2	35984										X							
hypothetical protein LOC681996	38080									X								
Hypoxanthine-guanine Phosphoribosyltransferase	24477	6.1													X			
Isocitrate dehydrogenase [NAD] subunit alpha, mitochondrial	39614	6.5	Q99NA5						X									
Isocitrate dehydrogenase [NAD] subunit alpha, mitochondrial precursor	39588									X								
isopentenyl-diphosphate Delta-isomerase 1	26385									X								
Inositol monophosphatase 1	50709	5.7	Q61G12															X
lipcortin I	38795									X								
L-lactate dehydrogenase B chain	36613	5.7	P42123						X									
Mitogen-activated protein kinase 1	63469	6.5	P63086	X														
Mitogen-activated protein kinase kinase kinase7	67201	6.7													X			
Mu-crystallin homolog	33533									X	X							
NADH dehydrogenase[ubiquinone] flavoprotein 1, mitochondrial precursor	50699												X					
NADH dehydrogenase[ubiquinone] 1 beta subcomplex subunit 10	20845												X					
N(G), N(G)-dimethylarginine dimethylaminohydrolase 2	29669									X								
Nitrilase homolog 1	32091	5.9	Q7TQ94						X									
Peroxiredoxin-1	22110	8.3													X			
Peroxiredoxin-1-like	22150												X					
Peroxiredoxin-2	21770												X					
Peroxiredoxin-6 *	24803									X								
Phosphatidylethanolamine-binding protein 1	20802	5.5	P31044				X											
Phoshhoglycerate mutase1	28832	6.7											X		X			
Phoshhoglycerate mutase2	28737									X								
Phospholysine phosphohistidine inorganic pyrophosphate phosphatase	29191	5.2	Q5I0D5															X
proteasome subunit alpha type-1	29499									X	X							
pyruvate dehydrogenase E1 alpha form 1 subunit	43169									X								
Phosphoglycerate Mutase 1	28832	6.7										X						
pyruvate kinase isozymes M1/M2	57781									X								
Rab GDP dissociation inhibitor alpha	50537	5	P50398						X									
Rab GDP dissociation inhibitor beta	50664	6.1	P50395				X											
rCG51928, isoform CRA_b	27055									X								
Ribonuclease inhibitor	49975	4.7	P29315						X									
Ribose-phosphate pyrophosphokinase 1 isoform 1	34812												X					
RNA-binding protein FUS	52642									X								
Secernin-1	46382	4.7	Q12765			X		X										
Septin-2	41488	6.1	Q15019						X						X			
Septin-8	55757	5.9	Q92599				X											
Serum albumin	68731	6.1	P02770			X	X		X									
SNW domain-containing protein 1	61425									X								
statin-related protein	50307									X								
synapsin-1 isoform a	73943									X								
synapsin-3	63309									X								
Transgelin-3	22501	6.8	P37805															X
T-complex protein 1 subunit alpha	60322												X					

Protein	MW	pI	Accession	1	2	3	4	5	6	7	8	9	10	11	12	13	14	15
T-complex protein 1 subunit alpha	60360	5.9	P28480	X	X													
Thioredoxin-like protein 1	32250	4.8	Q920J4															X
Transketolase	67631	7.2							X			X						
Transitional endoplasmic reticulum ATPase	89323	5.1	P55072			X		X										
tropomodulin-2	39468										X							
Tropomyosin alpha-3 chain	29007	4.7	Q63610	X	X													
Tropomyosin alpha-3 chain(HUMAN)	32819	4.7	P06753		X													
Tropomyosin alpha-4 chain	28510	4.7	P09495		X													
triosephosphate isomerase	26904									X								
Tubulin alpha-1A chain	50136	4.9	P68370					X										
Tubulin beta-2A chain	49907	4.8	Q13885															X
TUC 4b(CRMP 4)	73853										X							
Vesicle-fusing ATPase	82653	6.5	Q9QUL6											X				
Vimentin	53733	5.1	P31000					X										
V-type protein proton ATPase catalytic subunit A	68222										X							

*Peroxiredoxin 6 – Also identified in three of three patients with profound, yet undiagnosed, neuropathology.

APPENDIX III

Table 15. Entire set of potential clinical variables collected in the mild TBI study.

Paired ID		CT_TBI
BSI - ID		CT Scalp_Hematoma
Paired Sample		CT-Skull-Fracture
Greg ID		CT-Subdural_Hematoma_Acute
Sex		CT-Subarachnoid_Hemorrhage
Primary Race		CT-Contusion
Highest Education		CT-:Intracerebral_Hemorrhage
Interval		CT-:DAI
Injury_Mechanism		CT-Intraventricular_Hemorrhage
Neuro_Loss_Conscious		Age_at_MRI
LOC_Duration		Hours_Between_MRI_and_INJ
Post_Traumatic_Amnesia		MRI_TBI
LOC Post Traumatic Amnesia Length		MRI-Epidural_Hematoma
Arrival_GCS_Done		MRI-Subdural_Hematoma_Acute
Arrival_GCS_Eyes_Open		MRI-Scalp_Hematoma
Arrival_GCS_Best_Verbal		MRI_Subarachnoid_Hemorrhage
Arrival_GCS_Best_Motor		MRI-Contusion
Arrival_GCS_Total		MRI-Intracerebral_Hemorrhage
DC_Location_To		MRI-DAI
NSI-Dizzy1		MRI-Intraventricular_Hemorrhage
NSI_Loss_Balance		30_Day_assessments::Interval
NSI-Poor_Coordination		30_Day_assessments::SWLS_Ideal
NSI-Headaches		30_Day_assessments::SWLS_Excellent
NSI_Nausea		30_Day_assessments::SWLS_Satisfied
Vision_Prob		30_Day_assessments::SWLS_Gottn_Important_Thin
NSI_Sensitivity_Light		30_Day_assessments::SWLS_Change_Nothing
NSI_Hearng_Diff		30_Day_assessments::SWLS_Total
NSI_Sensitivity_Noise		30_Day_assessments::Epilepsy_Risk
NSI_Numb_Tinglng		30_Day_assessments::GOSE_Score
NSI_Change_Taste_Smell		90_Day_Assessments::Interval
NSI_Change_Appetite		90_Day_Assessments::SWLS_Ideal
NSI_Poor_Concentrtn		90_Day_Assessments::SWLS_Excellent
NSI_Forgetfulnss		90_Day_Assessments::SWLS_Satisfied
NSI_Diff_Makng_Decisns		90_Day_Assessments::SWLS_Gottn_Important_Thin
NSI_Slowd_Thinkng		90_Day_Assessments::SWLS_Change_Nothing
NSI_Fatigue		90_Day_Assessments::SWLS_Total
NSI_Diff_Sleepng		90_Day_Assessments::Epilepsy_Risk
NSI_Anxious		90_Day_Assessments::GOSE_Score
NSI_Depressd		
NSI_Irritability		
NSI_Poor_Frustrtn		

APPENDIX IV

Table 16. Surgical procedures performed within the first 24 hours on patients admitted with Moderate to Severe TBI.

Surgical procedures performed on Moderate to Severe TBI Patients
Decompressive Craniectomy
Right craniectomy, drainage of subdural hematoma
Right frontoparietal and temporal craniectomy, subdural hematoma evacuated + ICP monitor
Right frontotemporoparietal craniotomy + Decompressive craniectomy + removal of subdural hematoma and right frontal and temporal contusion + ICP Monitor
Left decompressive hemicraniectomy + Evacuate subdural hematoma + anterior temporal lobectomy + ICP monitor
Bilateral decompressive craniectomy for evacuation of acute subdural hematoma + ICP Monitor
Right frontotemporoparietal craniotomy + Evacuation of right acute subdural hematoma + Right subtemporal decompressive craniectomy + Partial evacuation of right temporal intracerebral contusion + ICP monitor
Right trauma craniotomy + Evacuation of subdural hematoma and control of hemorrhagic contusion + ICP Monitor
Left frontotemporal craniotomy + removal of acute subdural hematoma and left frontal contusion with bleeding + ICP monitor
Right craniotomy for evacuation of acute subdural hematoma + Partial evacuation and cauterization of right parietal contusion + Right subtemporal decompressive craniectomy + ICP Monitor
Decompressive craniectomy + Subdural hematoma was evacuated bilaterally + ICP Monitor
Left frontotemporal craniotomy and evacuation of acute epidural hematoma + ICP Monitor
Open reduction internal fixation of the C3-4 fracture + spinal cord decompression with drainage of epidural hematoma and disc herniation
Subdural Decompressive craniectomy + evacuated acute subdural hematoma + ICP Monitor
Bifrontal decompressive craniectomy + Evacuation of bilateral subdural hematomas and bifrontal brain contusion + ICP Monitor

Left frontotemporoparietal craniotomy for evacuation of acute subdural hematoma, removal of frontal subdural contusion + Subtemporal Craniectomy for decompression of the temporal lobe + ICP Monitor
Urgent right decompressive hemicraniectomy + Evacuation right acute subdural hematoma and frontal contusions
Left-sided craniectomy and excision of epidural, subdural, and intracerebral hemorrhage + ICP Monitor
Left craniotomy for acute epidural hematoma + Drainage of left and right acute subdural hematoma + Right craniotomy for contusion and acute subdural hematoma + Resection of anterolateral right contusion because of mass effect + ICP Monitor

APPENDIX V

Figure 20. Glasgow Coma Scale

Eyes Open	spontaneous	4
	to sound	3
	to pain	2
	never	1

Best Verbal Response	orientated	5
	confused conversation	4
	inappropriate words	3
	incomprehensible sounds	2
	none	1

Best Motor Response	obeys commands	6
	localise pain	5
	flexion (withdrawal)	4
	(abnormal)	3
	extension	2
	none	1

Total 3 - 15
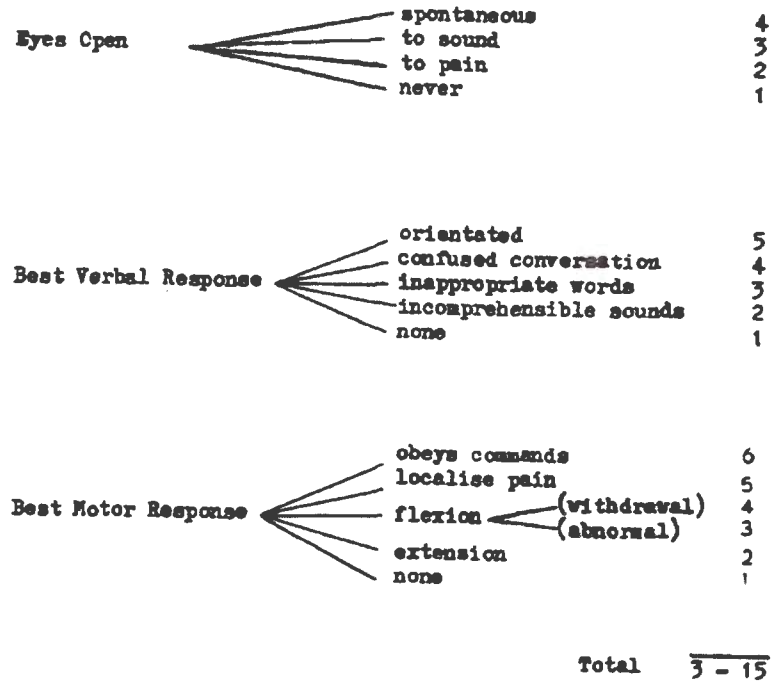
Fig. 1. Glasgow coma scale

One of the first officially published visual representations of the Glasgow Coma Scale

Original citations:

Teasdale G, Jennett B. 1974. Assessment of coma and impaired consciousness. A practical scale. *Lancet* 2(7872):81-84

Teasdale G, Jennett B. 1976. Assessment and prognosis of coma after head injury. *Acta Neurochir (Wien)* 34:45-55

APPENDIX VI

Table 17. Pillai's trace statistics

Mild to Moderate TBI

				Exact Statistic					Computed using alpha = 0.05
Multi variant analysis			**Value**	**F**	**Hypothesis df**	**Error df**	**Sig.**	**Partial Eta Squar ed**	**Observed Power**
Multi plex + PRDX6	TP1	Pillai's Trace	0.559	26.118	7	114	0.000	0.559	1
Multi plex + PRDX6	TP2	Pillai's Trace	0.75	50.641	7	118	0.000	0.75	1

Moderate to Severe TBI

				Exact Statistic					Computed using alpha = 0.05
Multi variant analysis			**Value**	**F**	**Hypothesis df**	**Error df**	**Sig.**	**Partial Eta Squared**	**Observed Power**
Multi plex	TP1	Pillai's Trace	0.499	21.11	6	127	0.000	0.499	1
Multi plex	TP2	Pillai's Trace	0.573	25.902	6	116	0.000	0.573	1
Multi plex	TP3	Pillai's Trace	0.602	28.452	6	113	0.000	0.602	1
Multi plex	TP4	Pillai's Trace	0.526	20.348	6	110	0.000	0.526	1

			Exact Statistic					Computed using alpha = 0.05
uni variant analysis		**Type III Sum of Squares**	**Value**	**F**	**df**	**Sig.**	**Partial Eta Squared**	**Observed Power**
PRDX6	TP1	8161733	0.499	54.8	1	0.000	0.404	1
PRDX6	TP2	2652157	0.573	44.8	1	0.000	0.362	1
PRDX6	TP3	1449363	0.602	31.5	1	0.000	0.285	1
PRDX6	TP4	357850	0.526	7.969	1	0.006	0.094	0.796

REFERENCES

1. Adamson DM, M. Audrey Burnam, Rachel M. Burns, Leah B. Caldarone, Robert A. Cox, Elizabeth D'Amico, Claudia Diaz, Christine Eibner, Gail Fisher, Todd C. Helmus, Terri Tanielian, Benjamin R. Karney, Beau Kilmer, Grant N. Marshall, Laurie T. Martin, Lisa S. Meredith, Karen N. Metscher, Karen Chan Osilla, Rosalie Liccardo Pacula, Rajeev Ramchand, Jeanne S. Ringel, Terry L. Schell, Jerry M. Sollinger, Lisa H. Jaycox, Mary E. Vaiana, Kayla M. Williams and Michael R. Yochelson., ed. 2008. *Invisible Wounds of War: Psychological and Cognitive Injuries, Their Consequences, and Services to Assist Recovery*. Santa Monica, CA: RAND Corporation.

2. Anderson RE, Hansson LO, Nilsson O, Dijlai-Merzoug R, Settergren G. 2001. High serum S100B levels for trauma patients without head injuries. *Neurosurgery* 48:1255-8; discussion 8-60

3. Ankeny DP, Popovich PG. 2009. Mechanisms and implications of adaptive immune responses after traumatic spinal cord injury. *Neuroscience* 158:1112-21

4. Ankeny DP, Popovich PG. 2010. B cells and autoantibodies: complex roles in CNS injury. *Trends Immunol* 31:332-8

5. Baker PR, Clauser, K.R. 2011. *Protein Prospector*. http://prospector.ucsf.edu.

6. Bazarian JJ, Beck C, Blyth B, von Ahsen N, Hasselblatt M. 2006. Impact of creatine kinase correction on the predictive value of S-100B after mild traumatic brain injury. *Restor Neurol Neurosci* 24:163-72

7. Bejot Y, Mossiat C, Giroud M, Prigent-Tessier A, Marie C. 2011. Circulating and brain BDNF levels in stroke rats. Relevance to clinical studies. *PLoS ONE* 6:e29405

8. Berger RP, Adelson PD, Pierce MC, Dulani T, Cassidy LD, Kochanek PM. 2005. Serum neuron-specific enolase, S100B, and myelin basic protein concentrations after inflicted and noninflicted traumatic brain injury in children. *J. Neurosurg.* 103:61-8

9. Berger RP, Hayes RL, Richichi R, Beers SR, Wang KK. 2012. Serum concentrations of ubiquitin C-terminal hydrolase-L1 and alphaII-spectrin breakdown product 145 kDa correlate with outcome after pediatric TBI. *J. Neurotrauma* 29:162-7

10. Berry M, Riches AC. 1974. An immunological approach to regeneration in the central nervous system. *Br. Med. Bull.* 30:135-40

11. Berzi A, Ayata CK, Cavalcante P, Falcone C, Candiago E, et al. 2008. BDNF and its receptors in human myasthenic thymus: implications for cell fate in thymic pathology. *J. Neuroimmunol.* 197:128-39

12. Biberthaler P, Linsenmeier U, Pfeifer KJ, Kroetz M, Mussack T, et al. 2006. Serum S-100B concentration provides additional information fot the indication of computed tomography in patients after minor head injury: a prospective multicenter study. *Shock* 25:446-53

13. Bohmer AE, Oses JP, Schmidt AP, Peron CS, Krebs CL, et al. 2011. Neuron-specific enolase, S100B, and glial fibrillary acidic protein levels as outcome predictors in patients with severe traumatic brain injury. *Neurosurgery* 68:1624-30; discussion 30-1

14. Bouras C, Riederer BM, Kovari E, Hof PR, Giannakopoulos P. 2005. Humoral immunity in brain aging and Alzheimer's disease. *Brain Res. Brain Res. Rev.* 48:477-87

15. Brait VH, Arumugam TV, Drummond GR, Sobey CG. 2012. Importance of T lymphocytes in brain injury, immunodeficiency, and recovery after cerebral ischemia. *J. Cereb. Blood Flow Metab.* 32:598-611

16. Burbelo PD, Hirai H, Leahy H, Lernmark A, Ivarsson SA, et al. 2008. A New Luminescence Assay for Autoantibodies to Mammalian Cell–Prepared Insulinoma-Associated Protein 2. *Diabetes Care* 31:1824-6

17. Camins A, Verdaguer E, Folch J, Canudas AM, Pallas M. 2006. The role of CDK5/P25 formation/inhibition in neurodegeneration. *Drug News Perspect* 19:453-60

18. Cardali S, Maugeri R. 2006. Detection of alphaII-spectrin and breakdown products in humans after severe traumatic brain injury. *J. Neurosurg. Sci.* 50:25-31

19. Carr ME, Jr., Masullo LN, Brown JK, Lewis PC. 2009. Creatine kinase BB isoenzyme blood levels in trauma patients with suspected mild traumatic brain injury. *Mil. Med.* 174:622-5

20. Cheung ZH, Gong K, Ip NY. 2008. Cyclin-dependent kinase 5 supports neuronal survival through phosphorylation of Bcl-2. *J. Neurosci.* 28:4872-7

21. Cheung ZH, Ip NY. 2008. Cdk5 in Dendrite and Synapse Development: Emerging Role as a Modulator of Receptor Tyrosine Kinase Signaling In *Cyclin Dependent Kinase 5 (Cdk5)*ed. NY Ip, L-H Tsai:51-68: Springer US.

22. Corso P, Finkelstein E, Miller T, Fiebelkorn I, Zaloshnja E. 2006. Incidence and lifetime costs of injuries in the United States. *Inj. Prev.* 12:212-8

23. Crews L, Ruf R, Patrick C, Dumaop W, Trejo-Morales M, et al. 2011. Phosphorylation of collapsin response mediator protein-2 disrupts neuronal maturation in a model of adult neurogenesis: Implications for neurodegenerative disorders. *Molecular Neurodegeneration* 6:67

24. Czeiter E, Mondello S, Kovacs N, Sandor J, Gabrielli A, et al. 2012. Brain injury biomarkers may improve the predictive power of the IMPACT outcome calculator. *J. Neurotrauma* 29:1770-8

25. Daly C, Rollins BJ. 2003. Monocyte chemoattractant protein-1 (CCL2) in inflammatory disease and adaptive immunity: therapeutic opportunities and controversies. *Microcirculation* 10:247-57

26. Davidson A, Diamond B. 2001. Autoimmune Diseases. *N. Engl. J. Med.* 345:340-50

27. Dekaban GA, Thawer S. 2009. Pathogenic antibodies are active participants in spinal cord injury. *J. Clin. Invest.* 119:2881-4

28. Demange L, Abdellah FN, Lozach O, Ferandin Y, Gresh N, et al. 2013. Potent inhibitors of CDK5 derived from roscovitine: Synthesis, biological evaluation and molecular modelling. *Bioorg. Med. Chem. Lett.* 23:125-31

29. Dhariwala FA, Rajadhyaksha MS. 2008. An unusual member of the Cdk family: Cdk5. *Cell. Mol. Neurobiol.* 28:351-69

30. Dhavan R, Tsai LH. 2001. A decade of CDK5. *Nat Rev Mol Cell Biol* 2:749-59

31. Dogan RN, Karpus WJ. 2004. Chemokines and chemokine receptors in autoimmune encephalomyelitis as a model for central nervous system inflammatory disease regulation. *Front. Biosci.* 9:1500-5

32. Doppenberg EM, Choi SC, Bullock R. 1997. Clinical trials in traumatic brain injury. What can we learn from previous studies? *Ann. N. Y. Acad. Sci.* 825:305-22

33. Faul M XL, Wald MM, Coronado VG. . 2010. Traumatic Brain Injury in the United States: Emergency Department Visits, Hospitalizations and Deaths 2002–2006. Atlanta, GA: National Center for Injury Prevention and Control, Centers for disease Control and Prevention

34. Field KJ, White WJ, Lang CM. 1993. Anaesthetic effects of chloral hydrate, pentobarbitone and urethane in adult male rats. *Lab. Anim.* 27:258-69

35. Folch J, Lees M, Sloane Stanley GH. 1957. A simple method for the isolation and purification of total lipides from animal tissues. *J. Biol. Chem.* 226:497-509

36. Folkerts MM, Berman RF, Muizelaar JP, Rafols JA. 1998. Disruption of MAP-2 immunostaining in rat hippocampus after traumatic brain injury. *J. Neurotrauma* 15:349-63

37. Gahmberg CG, Tian L, Ning L, Nyman-Huttunen H. 2008. ICAM-5--a novel two-facetted adhesion molecule in the mammalian brain. *Immunol. Lett.* 117:131-5

38. Gensel JC, Kigerl KA, Mandrekar-Colucci SS, Gaudet AD, Popovich PG. 2012. Achieving CNS axon regeneration by manipulating convergent neuro-immune signaling. *Cell Tissue Res.* 349:201-13

39. Gerberding JL. 2003. The Report to Congress on Mild Traumatic Brain Injury in the United States: Steps to Prevent a Serious Public Health Problem, Centers for Disease Control and Prevention, Atlanta

40. Goldman N. Future Directions in Integration of Biological and Social Theories. *Proc. 5th Annual Workshop on Biomarker Collection in Population-Based Health Research, Chicago, IL, 2007*: Chicago Core on Biomarkers in Population-Based Aging Research

41. Goryunova AV, Bazarnaya NA, Sorokina EG, Semenova NY, Globa OV, et al. 2007. Glutamate receptor autoantibody concentrations in children with chronic post-traumatic headache. *Neurosci. Behav. Physiol.* 37:761-4

42. Goshima Y, Sasaki Y, Uchida Y, Yamashita N, Nakamura F. 2008. CRMP Family Protein: Novel Targets for Cdk5 That Regulates Axon Guidance, Synapse Maturation, and Cell Migration

Cyclin Dependent Kinase 5 (Cdk5). ed. NY Ip, L-H Tsai:9-24: Springer US. Number of 9-24 pp.

43. Graham MR, Myers T, Evans P, Davies B, Cooper SM, et al. 2011. Direct hits to the head during amateur boxing is associated with a rise in serum biomarkers for brain injury. *Int J Immunopathol Pharmacol* 24:119-25

44. Gu L, Xiong X, Zhang H, Xu B, Steinberg GK, Zhao H. 2012. Distinctive effects of T cell subsets in neuronal injury induced by cocultured splenocytes in vitro and by in vivo stroke in mice. *Stroke* 43:1941-6

45. Han M, Nagele E, DeMarshall C, Acharya N, Nagele R. 2012. Diagnosis of Parkinson's disease based on disease-specific autoantibody profiles in human sera. *PLoS ONE* 7:e32383

46. Hefferan MP, Johe K, Hazel T, Feldman EL, Lunn JS, Marsala M. 2011. Optimization of immunosuppressive therapy for spinal grafting of human spinal stem cells in a rat model of ALS. *Cell Transplant.* 20:1153-61

47. Hensley K, Venkova K, Christov A, Gunning W, Park J. 2011. Collapsin Response Mediator Protein-2: An Emerging Pathologic Feature and Therapeutic Target for Neurodisease Indications. *Mol. Neurobiol.* 43:180-91

48. Hergenroeder GW, Redell JB, Moore AN, Dash PK. 2008. Biomarkers in the clinical diagnosis and management of traumatic brain injury. *Mol Diagn Ther* 12:345-58

49. Herrmann M, Curio N, Jost S, Wunderlich MT, Synowitz H, Wallesch CW. 1999. Protein S-100B and neuron specific enolase as early neurobiochemical markers of the severity of traumatic brain injury. *Restor Neurol Neurosci* 14:109-14

50. Herrmann M, Jost S, Kutz S, Ebert AD, Kratz T, et al. 2000. Temporal profile of release of neurobiochemical markers of brain damage after traumatic brain injury is associated with intracranial pathology as demonstrated in cranial computerized tomography. *J. Neurotrauma* 17:113-22

51. Ingebrigtsen T, Romner B. 2003. Biochemical serum markers for brain damage: a short review with emphasis on clinical utility in mild head injury. *Restor Neurol Neurosci* 21:171-6

52. Jacobowitz DM, Cole JT, McDaniel DP, Pollard HB, Watson WD. 2012. Microglia activation along the corticospinal tract following traumatic brain injury in the rat: A neuroanatomical study. *Brain Res.* 1465:80-9

53. Jacobowitz DM, Heydorn WE. 1984. Two-dimensional gel electrophoresis used in neurobiological studies of proteins in discrete areas of the rat brain. *Clin. Chem.* 30:1996-2002

54. Jacobowitz DM, O'Donohue TL. 1978. alpha-Melanocyte stimulating hormone: immunohistochemical identification and mapping in neurons of rat brain. *Proc. Natl. Acad. Sci. U. S. A.* 75:6300-4

55. Jun BH, Kang H, Lee YS, Jeong DH. 2012. Fluorescence-based multiplex protein detection using optically encoded microbeads. *Molecules* 17:2474-90

56. Kamchatov PR, Ruleva N, Dugin SF, Buriachkovskaia LI, Chugunov AV, et al. 2009. [Neurospecific proteins and autoantibodies in serum of patients with acute ischemic stroke]. *Zh. Nevrol. Psikhiatr. Im. S. S. Korsakova* 109:69-72

57. Kanwar JR, Sriramoju, B., Kanwar, R.K. 2011. Recent Advances in the Treatment of Neurological Autoimmune Disorders. In *Recent Advances in the Treatment of Neurological Autoimmune Disorders, Autoimmune Disorders - Current Concepts and Advances from Bedside to Mechanistic Insights*, ed. FP Huang: InTech.

58. Kaplan GB, Vasterling JJ, Vedak PC. 2010. Brain-derived neurotrophic factor in traumatic brain injury, post-traumatic stress disorder, and their comorbid conditions: role in pathogenesis and treatment. *Behav. Pharmacol.* 21:427-37

59. Karkela J, Bock E, Kaukinen S. 1993. CSF and serum brain-specific creatine kinase isoenzyme (CK-BB), neuron-specific enolase (NSE) and neural cell adhesion molecule (NCAM) as prognostic markers for hypoxic brain injury after cardiac arrest in man. *J. Neurol. Sci.* 116:100-9

60. Kasper LH, Shoemaker J. 2010. Multiple sclerosis immunology: The healthy immune system vs the MS immune system. *Neurology* 74 Suppl 1:S2-8

61. Kato K, Suzuki F, Shimizu A, Shinohara H, Semba R. 1986. Highly Sensitive Immunoassay for Rat Brain-Type Creatine Kinase: Determination in Isolated Purkinje Cells. *J. Neurochem.* 46:1783-8

62. Kilgannon P, Turner T, Meyer J, Wisdom W, Gallatin WM. 1998. Mapping of the ICAM-5 (telencephalin) gene, a neuronal member of the ICAM family, to a location between ICAM-1 and ICAM-3 on human chromosome 19p13.2. *Genomics* 54:328-30

63. Korfias S, Papadimitriou A, Stranjalis G, Bakoula C, Daskalakis G, et al. 2009. Serum biochemical markers of brain injury. *Mini Rev Med Chem* 9:227-34

64. Lisianyi NI, Liubych LD, Stepanenko IV, Berezhnii HA. 1998. [Humoral link of autoimmune reactions to neuron-specific enolase in post-radiation encephalopathy patients]. *Ukr. Biokhim. Zh.* 70:76-82

65. Lopes JP, Agostinho P. 2011. Cdk5: multitasking between physiological and pathological conditions. *Prog. Neurobiol.* 94:49-63

66. Lu P, Wang Y, Graham L, McHale K, Gao M, et al. 2012. Long-distance growth and connectivity of neural stem cells after severe spinal cord injury. *Cell* 150:1264-73

67. Mahad D, Callahan MK, Williams KA, Ubogu EE, Kivisakk P, et al. 2006. Modulating CCR2 and CCL2 at the blood-brain barrier: relevance for multiple sclerosis pathogenesis. *Brain* 129:212-23

68. Mahad DJ, Ransohoff RM. 2003. The role of MCP-1 (CCL2) and CCR2 in multiple sclerosis and experimental autoimmune encephalomyelitis (EAE). *Semin. Immunol.* 15:23-32

69. Marchi N, Bazarian JJ, Puvenna V, Janigro M, Ghosh C, et al. 2013. Consequences of repeated blood-brain barrier disruption in football players. *PLoS ONE* 8:e56805

70. Marshall LF, Marshall SB, Klauber MR, Van Berkum Clark M, Eisenberg H, et al. 1992. The diagnosis of head injury requires a classification based on computed axial tomography. *J. Neurotrauma* 9 Suppl 1:S287-92

71. Maruya SI, Myers JN, Weber RS, Rosenthal DI, Lotan R, El-Naggar AK. 2005. ICAM-5 (telencephalin) gene expression in head and neck squamous carcinoma tumorigenesis and perineural invasion! *Oral Oncol.* 41:580-8

72. Mazanetz MP, Fischer PM. 2007. Untangling tau hyperphosphorylation in drug design for neurodegenerative diseases. *Nat Rev Drug Discov* 6:464-79

73. McKeating EG, Andrews PJ, Mascia L. 1998. Relationship of neuron specific enolase and protein S-100 concentrations in systemic and jugular venous serum to injury severity and outcome after traumatic brain injury. *Acta Neurochir Suppl* 71:117-9

74. Mondello S, Linnet A, Buki A, Robicsek S, Gabrielli A, et al. 2012. Clinical utility of serum levels of ubiquitin C-terminal hydrolase as a biomarker for severe traumatic brain injury. *Neurosurgery* 70:666-75

75. Mondello S, Muller U, Jeromin A, Streeter J, Hayes RL, Wang KK. 2011. Blood-based diagnostics of traumatic brain injuries. *Expert Rev Mol Diagn* 11:65-78

76. Mondello S, Papa L, Buki A, Bullock MR, Czeiter E, et al. 2011. Neuronal and glial markers are differently associated with computed tomography findings and outcome in patients with severe traumatic brain injury: a case control study. *Crit Care* 15:R156

77. Morozov SG, Asanova LM, Gnedenko BB, Panchenko LF, Lavrova TN. 1996. [Autoantibodies against nerve tissue proteins long after cranio-cerebral injury]. *Vopr. Med. Khim.* 42:147-52

78. Nagele E, Han M, Demarshall C, Belinka B, Nagele R. 2011. Diagnosis of Alzheimer's disease based on disease-specific autoantibody profiles in human sera. *PLoS ONE* 6:e23112

79. Narayan RK, Michel ME, Ansell B, Baethmann A, Biegon A, et al. 2002. Clinical trials in head injury. *J. Neurotrauma* 19:503-57

80. Neff F, Wei X, Nolker C, Bacher M, Du Y, Dodel R. 2008. Immunotherapy and naturally occurring autoantibodies in neurodegenerative disorders. *Autoimmun Rev* 7:501-7

81. Neumann CA, Krause DS, Carman CV, Das S, Dubey DP, et al. 2003. Essential role for the peroxiredoxin Prdx1 in erythrocyte antioxidant defence and tumour suppression. *Nature* 424:561-5

82. Ning L, Tian L, Smirnov S, Vihinen H, Llano O, et al. 2013. Interactions between ICAM-5 and beta1 integrins regulate neuronal synapse formation. *J. Cell Sci.* 126:77-89

83. NRC. 1987. Biological markers in environmental health research. Committee on Biological Markers of the National Research Council. *Environ. Health Perspect.* 74:3-9

84. Nylen K, Ost M, Csajbok LZ, Nilsson I, Blennow K, et al. 2006. Increased serum-GFAP in patients with severe traumatic brain injury is related to outcome. *J. Neurol. Sci.* 240:85-91

85. O'Farrell PH. 1975. High resolution two-dimensional electrophoresis of proteins. *J. Biol. Chem.* 250:4007-21

86. Okie S. 2005. Traumatic brain injury in the war zone. *N. Engl. J. Med.* 352:2043-7

87. Papa L, Akinyi L, Liu MC, Pineda JA, Tepas JJ, 3rd, et al. 2010. Ubiquitin C-terminal hydrolase is a novel biomarker in humans for severe traumatic brain injury. *Crit. Care Med.* 38:138-44

88. Parham P. 2009. *The Immune System*. London: Garland Science. 506 pp.

89. Pelinka LE, Hertz H, Mauritz W, Harada N, Jafarmadar M, et al. 2005. Nonspecific increase of systemic neuron-specific enolase after trauma: clinical and experimental findings. *Shock* 24:119-23

90. Pelinka LE, Kroepfl A, Leixnering M, Buchinger W, Raabe A, Redl H. 2004. GFAP versus S100B in serum after traumatic brain injury: relationship to brain damage and outcome. *J. Neurotrauma* 21:1553-61

91. Pelinka LE, Kroepfl A, Schmidhammer R, Krenn M, Buchinger W, et al. 2004. Glial fibrillary acidic protein in serum after traumatic brain injury and multiple trauma. *J. Trauma* 57:1006-12

92. Phillips JP, Jones HM, Hitchcock R, Adama N, Thompson RJ. 1980. Radioimmunoassay of serum creatine kinase BB as index of brain damage after head injury. *Br. Med. J.* 281:777-9

93. Pineda JA, Lewis SB, Valadka AB, Papa L, Hannay HJ, et al. 2007. Clinical significance of alphaII-spectrin breakdown products in cerebrospinal fluid after severe traumatic brain injury. *J. Neurotrauma* 24:354-66

94. Power JH, Asad S, Chataway TK, Chegini F, Manavis J, et al. 2008. Peroxiredoxin 6 in human brain: molecular forms, cellular distribution and association with Alzheimer's disease pathology. *Acta Neuropathol* 115:611-22

95. Prager EM, Bergstrom HC, Grunberg NE, Johnson LR. 2011. The importance of reporting housing and husbandry in rat research. *Front Behav Neurosci* 5:38

96. PRB. 2008. Use of Biomarkers in Predicting Health and Mortality. In *Today's Research on Aging - Program and Policy Implications*. Washington, DC: Population Reference Bureau

97. Raabe A, Grolms C, Keller M, Dohnert J, Sorge O, Seifert V. 1998. Correlation of computed tomography findings and serum brain damage markers following severe head injury. *Acta Neurochir. (Wien).* 140:787-91; discussion 91-2

98. RAN. 2010. Biomarkers in Cancer - An introductory Guide to Advocates. Plano, TX: Research Advocacy Network

99. Ransohoff RM, Brown MA. 2012. Innate immunity in the central nervous system. *J. Clin. Invest.* 122:1164-71

100. Ring RH, Alder J, Fennell M, Kouranova E, Black IB, Thakker-Varia S. 2006. Transcriptional profiling of brain-derived-neurotrophic factor-induced neuronal plasticity: a novel role for nociceptin in hippocampal neurite outgrowth. *J. Neurobiol.* 66:361-77

101. Romner B, Ingebrigtsen T. 2001. High serum S100B levels for trauma patients without head injuries. *Neurosurgery* 49:1490; author reply 2-3

102. Ross SA, Cunningham RT, Johnston CF, Rowlands BJ. 1996. Neuron-specific enolase as an aid to outcome prediction in head injury. *Br. J. Neurosurg.* 10:471-6

103. Rothoerl RD, Woertgen C. 2001. High serum S100B levels for trauma patients without head injuries. *Neurosurgery* 49:1490-1; author reply 2-3

104. Rothoerl RD, Woertgen C, Holzschuh M, Metz C, Brawanski A. 1998. S-100 serum levels after minor and major head injury. *J. Trauma* 45:765-7

105. Rudehill S, Muhallab S, Wennersten A, von Gertten C, Al Nimer F, et al. 2006. Autoreactive antibodies against neurons and basal lamina found in serum following experimental brain contusion in rats. *Acta Neurochir. (Wien).* 148:199-205; discussion

106. Sandler SJ, Figaji AA, Adelson PD. 2010. Clinical applications of biomarkers in pediatric traumatic brain injury. *Childs Nerv. Syst.* 26:205-13

107. Schwartz M. 2001. Protective autoimmunity as a T-cell response to central nervous system trauma: prospects for therapeutic vaccines. *Prog. Neurobiol.* 65:489-96

108. Schwartz M, Kipnis J. 2011. A conceptual revolution in the relationships between the brain and immunity. *Brain. Behav. Immun.* 25:817-9

109. Selassie AW, Zaloshnja E, Langlois JA, Miller T, Jones P, Steiner C. 2008. Incidence of long-term disability following traumatic brain injury hospitalization, United States, 2003. *J. Head Trauma Rehabil.* 23:123-31

110. Sharma HS, Zimmermann-Meinzingen S, Johanson CE. 2010. Cerebrolysin reduces blood-cerebrospinal fluid barrier permeability change, brain pathology, and functional deficits following traumatic brain injury in the rat. *Ann. N. Y. Acad. Sci.* 1199:125-37

111. Skogseid IM, Nordby HK, Urdal P, Paus E, Lilleaas F. 1992. Increased serum creatine kinase BB and neuron specific enolase following head injury indicates brain damage. *Acta Neurochir. (Wien).* 115:106-11

112. Smith PK, Krohn RI, Hermanson GT, Mallia AK, Gartner FH, et al. 1985. Measurement of protein using bicinchoninic acid. *Anal. Biochem.* 150:76-85

113. Sorokina EG, Semenova Zh B, Bazarnaya NA, Meshcheryakov SV, Reutov VP, et al. 2009. Autoantibodies to glutamate receptors and products of nitric oxide metabolism in serum in children in the acute phase of craniocerebral trauma. *Neurosci. Behav. Physiol.* 39:329-34

114. Sorokina EM, Feinstein SI, Zhou S, Fisher AB. 2011. Intracellular targeting of peroxiredoxin 6 to lysosomal organelles requires MAPK activity and binding to 14-3-3epsilon. *Am J Physiol Cell Physiol* 300:C1430-41

115. Stein TD, Fedynyshyn JP, Kalil RE. 2002. Circulating autoantibodies recognize and bind dying neurons following injury to the brain. *J. Neuropathol. Exp. Neurol.* 61:1100-8

116. Tabachnick BG, Fidell, L.S. . 2006. *Using Multivariate Statistics, 5/E.* Pearson. 1008 pp.

117. Teasdale G, Jennett B. 1976. Assessment and prognosis of coma after head injury. *Acta Neurochir. (Wien).* 34:45-55

118. TechConnect U. 2011. Banyan Biomarkers, Inc. Monitoring Traumatic Brain Injury. In *UF TechConnect*, ed. Uo Florida. Gainsville, FL: UF Office of Technology Licensing

119. Thomas DG, Rabow L, Teasdale G. 1979. Serum myelin basic protein, clinical responsiveness, and outcome of severe head injury. *Acta Neurochir. Suppl. (Wien).* 28:93-5

120. Thompson RJ. 1980. Clinical applications of measurements of human brain-specific proteins. *Biochem. Soc. Trans.* 8:494-6

121. Thompson RJ, Graham JG, McQueen IN, Kynoch PA, Brown KW. 1980. Radioimmunoassay of brain-type creatine kinase-BB isoenzyme in human tissues and in serum of patients with neurological disorders. *J. Neurol. Sci.* 47:241-54

122. Tian L, Nyman H, Kilgannon P, Yoshihara Y, Mori K, et al. 2000. Intercellular adhesion molecule-5 induces dendritic outgrowth by homophilic adhesion. *J. Cell Biol.* 150:243-52

123. Toll EC, Seifalian AM, Birchall MA. 2011. The role of immunophilin ligands in nerve regeneration. *Regen Med* 6:635-52

124. Tolonen A, Turkka J, Salonen O, Ahoniemi E, Alaranta H. 2007. Traumatic brain injury is under-diagnosed in patients with spinal cord injury. *J Rehabil Med* 39:622-6

125. Tse MC, Lane C, Mott K, Onlamoon N, Hsiao HM, Perng GC. 2009. ICAM-5 modulates cytokine/chemokine production in the CNS during the course of herpes simplex virus type 1 infection. *J. Neuroimmunol.* 213:12-9

126. Tulsawani R, Kelly LS, Fatma N, Chhunchha B, Kubo E, et al. 2010. Neuroprotective effect of peroxiredoxin 6 against hypoxia-induced retinal ganglion cell damage. *BMC Neurosci* 11:125

127. van Bavel CC, Dieker J, Muller S, Briand JP, Monestier M, et al. 2009. Apoptosis-associated acetylation on histone H2B is an epitope for lupus autoantibodies. *Mol. Immunol.* 47:511-6

128. Vos PE, Lamers KJ, Hendriks JC, van Haaren M, Beems T, et al. 2004. Glial and neuronal proteins in serum predict outcome after severe traumatic brain injury. *Neurology* 62:1303-10

129. Waldrop MA, Suckow AT, Marcovina SM, Chessler SD. 2007. Release of glutamate decarboxylase-65 into the circulation by injured pancreatic islet beta-cells. *Endocrinology* 148:4572-8

130. Wang KK, Ottens AK, Liu MC, Lewis SB, Meegan C, et al. 2005. Proteomic identification of biomarkers of traumatic brain injury. *Expert Rev Proteomics* 2:603-14

131. Wang R, Chen J, Zhou S, Li C, Yuan G, et al. 1995. [Enzyme-linked immunoadsorbent assays for myelin basic protein and antibodies to myelin basic protein in serum and CSF of patients with diseases of the nervous system]. *Hua Xi Yi Ke Da Xue Xue Bao* 26:131-4

132. Warden D. 2006. Military TBI during the Iraq and Afghanistan wars. *J. Head Trauma Rehabil.* 21:398-402

133. Warren MW, Kobeissy FH, Liu MC, Hayes RL, Gold MS, Wang KK. 2005. Concurrent calpain and caspase-3 mediated proteolysis of alpha II-spectrin and tau in rat brain after methamphetamine exposure: a similar profile to traumatic brain injury. *Life Sci.* 78:301-9

134. Warren MW, Zheng W, Kobeissy FH, Cheng Liu M, Hayes RL, et al. 2007. Calpain- and caspase-mediated alphaII-spectrin and tau proteolysis in rat cerebrocortical neuronal cultures after ecstasy or methamphetamine exposure. *Int J Neuropsychopharmacol* 10:479-89

135. Wekerle H. 2006. Breaking ignorance: the case of the brain. *Curr. Top. Microbiol. Immunol.* 305:25-50

136. Wiesmann M, Steinmeier E, Magerkurth O, Linn J, Gottmann D, Missler U. 2010. Outcome prediction in traumatic brain injury: comparison of neurological status, CT findings, and blood levels of S100B and GFAP. *Acta Neurol. Scand.* 121:178-85

137. Willson VJ, Jones HM, Morgan PM, Thompson RJ. 1980. A two-site immunoradiometric assay for the BB isoenzyme of human creatine kinase. *Biochem. Soc. Trans.* 8:621-2

138. Wilson JT, Pettigrew LE, Teasdale GM. 1998. Structured interviews for the Glasgow Outcome Scale and the extended Glasgow Outcome Scale: guidelines for their use. *J. Neurotrauma* 15:573-85

139. Woertgen C, Rothoerl RD, Brawanski A. 2001. Neuron-specific enolase serum levels after controlled cortical impact injury in the rat. *J. Neurotrauma* 18:569-73

140. Woertgen C, Rothoerl RD, Holzschuh M, Metz C, Brawanski A. 1997. Comparison of serial S-100 and NSE serum measurements after severe head injury. *Acta Neurochir. (Wien).* 139:1161-4; discussion 5

141. Woertgen C, Rothoerl RD, Wiesmann M, Missler U, Brawanski A. 2002. Glial and neuronal serum markers after controlled cortical impact injury in the rat. *Acta Neurochir Suppl* 81:205-7

142. Yang H. 2012. Structure, Expression, and Function of ICAM-5. *Comp Funct Genomics* 2012:368938

143. Yong VW, Marks S. 2010. The interplay between the immune and central nervous systems in neuronal injury. *Neurology* 74 Suppl 1:S9-S16

144. Zafonte R, Friedewald WT, Lee SM, Levin B, Diaz-Arrastia R, et al. 2009. The citicoline brain injury treatment (COBRIT) trial: design and methods. *J. Neurotrauma* 26:2207-16

145.   Zurek J, Fedora M. 2012. The usefulness of S100B, NSE, GFAP, NF-H, secretagogin and Hsp70 as a predictive biomarker of outcome in children with traumatic brain injury. *Acta Neurochir. (Wien).* 154:93-103;